UNIVERSIDADE FEDERAL DE VIÇOSA

AUDERLAN DE MACENA PEREIRA

PHOTOSYNTHESIS IMPROVEMENT AND THE RELATIONSHIP BETWEEN PHOTOSYNTHETIC PIGMENTS AND PRIMARY METABOLISM IN TOMATO LEAVES

VIÇOSA MINAS GERAIS
2019

AUDERLAN DE MACENA PEREIRA

PHOTOSYNTHESIS IMPROVEMENT AND THE RELATIONSHIP BETWEEN PHOTOSYNTHETIC PIGMENTS AND PRIMARY METABOLISM IN TOMATO LEAVES

Thesis presented to the Universidade Federal de Viçosa, as part of the requirements of the Plant Physiology Graduate Program, to obtaining the title of *Doctor Scientiae*.

Advisor: Wagner L. Araújo

Co-advisor: Auxiliadora O. Martins

VIÇOSA MINAS GERAIS
2019

AUDERLAN DE MACENA PEREIRA

PHOTOSYNTHESIS IMPROVEMENT AND THE RELATIONSHIP BETWEEN PHOTOSYNTHETIC PIGMENTS AND PRIMARY METABOLISM IN TOMATO LEAVES

Thesis presented to the Universidade Federal de Viçosa, as part of the requirements of the Plant Physiology Graduate Program, to obtaining the title of *Doctor Scientiae*.

APPROVED: November 21th, 2019.

Assent:

Auderlan de Macena Pereira
Author

Wagner L. Araújo
Advisor

To God,
my parents, Francisca and Adegilson,
my girlfriend Clara Alice,
my brother Emerson,
to my family and friends
and teachers.

I dedicate

ACKNOWLEDGEMENTS

First and foremost, I would like to thank God for the gift of life and the opportunities for learning.

I am very grateful to the Universidade Federal de Viçosa (UFV), especially to the Plant Physiology Graduate Program, for the support and for providing all the necessary conditions for the development of this work.

I also would like to thank my advisor Wagner L. Araújo, for having welcomed me into his labs and guided me during my PhD studies, contributing to the construction of this work and to becoming a better person and professional. I also thank Prof. Adriano Nunes-Nesi for his academic contributions that also contributed to my professional development.

I thank my co-adviser, Auxiliadora O. Martins (Dora), for the support and active and direct participation in the development of this work, for the time availability and assistance, living up to her name, whenever necessary.

I also thank the contributions of teachers Agustin, Dimas and Samuel. To all my colleagues, former and current members, from the "UCP Group" for their friendship, companionship and support, especially Vitor, Jorge, William, Lucas and Victor Fernandes.

I would also like to acknowledge Professor Dr. Lázaro E. P. Peres (Luiz de Queiroz College of Agriculture -ESALQ/USP, Brazil) for sharing the seeds used in this work.

This study was financed in part by the Coordenação de Aperfeiçoamento de Pessoal de Nível Superior (CAPES/Brazil– Finance Code 001), the Max Planck Society, the National Council for Scientific and Technological Development (CNPq) and FAPEMIG (Minas Gerais State Research Assistance Foundation). Scholarships granted by CAPES are also gratefully acknowledged.

Thanks are also due to my parents, Francisca and Adegilson, who always supported me and were committed to my future. My girlfriend Clara Alice, for the unconditional support and constant presence in my life. To my brother Emerson for their support and encouragement. To all my friends of the group "Las Peladas", especially Dalton, João and Daniel, for helping me in one of the most difficult moments I have been through and thus making it possible to finish this work. And last but not least to all my teachers, from primary to here.

“The man without patience in this life is nothing”

Seu Zuzu

ABSTRACT

PEREIRA, Auderlan de Macena, D.Sc., Universidade Federal de Viçosa, November, 2019. **Photosynthesis improvement and the relationship between photosynthetic pigments and primary metabolism in tomato leaves**. Advisor: Wagner Luiz Araújo. Co-advisor: Auxiliadora Oliveira Martins.

Photosynthesis is responsible for the primary productivity and maintenance of life on the planet, boosting biological activity and contributing to the maintenance of the environment. Traditional crop improvement has been sufficient to keep up with the growing demand for food. However, advances in this area have not focused on photosynthesis, per se, but on fixed carbon partitioning. In the near future other approaches must be used to meet the increasing demand. Thus, several paths may be followed, from improving metabolic pathways related to CO_2 fixation, inclusion of metabolic mechanisms from other species and improvements in energy uptake by plants. For the use of energy, it must be first absorbed by photosynthetic pigments, transferring it in the form of excitation energy to the reaction centers where it is converted into biochemical energy. The carbon products fixed in photosynthesis are further used as energy source and building blocks by several metabolic routes. Photosynthetic pigments are also produced from carbon skeletons provided by the primary metabolism, and therefore changes in carbon flow to pigment biosynthesis will likely lead to consequences in the parts of metabolism. In this context, the main goals of this work were: (*i*) to review and present recent advances related to the improvement of photosynthesis in plants, showing promising advances in the field of plant photosynthesis optimization, with well-established future directions; (*ii*) to investigate how high pigment mutations (*hp1* and *hp2*) influence tomato metabolic machinery and how these plants adjust themselves to different light conditions; and (*iii*) to increase our understanding of how mutations that alter carotenoid biosynthesis [namely *crimson* (*old gold-og*), *Delta carotene* (*Del*) and *tangerine* (*t*)] affect the metabolic machinery of tomato plants. Regarding mutations associated with pigment biosynthesis, the data obtained clearly show that extensive metabolic reprogramming occurs allowing plants to withstand changes in the biosynthesis of photosynthetic pigments. Although the mutants were characterized by higher net photosynthesis (*A*), lower stomatal limitation, higher V_{cmax} and anatomical modifications that favor photosynthesis, we found that carbohydrate levels are not increased. Another conspicuous feature is that shading

minimizes the above differences between mutants and WT, or even fully reversed this in the case of certain metabolites. We further observed that mutations *og*, *Del* and *t* did not greatly affect vegetative growth, leaf anatomy and gas exchange parameters. However, an exquisite metabolic reprogramming was recorded. Taken together, our results show that despite minor impacts on growth and gas exchange, carbon flux is extensively affected, leading to adjustments in tomato metabolism to support changes in carotenoid biosynthesis. It is important to mention that such metabolic alterations seems to have little impacts on growth parameters, although yield is strongly affected. Our results also open novel research avenues, indicating new possibilities for better understanding the relationship between photosynthetic pigments and plant metabolism, as well as the enhancement of photosynthesis.

Keywords: Luminosity. Carotenoids. Carbon deviation. Shading.

RESUMO

PEREIRA, Auderlan de Macena, D.Sc., Universidade Federal de Viçosa, novembro de 2019. **Melhorias na fotossíntese e a relação entre pigmentos fotossintéticos e metabolismo primário em folhas de tomateiro**. Orientador: Wagner Luiz Araújo. Coorientadora: Auxiliadora Oliveira Martins.

A fotossíntese é responsável pela produtividade primária e manutenção da vida no planeta, impulsionando a atividade biológica e contribuindo para a manutenção do ambiente. O melhoramento tradicional das culturas tem sido suficiente para acompanhar a crescente demanda por alimentos; no entanto, avanços nessa área não tem focado na fotossíntese em si, mas no particionamento do carbono fixado. Porém, em um futuro próximo outras abordagens deverão ser utilizadas para alcançar a demanda cada vez mais crescente. Dentre tais abordagens, diversos caminhos podem ser seguidos, desde o aprimoramento de rotas metabólicas relacionadas à fixação do CO_2, à inclusão de mecanismos metabólicos de outras espécies e melhorias na capacidade de captação de energia pelas plantas. Para que a energia luminosa seja efetivamente utilizada pelas plantas, primeiro precisa ser absorvida pelos pigmentos fotossintéticos, que a transferem na forma de energia de excitação para os centros de reação, onde é convertida em energia bioquímica. Os pigmentos fotossintéticos são também produzidos a partir de esqueletos de carbono fornecidos pelo metabolismo primário e, desse modo, alterações no fluxo de carbono para a biossíntese de pigmentos possivelmente terá consequências em outras partes do metabolismo. Diante disso, nossos objetivos foram: (*i*) revisar e apresentar os recentes avanços relacionados ao melhoramento da fotossíntese em plantas, indicando avanços promissores no campo da otimização da fotossíntese em plantas, com direcionamentos futuros bem estabelecidos; (*ii*) investigar como as mutações high pigment (*hp1* e *hp2*) influenciam a maquinaria metabólica do tomateiro e como essas plantas se ajustam a diferentes condições de luminosidade; e (*iii*) compreender como as mutações que alteram a biossíntese de carotenoides [nomeadamente *crimson* (*old gold-og*), *Delta carotene* (*Del*) and *tangerine* (*t*)] afetam a maquinaria metabólica de plantas de tomateiro. Com relação as mutações ligadas a biossíntese de pigmentos, os dados obtidos indicam que uma extensa reprogramação metabólica ocorre para que as plantas possam suportar significante alterações na biossíntese de pigmentos fotossintéticos. Embora os mutantes *hp1* e *hp2* tenham sido caracterizados por maiores taxas fotossintéticas, menores limitações

estomáticas associadas a modificações anatômicas que favorecem a fotossíntese, não se observaram alterações nos níveis de carboidratos. Cabe mencionar também que o sombreamento minimiza as diferenças entre mutantes *hp* e o tipo selvagem. Foi também observado que as mutações *og*, *Del* e *t* tem pouco impacto no crescimento vegetativo, anatomia foliar e parâmetros de trocas gasosas. Não obstante, uma extensa reprogramação metabólica foi observada indicando que ajustes metabólicos ocorrem para suportar as alterações na biossíntese de carotenoides. É importante mencionar também que, aparentemente, tais alterações metabólicas interferem pouco ou nada em parâmetros associados ao crescimento, embora a produção seja afetada. Os resultados aqui apresentados abrem também diversas perspectivas para trabalhos futuros ao indicar novas possibilidades para se compreender melhor a relação entre pigmentos fotossintéticos e metabolismo em plantas, bem como o incremento da fotossíntese.

Palavras-chave: Luminosidade. Carotenoides. Desvio de carbono. Sombreamento.

CONTENTS

1. GENERAL INTRODUCTION

Historically speaking, agriculture has played a major role during not only the development of civilizations but also the rapid growth of populations over the years thanks to increased food production (Jacob, 2005). However, the ever-increasing demand for food represents a huge burden on the available arable land, requiring further increases in agricultural productivity (Tilman et al., 2011; Ort et al., 2015). Accordingly, the rise in food demand requires the development of novel agricultural approaches to enhance sustainable production by using smaller area for planting (Aqeel-Ur-Rehman and Shaikh, 2009).

Photosynthesis is one of the most important biochemical processes responsible for maintaining life on the planet not only for helping to boost biological activity but also due to the maintenance of the global environment (Cavalier-Smith, 2006). Briefly, the energy available on Earth is virtually made available through photosynthesis, a pro

cess whereby organisms containing special pigments capture and convert light energy into biochemical energy, used for CO_2 fixation and biosynthesis of carbohydrates that form the building blocks for biomass (McKendry, 2002). Accordingly, it has been postulated that, in order to increase agricultural production, manipulation of photosynthesis in plants presents itself as a suitable approach (Gifford and Evans, 1981; Zhu et al., 2010; South et al., 2019). This is clearly due to the fact that this process represents the CO_2 input for biomass production (McKendry, 2002). CO_2 incorporation into ribulose-1,5-bisphosphate (RuBP) by Rubisco is the first step in plant carbohydrate metabolism which is further used to build biomass and produce energy during growth and development (Parry et al., 2013). This fact aside, Rubisco is characterized by a relatively inefficiency as it can be deduced by its slow catalytic carboxylation rate and its oxygenation activity, which is a major barrier to increasing leaf-level carbon assimilation rate (Ort et al., 2015). Nevertheless, Rubisco activity is one of the main targets for improve photosynthesis and has been extensively explored over the last years (Whitney et al., 2011; Carmo-Silva et al., 2015; Sharwood, 2017). It is important to mention, however, that while the Rubisco properties clearly represent a barrier to increase photosynthetic rate and harnessing sunlight, it has been postulated that these limitations can be substantially mitigated by improvements in canopy light sharing, by

re-engineering Rubisco or by actively concentrating CO_2 at the Rubisco's active site (Ort et al., 2015).

Light is essential for providing energy to first stage of the CO_2 fixation and therefore it has a complex and yet not fully understood influence on crop growth, development and production (Papadopoulos and Hao, 1997; Yamori and Shikanai, 2016). It should be stressed that prior light energy to be used by any system, light must first be absorbed by specific pigments. Thus, antenna complex pigments, mainly chlorophylls and carotenoids, absorb light energy and transfer it as excitation energy to the reaction centers, where it is further converted to biochemical energy (Murchie and Niyogi, 2011). It is important to mention, however, that under high light conditions, the generation of reactive oxygen species (ROS), which are highly harmful to cellular integrity and functionality (Barber and Andersson, 1992), can eventually increase. Although light excess is potentially harmful, plants have a multitude of mechanisms to manage the excess of energy absorbed (Murchie and Niyogi, 2011). Among, these mechanisms allowing dissipation of excess energy the action of the carotenoids, specifically via xanthophyll's cycle, is of importance (Demmig-Adams, 1990). In this way, pigments are of fundamental significance to the photosynthetic processes allowing either light capture or the protection of photosynthetic apparatus.

Other pigment-related molecules such as phytochrome, which are protein pigments, play a key role in plant development and are capable of absorbing light in the red and far-red range wavelength between 660 and 730 nm (Hughes, 2010). It is important to highlight that light not only serves as a source of energy for photosynthesis, but it also acts as a stimulus that triggers several complex physiological responses. Briefly, such responses are initially activated by phytochromes, responsible for both light perception and a range of environmental responses, due to its role in regulating the transcription of specific genes, influencing several biochemical and molecular mechanisms (Lieberman et al., 2004; Carvalho et al., 2011).

Photosynthesis products are used as energy source and building blocks for maintenance growth and development by various metabolic pathways that might compete in an organized and balanced manner. Even though central metabolism is most likely more resilient to changes given its various regulatory layers, these layers can be successfully circumvented, for instance, by genetic manipulation, in order to force a high flow through a

specific set of reactions. Indeed, the interactive connected nature of the metabolic pathways makes inevitably that it would lead to consequences on other parts of metabolism (Sweetlove et al., 2017). Yet, our knowledge on how exactly changes in the biosynthesis of carotenoids in impacts leaf primary metabolism and plant growth in general remains rather fragmented. Thus, here we postulated that an enhancement of the carotenoid levels, observed in several tomato (*Solanum lycopersicum* L.) mutant lines, would significantly alter primary metabolism and growth. Accordingly, the work presented here is focused on the investigation of the role of carotenoids on the context of plant growth and leaf metabolism. To this end, a range of complementary approaches were used and thus this thesis is organized as a compilation of three independent chapters which in the first we review and present recent advances related to the improvement of photosynthesis in agricultural crops, and in the last two chapters we discuss how and to which extent mutations that alter pigments concentration affect the growth, development and production in tomato plants. In each chapter an introduction and discussion as well as details of the methods used are included. At the end, one chapter entitled "Concluding Remarks" synthesizes the main findings of this work and the main challenges and perspectives in understanding the role played by carotenoids during plant development and in the absence of stress are briefly discussed.

Chapter I - Engineering photosynthesis: progress and perspectives

Given the recognized importance of photosynthesis, as the basis of the primary productivity in Earth, in chapter I, we present an overview of the latest advances in attempts to improve photosynthetic performance in plants. We focused on the key points considered key to the enhancement of photosynthesis including Rubisco reengineering, Calvin-Benson cycle optimization, light use efficiency, the introduction of C_4 cycle in C_3 plants and the inclusion of others CO_2 concentrating mechanisms (CCMs) and provide compelling evidence that there is still room for further improvements. Finally, we conclude this chapter presenting future perspectives and possible directions on this subject.

Chapter II - Differential metabolic reprogramming in tomato HIGH PIGMENT mutants submitted to shading conditions

In this chapter, we hypothesized that the high pigments levels observed in the *hp1* and *hp2* mutants may represent an additional energy expense for these plants and that major metabolic adjustments are required to allow maintenance of successful performance of tomato plants grown under different sunlight conditions. By coupling morphological, physiological and biochemical analyses of leaves from tomato *hp* mutant plants grown under low light or high light conditions, we investigate different aspects of the influence of high pigment on plant growth and primary metabolism. Combined results indicate that *hp* mutations greatly affect production and that extensive physiological and metabolic reprogramming occurs to support greater pigment biosynthesis that are likely involved in protection against light-induced oxidative stress. In summary, complex metabolic adjustments appears to act in *hp* mutant plant not to improve photosynthetic performance *per se* but rather to afford protection associated with energy dissipation and ROS scavenging in leaves.

Chapter III - Differential leaf pigmentation in tomato culminate with a complex metabolic reprogramming without growth impacts

In chapter III, we further explored the metabolic and physiologic impacts of pigmentation-related mutations on tomatoes. To reach this goal, we investigate how the metabolic machinery of tomato adjusts itself to varying carotenoid biosynthesis and whether these adjustments are supported by clear reprogramming of photosynthetic and primary metabolism. We sought to observe the effects of mutations on well characterized tomato carotenoid mutant plants [namely *crimson* (*old gold*), *Delta carotene* (*Del*) and *tangerine* (*t*)] grown under natural fluctuation conditions by analysing photosynthetic traits, antioxidant capacity, as well as primary metabolite profiles. Taken together, our results show that changes in carotenoid biosynthesis culminated with minor, if any, impacts on vegetative growth, although carbon flux is seemingly extensively modified by changes in carotenoid biosynthesis. We further posit that metabolic adjustments are likely important to sustain

photosynthetic performance supporting the maintenance of growth and that significant phenotype plasticity would be expected under stressful conditions.

Literature cited

Aqeel-Ur-Rehman, Shaikh ZA (2009) Smart agriculture. Applications of Modern High Performance Networks 120–129

Barber J, Andersson B (1992) Too much of a good thing: light can be bad for photosynthesis. Trends in Biochemical Sciences **17**: 61–66

Carmo-Silva E, Scales JC, Madgwick PJ, Parry MAJ (2015) Optimizing Rubisco and its regulation for greater resource use efficiency. Plant, Cell and Environment **38**: 1817–1832

Carvalho RF, Aidar ST, Azevedo RA, Dodd IC, Peres LEP (2011) Enhanced transpiration rate in the high pigment 1 tomato mutant and its physiological significance. Plant Biology **13**: 546–550

Cavalier-Smith T (2006) Cell evolution and Earth history: Stasis and revolution. Philosophical Transactions of the Royal Society B: Biological Sciences **361**: 969–1006

Demmig-Adams B (1990) Carotenoids and photoprotection in plants: A role for the xanthophyll zeaxanthin. BBA - Bioenergetics **1020**: 1–24

Gifford RM, Evans LT. (1981) Photosynthesis, carbon partitioning, and yield. Annual Review of Plant Biology **32**: 485–509

Hughes J (2010) Phytochrome three-dimensional structures and functions. Biochemical Society Transactions **38**: 710–716

Jacob LW (2005) From foraging to farming: explaining the neolithic revolution. Journal of Economic Surveys **19**: 561–586

Lieberman M, Segev O, Gilboa N, Lalazar A, Levin I (2004) The tomato homolog of the gene encoding UV-damaged DNA binding protein 1 (DDB1) underlined as the gene that causes the high pigment-1 mutant phenotype. Theoretical and Applied Genetics **108**: 1574–1581

McKendry P (2002) Energy production from biomass (part 1): Overview of biomass. Bioresource Technology **83**: 37–46

Murchie EH, Niyogi KK (2011) Manipulation of Photoprotection to Improve Plant Photosynthesis. Plant Physiology **155**: 86–92

Ort DR, Merchant SS, Alric J, Barkan A, Blankenship RE, Bock R, Croce R, Hanson MR, Hibberd JM, Long SP, et al (2015) Redesigning photosynthesis to sustainably meet global food and bioenergy demand. Proceedings of the National Academy of Sciences of the United States of America **112**: 8529–8536

Papadopoulos AP, Hao X (1997) Effects of three greenhouse cover materials on tomato growth, productivity, and energy use. Scientia Horticulturae **70**: 165–178

Parry MAJ, Andralojc PJ, Scales JC, Salvucci ME, Carmo-Silva AE, Alonso H, Whitney SM (2013) Posidonia oceanica cadmium induces changes in DNA Rubisco activity and regulation as targets for crop methylation an. Journal of Experimental Botany **64**: 695–709

Sharwood RE (2017) Engineering chloroplasts to improve Rubisco catalysis: prospects for translating improvements into food and fiber crops. New Phytologist **213**: 494–510

South PF, Cavanagh AP, Liu HW, Ort DR (2019) Synthetic glycolate metabolism pathways stimulate crop growth and productivity in the field. Science **363**: 1-9

Sweetlove LJ, Nielsen J, Fernie AR (2017) Engineering central metabolism – a grand challenge for plant biologists. Plant Journal **90**: 749–763

Tilman D, Balzer C, Hill J, Befort BL (2011) Global food demand and the sustainable intensification of agriculture. Proceedings of the National Academy of Sciences of the United States of America **108**: 20260–20264

Whitney SM, Houtz RL, Alonso H (2011) Advancing our understanding and capacity to engineer nature's CO_2-sequestering enzyme, Rubisco. Plant Physiology **155**: 27–35

Yamori W, Shikanai T (2016) Physiological functions of cyclic electron transport around photosystem i in sustaining photosynthesis and plant growth. Annual Review of Plant Biology **67**: 81–106

Zhu XG, Long SP, Ort DR (2010) Improving photosynthetic efficiency for greater yield. Annual Review of Plant Biology **61**: 235–261

2. CHAPTER I:

Engineering photosynthesis: progress and perspectives

REVIEW

Engineering photosynthesis: progress and perspectives

Douglas J. Orr [1], Auderlan M. Pereira[2,3], Paula da Fonseca Pereira[2,3], Ítalo A. Pereira-Lima[2,3], Agustin Zsögön[3], Wagner L. Araújo [2,3]

[1]Lancaster Environment Centre, Lancaster University, Lancaster, LA1 4YQ, UK
[2]Max-Planck Partner Group at the Departamento de Biologia Vegetal, Universidade Federal de Viçosa, Viçosa, Minas Gerais, Brazil
[3]Departamento de Biologia Vegetal, Universidade Federal de Viçosa, Viçosa, Minas Gerais, Brazil

v1 **First published:** N/A, **N/A**: N/A (doi: N/A)
Latest published: N/A, **N/A**: N/A (doi: N/A)

Abstract

Photosynthesis is the basis of primary productivity on the planet. Crop breeding has sustained steady improvements in yield to keep pace with population growth increases. Yet these advances have not resulted from improving the photosynthetic process *per se* but rather of altering the way carbon is partitioned within the plant. Mounting evidence suggests that the rate at which crop yields can be boosted by traditional plant breeding approaches is wavering, and they may reach a "yield ceiling" in the foreseeable future. Further increases in yield will likely depend on the targeted manipulation of plant metabolism. Improving photosynthesis poses one such route, with simulations indicating it could have a significant transformative influence on enhancing crop productivity. Here, we summarize recent advances of alternative approaches for the manipulation and enhancement of photosynthesis and their possible application for crop improvement.

Open Peer Review

Referee Status: *AWAITING PEER REVIEW*

F1000 Faculty Reviews are commissioned from members of the prestigious F1000 Faculty. In order to make these reviews as comprehensive and accessible as possible, peer review takes place before publication; the referees are listed below, but their reports are not formally published.

Discuss this article

Comments (0)

Corresponding author: Wagner L. Araújo (wlaraujo@ufv.br)

Author roles: Orr DJ: Conceptualization, Writing – Original Draft Preparation, Writing – Review & Editing; **Pereira AM**: Writing – Original Draft Preparation; **da Fonseca Pereira P**: Writing – Original Draft Preparation; **Pereira-Lima ÍA**: Writing – Original Draft Preparation; **Zsögön A**: Writing – Original Draft Preparation, Writing – Review & Editing; **Araújo WL**: Conceptualization, Writing – Review & Editing

Competing interests: The authors declare that they have no competing interests.

How to cite this article: Orr DJ, Pereira AM, da Fonseca Pereira P *et al.* **Engineering photosynthesis: progress and perspectives** *F1000Research* , : (doi: $version.doi)

Grant information: This work was made possible through financial support from the Max Planck Society, the National Council for Scientific and Technological Development (CNPq-Brazil grant no. 402511/2016-6), and the Foundation for Research Assistance of the Minas Gerais State (FAPEMIG-Brazil grant no. APQ 01078-15) to WLA. We also thank the scholarships granted by the Brazilian Federal Agency for Support and Evaluation of Graduate Education (CAPES-Brazil) to AMP and IAP-L. Research fellowship granted by CNPq-Brazil (grant no. 306281/2016-3) to WLA is also gratefully acknowledged.
The funders had no role in study design, data collection and analysis, decision to publish, or preparation of the manuscript.

First published: N/A, **N/A**: N/A (doi: N/A)

Introduction

Photosynthesis consists of a series of biochemical reactions whereby plants use sunlight to reduce atmospheric CO_2 into carbohydrates, releasing O_2 as a byproduct. The first photosynthetic organisms appeared at least 2.5 billion years ago (Archean Eon) and were single-celled ocean-dwelling prokaryotes. Thus, photosynthesis was originally an aquatic-based process occurring in a strongly reducing atmosphere[1]. The transition to a terrestrial environment and to an oxidizing atmosphere subsequently shaped the photosynthetic pathway into its current form[2,3]. Plant cells contain chloroplasts, which are organelles that originated from endosymbiosis of a cyanobacteria-like organism. Chloroplasts harbor the photosynthetic machinery and confer upon plants their characteristic green color. Sunlight within the visible spectrum is captured by chlorophyll and other accessory pigments and used to energize electrons derived from a water molecule in the thylakoid membrane of the chloroplasts. High-energy electrons are then transferred to carrier molecules, which can donate them for the reduction of gaseous CO_2 to triose-phosphates in the chloroplast stroma. The enzyme responsible for the first step in CO_2 fixation is ribulose-1,5-bisphosphate carboxylase/oxygenase (Rubisco). The Calvin-Benson cycle allows for the regeneration of the ribulose-1,5-bisphosphate molecule (RuBP)[4], whereas the fixed CO_2 molecule moves on to anabolic pathways for sucrose and starch biosynthesis.

The high energetic value of sucrose and starch drove the domestication of plants to create crops, spawning the agricultural revolution and the transition from a hunter-gatherer to the current agricultural-industrial society[5]. It is thus clear that photosynthesis is a cornerstone of human civilization and, as such, the object of intense basic and applied research in the face of mounting pressure to feed an increasing population[6,7]. Decades of research have provided a detailed picture of the intricacies of the photosynthetic process and suggested potential avenues for its improvement[8]. A broad range of opportunities have been identified to improve photosynthetic efficiency; for recent detailed reviews, see 7,9–11. We now know, for instance, that owing to the complex interaction between physiological and environmental parameters photosynthetic rate does not directly extrapolate to whole plant growth rate[12]. Breeders have managed to increase yields via processes that alter carbon partitioning rather than improving photosynthesis[13]. Breeding better crops through improved photosynthesis is a long-sought goal but so far has remained unrealized because of the multiplicity of challenges involved[12]. Here, we briefly review the current state of the ongoing efforts in molecular engineering to improve photosynthesis, plant growth, and yield (Figure 1).

We start by summarizing recent efforts to optimize Rubisco performance. Rubisco is an ancient enzyme that evolved in a CO_2-rich atmosphere devoid of O_2. It is a slow (turnover rate of ~3–5 s^{-1} compared to around >100 s^{-1} for most enzymes) and error-prone enzyme (fixing O_2 instead of CO_2 in up to one-third of reactions)[14]. The unavoidable side reaction with O_2, oxygenation of RuBP, leads to the photorespiratory cycle, which "recycles" unproductive reaction products[15]. However, this recycling comes at the cost of previously fixed carbon and a further loss of chemical energy[16]. To make up for such shortcomings, plants

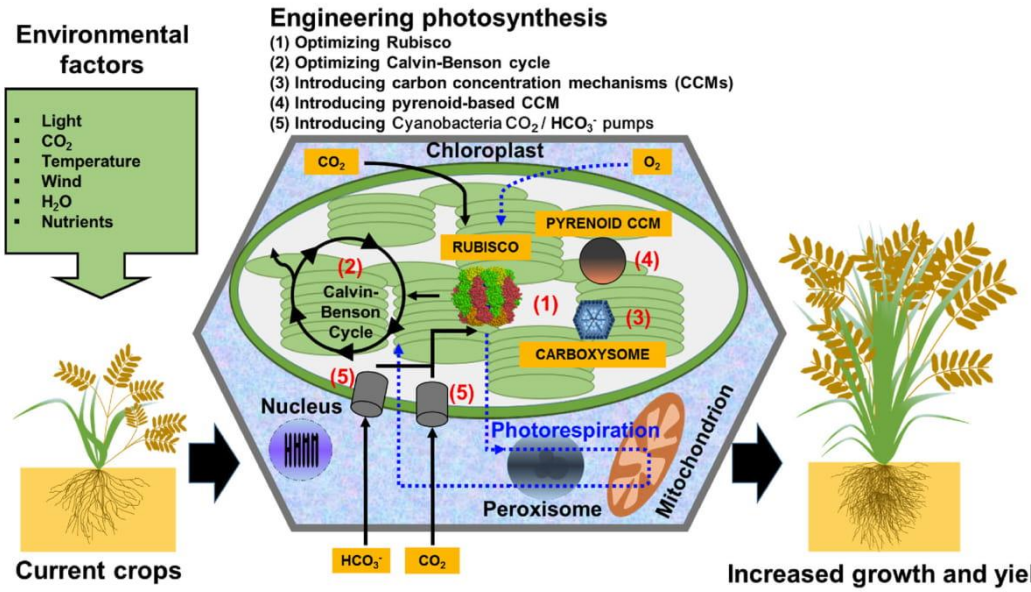

Figure 1. A number of routes are being studied to improve photosynthesis in crop plants. These include (1) improving the efficiency of the primary CO_2-fixing enzyme Rubisco, (2) optimizing elements of the Calvin-Benson cycle, (3) introducing the carboxysome-based carbon concentrating mechanism (CCM) from cyanobacteria, (4) introducing an algal pyrenoid CCM, and (5) improving the photochemical response of photosynthesis to rapid changes in light conditions. Further studies are also related to attempts to convert C_3 crops such as rice to the more efficient C_4-type photosynthesis.

generally contain large amounts of Rubisco (up to 50% of leaf total protein), which entails a large N-investment[17]. Despite the significant natural variation in Rubisco catalysis and structure, it maintains a conserved, complex, catalytic mechanism that intrinsically imparts a trade-off between an enzyme specificity for CO_2 over O_2 and its catalytic speed. Next, we synthesize recent work aimed at optimizing other enzymes of the Calvin-Benson cycle. Theoretical and experimental data suggest that under non-Rubisco-limiting conditions other enzymes in the cycle begin to limit photosynthetic rate[18]. We summarize recent progress on the manipulation of carbon concentrating mechanisms (CCMs), which are evolutionary solutions to counter Rubisco inefficiency. Well-known examples in plants include C_4 photosynthesis and crassulacean acid metabolism (CAM)[19,20]. C_4 and CAM photosynthesis are highly efficient processes[21]; however, plants using these processes are relatively restricted in number within the plant kingdom[22,23]. Exciting recent developments in efforts to introduce CCMs from non-plants are also discussed and summarized in Figure 1. We additionally emphasize the challenges and opportunities to further understand the complex interplay between photosynthesis and related metabolic processes that has limited success in the manipulation and improvement of photosynthesis.

Engineering Rubisco

The observed inefficiencies of Rubisco such as a slow CO_2-fixation rate and poor specificity for CO_2 over O_2 have made it a key engineering target to improve photosynthesis in crop plants (for reviews, see 8,17,24). Whilst there is a good understanding of the reaction mechanism[25,26], engineering efforts have yet to produce the holy grail of a "super Rubisco", as efforts to modify one aspect of its catalytic biochemistry typically come at a cost to another[8,17]. A notable discovery was that a single amino acid mutation acted as a catalytic "switch" to convert Rubisco from different *Flaveria* species from a "C_3 style" enzyme to a "C_4 style" and vice versa[27]. This clearly demonstrates the potential for manipulating the performance of Rubisco with targeted changes inferred from comparisons of natural diversity in enzyme sequence and catalysis. This has spurred a recent influx of data on the natural diversity of Rubisco in a bid to identify amino acid changes that can improve its catalysis in plants[28–36]. Insights into how Rubisco and other photosynthetic traits have co-evolved are critical to guiding kinetic characteristics for an improved crop Rubisco under differing environmental scenarios (e.g. 37,38). Rubisco screens extending outside of the plant realm have also proved highly informative. For example, the Rubisco from diatom and haptophyte micro-algae has undergone differing selection pressures that see its kinetic properties diverge from the canonical trade-off between catalytic rate and affinity for CO_2[39,40], providing possible new areas of exploration for improving Rubisco efficiency[41].

A key challenge in engineering Rubisco in plants is that it is a hefty 550 kDa hexadecameric complex comprising eight large subunits (*ca.* 52 kDa each) and eight small subunits (*ca.* 13 to 15 kDa). It is produced through an exquisite synthesis and assembly process that is dependent on a number of nucleus- and chloroplast-encoded components[42]. Typically, research has focused on the chloroplast-encoded large subunits, which contain the catalytic sites and can be routinely manipulated in tobacco for functional genomic studies[24,43]. More recent reports have highlighted the impact on catalysis of manipulating the small subunits[44–47]. The nuclear-encoded small subunit gene family (RbcS) is therefore a growing target for engineering, as nuclear transformation is already established in many species compared to the relatively few species amenable to chloroplast transformation[42,48]. An alternative approach to altering the extant Rubisco in a crop species is to replace it with better-performing natural variants, although this is subject to similar technical limitations. Introduction of foreign Rubisco is typically hampered by the complicated assembly requirements of the enzyme in the chloroplast (see 49), though important advances have been made in co-engineering introduced Rubisco alongside assembly chaperones[50]. Besides efforts to introduce a cyanobacterial CCM into higher plants (see below), the Rubisco from *Synechococcus elongatus* has now been successfully introduced into tobacco[51] and can support growth at elevated CO_2[52]. Whilst supporting much higher catalytic rates than higher plant Rubisco, the Rubisco from cyanobacteria has lower CO_2 affinity and specificity for CO_2 over O_2. Thus, for cyanobacteria Rubisco to support plant growth at ambient CO_2 levels, co-engineering of a functional CCM is required[53].

Calvin-Benson cycle optimization

It has long been recognized that other enzymes in the Calvin-Benson cycle represent viable targets to accelerate carbon fixation in plants (reviewed in 9,18,54–56). Recently, efforts have built on prior success in overexpressing SBPase (sedoheptulose-1,7-bisphosphatase) to improve growth in tobacco and rice[55,57,58]. These efforts have now expanded to include other Calvin-Benson enzymes in a combinatorial manner to avoid creating new bottlenecks in different parts of the cycle[59,60]. Increases in plant biomass have also been obtained by jointly manipulating genes in the Calvin-Benson cycle and the photorespiratory pathway[60]. An alternative approach has been to avert the CO_2 and energy costs of photorespiration by introducing synthetic "photorespiratory bypass" pathways in the chloroplast that direct CO_2 release in the proximity of Rubisco[61–64]. The potential benefits and caveats of the differing bypass strategies are reviewed in 65,66.

In addition to the overexpression of native enzymes (Figure 1), a number of studies have also shown effects through the expression of foreign membrane transporter proteins in both model[59,67–69] and crop species such as soybean and rice[70,71]. These genes are derived from cyanobacteria and include the frequently studied but functionally unknown membrane transporter protein IctB[72]. Introducing IctB has not always improved crop growth: for example, in one case changes were noted in photosynthetic rate without an increase in biomass[71]. In contrast, IctB expression improved growth in key crop species such as wheat[73] in the glasshouse and soybean in the field[70]. Importantly, extended field testing under future environmental scenarios through free-air CO_2 enrichment (FACE) experiments indicated that IctB no longer provided a growth benefit[74]. This finding underscores the frequent discontinuity in crop yield predictions between glasshouse and field trials and the importance of FACE field studies for screening the suitability of natural and engineered crops for future climates.

Optimizing response to changes in light-use efficiency

Major losses of energy conversion during plant biomass formation occur during light absorption and the photochemical reactions[75]. Dramatic increases in tobacco growth rate in the field were obtained recently by improving the rate of relaxation of photoprotection (non-photochemical quenching, NPQ). NPQ is the process by which plants dissipate excess light as heat when they receive more than they are capable of using[76]. Modeling suggested this as an area where there is room for improvement[77,78]. Combinations of genes involved in photoprotection were transformed into tobacco and those that accelerated the relaxation of NPQ increased the rate of biomass production by as much as 20% in glasshouse trials and around 15% in duplicated field trials[76]. The modifications involved introducing multiple genes expressing key components of the xanthophyll cycle and the PsbS subunit of photosystem-II. This combination allowed the plants to more quickly adapt to fluctuating light, turning off photoprotection and using light for photosynthesis rather than continuing to dissipate it as heat after a decrease in light level. The conservation of NPQ across plants suggests this approach may also serve to improve the growth of other crops. However, the mechanisms allowing plant cells to cope with the excess energy, such as NPQ, tend to decrease the overall efficiency of energy storage, since surface cells exposed to the light dissipate much of the available energy whereas cells in the lower layers remain light limited[79]. Thus, the temptation to increase the capacity to process the influx of energy by the photosynthetic apparatus is a challenge that must be pursued to ameliorate energy losses during plant photosynthesis (reviewed in 79). Increasing light energy capture might also be feasible by incorporating the bacteriochlorophylls found in many anoxygenic photosynthetic organisms into one of the photosystems in plants with the aim of extending the light absorption spectrum by plants to the far red region out to ~1,100 nm[79].

Changes in the antenna size of the photosystems have also been suggested as a route that could enhance solar conversion efficiency while reducing NPQ. This assumption is based on the fact that the antennae trap more light than can be used for photochemistry. Based on this, the theory is that in plants with a reduced number of light-harvesting pigments (e.g. chlorophyll and carotenoids) per photosystem, solar energy conversion efficiency could be significantly enhanced[11,80–82]. Changes in the leaf optical properties would alleviate over-absorption and mitigate efficiency losses associated with wasteful dissipation of sunlight by the upper canopy. Furthermore, they could bring about enhancements of photosynthetic productivity due to greater transmittance of light to lower layers, thus improving canopy light distribution and canopy photosynthesis. This truncated light-harvesting antenna (TLA) concept[80,81] has been successfully applied in microalgae[83–85] and cyanobacteria[86]. Recent work has shown that TLA enhances both photosynthesis and plant canopy biomass accumulation under high-density cultivation conditions in both tobacco[82] and rice[87]. This approach presents intrinsic practical limitations and challenges[81], but ongoing research suggests that expanded efforts could ultimately optimize this exciting biotechnological process.

Synthetic biology for CO_2 fixation in non-plants

Synthetic photosynthesis has made exciting progress recently via the incorporation of a non-native Calvin-Benson-like carbon assimilation in *Escherichia coli*. The highlight was the production of a bacterium that is capable of making sugars and other life-preserving metabolites from atmospheric CO_2[88,89]. Although at this stage both energy and reducing power are required through the oxidation of an external organic acid in an isolated metabolic module and thus no net carbon gain is achieved, this discovery clearly proves the potential of synthetic biology to optimize pathways of biotechnological significance and may even lead to new avenues for optimizing CO_2 fixation in plants[89]. Along such lines is the successful development of a synthetic carbon fixation pathway that functions efficiently *in vitro* but faces significant challenges for it to be compatible in a biological context[90].

Introducing the C_4 cycle in C_3 crops

C_4 photosynthesis has evolved independently of C_3 photosynthesis in several angiosperm families during the last 25 million years in at least 66 independent events[91]. Despite the frequency of these events, the evolution of C_4 photosynthesis is not distributed evenly in the plant kingdom[92]. This multiple parallel evolution appears to have occurred as an adaptive response to low atmospheric CO_2 concentrations and high temperature[22]. The transition from C_3 to C_4 plants requires the evolution of both morphological and physiological traits. Among these, the differentiation of photosynthetically active vascular bundle sheath cells, modification in the biochemistry of several enzymes, and increased intercellular and intracellular transport of metabolites are of pivotal significance. This makes the evolution of such a complex trait system in one single step highly unlikely[93]. The first evidence of evolutionary intermediate C_3–C_4 forms was reported in the 1970s[94], and this spurred intensive efforts to understand the mechanistic bases of the transition from C_3 to C_4.

A better understanding of the initial events that occurred during the C_3 evolution to C_3–C_4 intermediates and then to C_4 plants can contribute to increasing photosynthetic efficiency in C_3 plants. Whilst C_4 photosynthesis requires considerable additional ATP, the plants benefit from enhanced biomass production and improvements in nitrogen and water use efficiencies. Using complementary approaches, including genome and transcriptome analyses, the international C_4 rice consortium is working toward introducing the C_4 mechanism into rice[95]. This research initiative has already produced exciting results, including the identification of metabolite transporters and transcription factors[95,96]. Although the genes identified are potentially useful for engineering C_4 rice, clearly further investigation is required. Additional examination of temporal, spatial, and environmental dynamics spanning C_3 through C_3–C_4 intermediacy and true C_4 species will no doubt be highly informative for identifying useful genes and regulatory components (e.g. 97,98).

Recent efforts have expanded the number of genera studied beyond *Flaveria* species to include *Cleome* and *Moricandia*, two close relatives of the model C_3 *Arabidopsis*, which both contain intermediate as well as true C_4 species[92,99]. This provides a

powerful opportunity to accelerate advances through comparison with the large amount of data already available for *Arabidopsis* in order to find the minimal genetic basis of C_4 photosynthesis. This strategy has the growing potential to promote substantial increments in the yield of C_3 crops usually cultivated in dry and hot areas[95]. Importantly, at least some of the technical difficulties associated with separately isolating pure bundle sheath and mesophyll cells from C_3 plants have been overcome in *Arabidopsis*[100]. A very large-scale analysis of the bundle sheath translatome in *Arabidopsis* demonstrated its high similarity with the translatome in the root pericycle cells[100]. This study not only provides the foundation to enhance our understanding of the evolutionary function of bundle sheath cells in C_3 plants but also indicates that a highly similar and conserved regulatory network might sustain bundle sheath and pericycle cell functionality in *Arabidopsis thaliana.* Although several open questions remain, it seems clear that these types of studies are likely to be key to understanding the genetic triggers needed to re-organize the anatomy, gene expression, and biochemistry within C_4 plants, possibly paving the way toward producing C_4 rice.

Whilst perhaps less advanced than the efforts to understand and engineer C_4 photosynthesis, a number of groups are working to better understand the key elements required for CAM photosynthesis[101,102]. CAM plants are typically highly efficient in their use of water, and engineering of CAM into food or bioenergy crops may prove most beneficial by improving crop water use efficiency and expanding the land area capable of supporting agriculture[103]. CAM species may also serve as a suitable source of high-temperature-adapted enzymes of potential application in photosynthetic engineering[104].

Introducing non-plant CCMs into C_3 plants

One approach to improving plant photosynthesis is using engineering to implement CCMs from other photosynthetic organisms such as cyanobacteria or algae. While components of the CCM in cyanobacteria and algae can differ, both systems function to create a high-CO_2 environment around Rubisco to overcome its catalytic shortcomings. Among the core components of CCMs are inorganic carbon transporters and the co-localization of carbonic anhydrase (catalyzing the interconversion of HCO_3^- and CO_2) around Rubisco to maintain high CO_2 levels. In some instances, this association is contained within a protein micro-compartment to limit CO_2 escape and ensure high HCO_3^- levels can be sustained in the cytosol.

Cyanobacterial CCM

Amongst the CCMs currently being engineered into plants, the cyanobacterial carboxysome-based system has made the most striking progress in recent years. With a stronger—but still incomplete—understanding of the construction of this bacterial microcompartment (for in-depth reviews, see 72,105–109), significant progress has been made in assembling partial carboxysomes in higher plants using tobacco as a model system[110]. Lin and colleagues[111] demonstrated the assembly of various complex structures by expressing as few as three β-carboxysome proteins. As mentioned above, parallel work on introducing a cyanobacterial Rubisco into tobacco was also successful[51,52], with plants expressing cyanobacteria Rubisco and either the chaperone RbcX or the carboxysomal CcmM35 protein viable at elevated CO_2. These are key advances to build upon through the addition of further components to assemble a fully functional carboxysome shell[53], and combining these to localize Rubisco inside the carboxysome will be a critical next step toward functionality. The internal components such as CcmM35 are thought to be important for the true icosahedral structure to be formed[111,112]. The ability to assemble bacterial microcompartments also has implications beyond crop productivity[113].

An important consideration for introducing a full cyanobacterial CCM into higher plants is creating a compatible HCO_3^-/CO_2 environment by concentrating CO_2 inside the carboxysome shell, removing stromal carbonic anhydrase, and introducing HCO_3^- pumps to increase the bicarbonate concentration in the stroma[53,112,114]. Progress has been made in attempting to introduce transporters into tobacco[67,115], and issues related to correct localization are being targeted through a better understanding of transit peptides (e.g. 115,116). Recent progress in other bacterial microcompartments beyond the cyanobacterial carboxysome are also providing key insights for targeting protein localization and the assembly of these complex structures (reviewed in 110).

Pyrenoids

Although engineering an algal pyrenoid-based CCM into higher plants is less developed than cyanobacteria CCMs[112], there have recently been a number of key discoveries related to pyrenoid structure and function in the model *Chlamydomonas reinhardtii* (see 105,109,115,116). Discoveries such as the highly disordered linker protein essential pyrenoid component 1 (EPYC1) that pulls Rubisco together[108] and that a loop structure on the Rubisco small subunit is necessary for pyrenoid formation[117] supply targets for engineering in plants. For example, mutagenesis of this loop region has shown its modification has no effects on Rubisco catalysis in *Arabidopsis*[45]. Recent advances in the availability of a mutant Chlamydomonas library for functional studies[118] will likely accelerate advances in understanding, and engineering, algal pyrenoids. Increasing data on the CCM of other non-green micro-algae may also help better understand pyrenoid function and structural diversity[40,119].

Future perspectives and directions

Conventional crop breeding has thus far been sufficient to avert the dire Malthusian predictions of food shortage for a growing human population. Most projections suggest that novel yield-enhancing solutions are needed to avoid global crop production reaching a plateau. Genetic manipulation has been used to successfully engineer simple traits, such as insect and weed resistance. More refined molecular tinkering holds the promise of spectacular gains if fundamental pathways are targeted. Photosynthesis is one such pathway.

Synthetic biology is making large steps in engineering alternate CCM mechanisms into higher plants, in addition to efforts in manipulating elements of the Calvin-Benson cycle already present. Although mesophyll conductance to CO_2 had been a relatively overlooked limiting factor until recently, it is now considered a promising potential target for increasing photosynthesis[120]. It seems clear that expanded research efforts are

currently required to build upon many of the technologies described above by, for example, enhancing our understanding of CAM metabolism and introducing alternative non-plant CCMs into C_3 plants. Overcoming these challenges will require sustained investments in long-term research programs, with some of these research areas currently being advanced through large-scale, privately funded projects.

Ultimately, in the case of C_4 rice, necessity for development in a C_4 species as well as sufficiency for engineering C_4 rice will need to be considered when determining gene function. Existing candidate regulators are currently being functionally validated, and this is ongoing: knockdown experiments in maize and setaria are examining necessity, while overexpression in rice is being used to scrutinize sufficiency. Future advances in engineering C_4 rice will need to involve integrated analysis of these experiments together with further comprehension of the related gene regulatory networks. We posit that the successful integration of these different characteristics, as discussed above, coupled with the identification of the key regulators of C_4 morphoanatomical pattern and the development of a strategy of how the C_3 plant could be genetically altered allowing both the introduction and the establishment of the C_4 pathway should be a significant breakthrough in the field of synthetic biology. Recent advances and ongoing incremental findings suggest that improved crop photosynthesis could assist towards feeding a growing population in the near future.

Competing interests

The authors declare that they have no competing interests.

Grant information

This work was made possible through financial support from the Max Planck Society, the National Council for Scientific and Technological Development (CNPq-Brazil grant no. 402511/2016-6), and the Foundation for Research Assistance of the Minas Gerais State (FAPEMIG-Brazil grant no. APQ 01078-15) to WLA. We also thank the scholarships granted by the Brazilian Federal Agency for Support and Evaluation of Graduate Education (CAPES-Brazil) to AMP and IAP-L. Research fellowship granted by CNPq-Brazil (grant no. 306281/2016-3) to WLA is also gratefully acknowledged.

The funders had no role in study design, data collection and analysis, decision to publish, or preparation of the manuscript.

Acknowledgements

DJO acknowledges support through a sub-contract from the University of Illinois as part of the Bill and Melinda Gates Foundation award "RIPE: Realizing Increases in Photosynthetic Efficiency". We also thank the reviewers for their suggestions and comments which helped improve the manuscript and apologize to our colleagues whose work could not be cited due to space limitations.

References

F1000 recommended

1. Niklas KJ: **Plant Evolution.** 1st ed. Chicago, USA: University of Chicago Press, 2016; 560.
Reference Source

2. Hohmann-Marriott MF, Blankenship RE: **Evolution of photosynthesis.** *Annu Rev Plant Biol.* 2011; **62**: 515–48.
PubMed Abstract | Publisher Full Text

3. Nelson N, Ben-Shem A: **The complex architecture of oxygenic photosynthesis.** *Nat Rev Mol Cell Biol.* 2004; **5**(12): 971–82.
PubMed Abstract | Publisher Full Text

4. Martin W, Scheibe R, Schnarrenberger C: **The Calvin Cycle and its regulation.** In Springer Netherlands 2000; 9–51.
Publisher Full Text

5. Harlan JR: **Crops and man.** American Society of Agronomy. 1975.
Reference Source

6. Evans LT: **Feeding the ten billion: plants and population growth.** Cambridge, UK: Cambridge University Press, 1998.
Reference Source

7. F Ort DR, Merchant SS, Alric J, *et al.*: **Redesigning photosynthesis to sustainably meet global food and bioenergy demand.** *Proc Natl Acad Sci U S A.* 2015; **112**(28): 8529–36.
PubMed Abstract | Publisher Full Text | Free Full Text | F1000 Recommendation

8. Whitney SM, Houtz RL, Alonso H: **Advancing our understanding and capacity to engineer nature's CO_2-sequestering enzyme, Rubisco.** *Plant Physiol.* 2011; **155**(1): 27–35.
PubMed Abstract | Publisher Full Text | Free Full Text

9. Raines CA: **Increasing photosynthetic carbon assimilation in C_3 plants to improve crop yield: current and future strategies.** *Plant Physiol.* 2011; **155**(1): 36–42.
PubMed Abstract | Publisher Full Text | Free Full Text

10. Maurino VG, Weber AP: **Engineering photosynthesis in plants and synthetic microorganisms.** *J Exp Bot.* 2013; **64**(3): 743–51.
PubMed Abstract | Publisher Full Text

11. F Long SP, Marshall-Colon A, Zhu X: **Meeting the global food demand of the future by engineering crop photosynthesis and yield potential.** *Cell.* 2015; **161**(1): 56–66.
PubMed Abstract | Publisher Full Text | F1000 Recommendation

12. Evans JR: **Improving photosynthesis.** *Plant Physiol.* 2013; **162**(4): 1780–93.
PubMed Abstract | Publisher Full Text | Free Full Text

13. Fischer A, Byerlee D, Edmeades G: **Crop yields and global food security: will yield increase continue to feed the world?** Canberra, Australia: Australian Centre for International Agricultural Research, 2014; 634.
Reference Source

14. F Tcherkez GG, Farquhar GD, Andrews TJ: **Despite slow catalysis and confused substrate specificity, all ribulose bisphosphate carboxylases may be nearly perfectly optimized.** *Proc Natl Acad Sci U S A.* 2006; **103**(19): 7246–51.
PubMed Abstract | Publisher Full Text | Free Full Text | F1000 Recommendation

15. Timm S, Florian A, Fernie AR, *et al.*: **The regulatory interplay between photorespiration and photosynthesis.** *J Exp Bot.* 2016; **67**(10): 2923–9.
PubMed Abstract | Publisher Full Text

16. Betti M, Bauwe H, Busch FA, *et al.*: **Manipulating photorespiration to increase plant productivity: recent advances and perspectives for crop improvement.** *J Exp Bot.* 2016; **67**(10): 2977–88.
PubMed Abstract | Publisher Full Text

17. F Carmo-Silva E, Scales JC, Madgwick PJ, *et al.*: **Optimizing Rubisco and its regulation for greater resource use efficiency.** *Plant Cell Environ.* 2015; **38**(9): 1817–32.
PubMed Abstract | Publisher Full Text | F1000 Recommendation

18. Raines CA: **The Calvin cycle revisited.** *Photosynth Res.* 2003; **75**(1): 1–10.
PubMed Abstract | Publisher Full Text

19. Bräutigam A, Schlüter U, Eisenhut M, *et al.*: **On the Evolutionary Origin of CAM Photosynthesis.** *Plant Physiol.* 2017; **174**(2): 473–7.
PubMed Abstract | Publisher Full Text | Free Full Text

20. Winter K, Holtum JA, Smith JA: **Crassulacean acid metabolism: a continuous or discrete trait?** *New Phytol.* 2015; **208**(1): 73–8.
PubMed Abstract | Publisher Full Text

21. F Zhu X, Long SP, Ort DR: **What is the maximum efficiency with which photosynthesis can convert solar energy into biomass?** *Curr Opin Biotechnol.* 2008; **19**(2): 153–9.
PubMed Abstract | Publisher Full Text | F1000 Recommendation

22. Sage RF: **A portrait of the C_4 photosynthetic family on the 50th anniversary of its discovery: species number, evolutionary lineages, and Hall of Fame.** *J Exp Bot.* 2017; **68**(2): 4039–56.
PubMed Abstract | Publisher Full Text

23. Huang P, Studer AJ, Schnable JC, *et al.*: **Cross species selection scans identify components of C_4 photosynthesis in the grasses.** *J Exp Bot.* 2017; **68**(2): 127–35.
PubMed Abstract | Publisher Full Text | Free Full Text

24. Sharwood RE: **Engineering chloroplasts to improve Rubisco catalysis: prospects for translating improvements into food and fiber crops.** *New Phytol.* 2017; **213**(2): 494–510.
PubMed Abstract | Publisher Full Text

25. Tcherkez G: **Modelling the reaction mechanism of ribulose-1,5-bisphosphate carboxylase/oxygenase and consequences for kinetic parameters.** *Plant Cell Environ.* 2013; **36**(9): 1586–96.
PubMed Abstract | Publisher Full Text

26. Andersson I: **Catalysis and regulation in Rubisco.** *J Exp Bot.* 2008; **59**(7): 1555–68.
PubMed Abstract | Publisher Full Text

27. Whitney SM, Sharwood RE, Orr D, *et al.*: **Isoleucine 309 acts as a C_4 catalytic switch that increases ribulose-1,5-bisphosphate carboxylase/oxygenase (rubisco) carboxylation rate in *Flaveria*.** *Proc Natl Acad Sci USA.* 2011; **108**(35): 14688–93.
PubMed Abstract | Publisher Full Text | Free Full Text

28. F Sharwood RE, Ghannoum O, Kapralov MV, *et al.*: **Temperature responses of Rubisco from Paniceae grasses provide opportunities for improving C3 photosynthesis.** *Nat Plants.* 2016; **2**: 16186.
PubMed Abstract | Publisher Full Text | F1000 Recommendation

29. Perdomo JA, Cavanagh AP, Kubien DS, *et al.*: **Temperature dependence of *in vitro* Rubisco kinetics in species of Flaveria with different photosynthetic mechanisms.** *Photosynth Res.* 2015; **124**(1): 67–75.
PubMed Abstract | Publisher Full Text

30. Orr DJ, Alcântara A, Kapralov MV, *et al.*: **Surveying Rubisco Diversity and Temperature Response to Improve Crop Photosynthetic Efficiency.** *Plant Physiol.* 2016; **172**(2): 707–17.
PubMed Abstract | Publisher Full Text | Free Full Text

31. Hermida-Carrera C, Kapralov MV, Galmés J: **Rubisco Catalytic Properties and Temperature Response in Crops.** *Plant Physiol.* 2016; **171**(4): 2549–61.
PubMed Abstract | Publisher Full Text | Free Full Text

32. Galmés J, Kapralov MV, Andralojc PJ, *et al.*: **Expanding knowledge of the Rubisco kinetics variability in plant species: environmental and evolutionary trends.** *Plant Cell Environ.* 2014; **37**(9): 1989–2001.
PubMed Abstract | Publisher Full Text

33. Galmés J, Medrano H, Flexas J: **Acclimation of Rubisco specificity factor to drought in tobacco: discrepancies between *in vitro* and *in vivo* estimations.** *J Exp Bot.* 2006; **57**(14): 3659–67.
PubMed Abstract | Publisher Full Text

34. Galmés J, Andralojc PJ, Kapralov MV, *et al.*: **Environmentally driven evolution of Rubisco and improved photosynthesis and growth within the C_3 genus *Limonium* (Plumbaginaceae).** *New Phytol.* 2014; **203**(3): 989–99.
PubMed Abstract | Publisher Full Text

35. Galmés J, Kapralov MV, Copolovici LO, *et al.*: **Temperature responses of the Rubisco maximum carboxylase activity across domains of life: phylogenetic signals, trade-offs, and importance for carbon gain.** *Photosynth Res.* 2015; **123**(2): 183–201.
PubMed Abstract | Publisher Full Text

36. Prins A, Orr DJ, Andralojc PJ, *et al.*: **Rubisco catalytic properties of wild and domesticated relatives provide scope for improving wheat photosynthesis.** *J Exp Bot.* 2016; **67**(6): 1827–38.
PubMed Abstract | Publisher Full Text | Free Full Text

37. Galmés J, Ribas-Carbó M, Medrano H, *et al.*: **Rubisco activity in Mediterranean species is regulated by the chloroplastic CO_2 concentration under water stress.** *J Exp Bot.* 2011; **62**(2): 653–65.
PubMed Abstract | Publisher Full Text | Free Full Text

38. Galmés J, Molins A, Flexas J, *et al.*: **Coordination between leaf CO_2 diffusion and Rubisco properties allows maximizing photosynthetic efficiency in *Limonium* species.** *Plant Cell Environ.* 2017; **40**(10): 2081–2094.
PubMed Abstract | Publisher Full Text

39. F Young JN, Heureux AM, Sharwood RE, *et al.*: **Large variation in the Rubisco kinetics of diatoms reveals diversity among their carbon-concentrating mechanisms.** *J Exp Bot.* 2016; **67**(11): 3445–56.
PubMed Abstract | Publisher Full Text | Free Full Text | F1000 Recommendation

40. Heureux AMC, Young JN, Whitney SM, *et al.*: **The role of Rubisco kinetics and pyrenoid morphology in shaping the CCM of haptophyte microalgae.** *J Exp Bot.* 2017; **68**(14): 3959–3969.
PubMed Abstract | Publisher Full Text

41. Hanson DT: **Breaking the rules of Rubisco catalysis.** *J Exp Bot.* 2016; **67**(11): 3180–2.
PubMed Abstract | Publisher Full Text | Free Full Text

42. Maliga P, Bock R: **Plastid biotechnology: food, fuel, and medicine for the 21st century.** *Plant Physiol.* 2011; **155**(4): 1501–10.
PubMed Abstract | Publisher Full Text | Free Full Text

43. Whitney SM, Sharwood RE: **Construction of a tobacco master line to improve Rubisco engineering in chloroplasts.** *J Exp Bot.* 2008; **59**(7): 1909–21.
PubMed Abstract | Publisher Full Text

44. Ishikawa C, Hatanaka T, Misoo S, *et al.*: **Functional incorporation of sorghum small subunit increases the catalytic turnover rate of Rubisco in transgenic rice.** *Plant Physiol.* 2011; **156**(3): 1603–11.
PubMed Abstract | Publisher Full Text | Free Full Text

45. Atkinson N, Leitão N, Orr DJ, *et al.*: **Rubisco small subunits from the unicellular green alga *Chlamydomonas* complement Rubisco-deficient mutants of Arabidopsis.** *New Phytol.* 2017; **214**(2): 655–67.
PubMed Abstract | Publisher Full Text | Free Full Text

46. Morita K, Hatanaka T, Misoo S, *et al.*: **Unusual small subunit that is not expressed in photosynthetic cells alters the catalytic properties of rubisco in rice.** *Plant Physiol.* 2014; **164**(1): 69–79.
PubMed Abstract | Publisher Full Text | Free Full Text

47. F Laterre R, Pottier M, Remacle C, *et al.*: **Photosynthetic Trichomes Contain a Specific Rubisco with a Modified pH-Dependent Activity.** *Plant Physiol.* 2017; **173**(4): 2110–20.
PubMed Abstract | Publisher Full Text | Free Full Text | F1000 Recommendation

48. Bock R: **Engineering plastid genomes: methods, tools, and applications in basic research and biotechnology.** *Annu Rev Plant Biol.* 2015; **66**: 211–41.
PubMed Abstract | Publisher Full Text

49. Bracher A, Whitney SM, Hartl FU, *et al.*: **Biogenesis and Metabolic Maintenance of Rubisco.** *Annu Rev Plant Biol.* 2017; **68**: 29–60.
PubMed Abstract | Publisher Full Text

50. Whitney SM, Birch R, Kelso C, *et al.*: **Improving recombinant Rubisco biogenesis, plant photosynthesis and growth by coexpressing its ancillary RAF1 chaperone.** *Proc Natl Acad Sci USA.* 2015; **112**(11): 3564–9.
PubMed Abstract | Publisher Full Text | Free Full Text

51. Lin MT, Occhialini A, Andralojc PJ, *et al.*: **A faster Rubisco with potential to increase photosynthesis in crops.** *Nature.* 2014; **513**(7519): 547–50.
PubMed Abstract | Publisher Full Text | Free Full Text

52. Occhialini A, Lin MT, Andralojc PJ, *et al.*: **Transgenic tobacco plants with improved cyanobacterial Rubisco expression but no extra assembly factors grow at near wild-type rates if provided with elevated CO_2.** *Plant J.* 2016; **85**(1): 148–60.
PubMed Abstract | Publisher Full Text | Free Full Text

53. Price GD, Howitt SM: **Plant science: Towards turbocharged photosynthesis.** *Nature.* 2014; **513**(7519): 497–8.
PubMed Abstract | Publisher Full Text

54. Singh J, Pandey P, James D, *et al.*: **Enhancing C3 photosynthesis: an outlook on feasible interventions for crop improvement.** *Plant Biotechnol J.* 2014; **12**(9): 1217–30.
PubMed Abstract | Publisher Full Text

55. Feng L, Wang K, Li Y, *et al.*: **Overexpression of SBPase enhances photosynthesis against high temperature stress in transgenic rice plants.** *Plant Cell Rep.* 2007; **26**(9): 1635–46.
PubMed Abstract | Publisher Full Text

56. Ainsworth EA, Yendrek CR, Skoneczka JA, *et al.*: **Accelerating yield potential in soybean: potential targets for biotechnological improvement.** *Plant Cell Environ.* 2012; **35**(1): 38–52.
PubMed Abstract | Publisher Full Text

57. F Lefebvre S, Lawson T, Zakhleniuk OV, *et al.*: **Increased sedoheptulose-1,7-bisphosphatase activity in transgenic tobacco plants stimulates photosynthesis and growth from an early stage in development.** *Plant Physiol.* 2005; **138**(1): 451–60.
PubMed Abstract | Publisher Full Text | Free Full Text | F1000 Recommendation

58. Rosenthal DM, Locke AM, Khozaei M, *et al.*: **Over-expressing the C_3 photosynthesis cycle enzyme Sedoheptulose-1-7 Bisphosphatase improves photosynthetic carbon gain and yield under fully open air CO_2 fumigation (FACE).** *BMC Plant Biol.* 2011; **11**: 123.
PubMed Abstract | Publisher Full Text | Free Full Text

59. F Simkin AJ, McAusland L, Headland LR, *et al.*: **Multigene manipulation of photosynthetic carbon assimilation increases CO2 fixation and biomass yield in tobacco.** *J Exp Bot.* 2015; **66**(13): 4075–90.
PubMed Abstract | Publisher Full Text | Free Full Text | F1000 Recommendation

60. Simkin AJ, Lopez-Calcagno PE, Davey PA, *et al.*: **Simultaneous stimulation of sedoheptulose 1,7-bisphosphatase, fructose 1,6-bisphophate aldolase and the photorespiratory glycine decarboxylase-H protein increases CO_2 assimilation, vegetative biomass and seed yield in Arabidopsis.** *Plant Biotechnol J.* 2017; **15**(7): 805–16.
PubMed Abstract | Publisher Full Text | Free Full Text

61. Maier A, Fahnenstich H, von Caemmerer S, *et al.*: **Transgenic Introduction of**

a Glycolate Oxidative Cycle into *A. thaliana* Chloroplasts Leads to Growth Improvement. *Front Plant Sci.* 2012; **3**: 38.
PubMed Abstract | Publisher Full Text | Free Full Text

62. F Kebeish R, Niessen M, Thiruveedhi K, *et al.*: **Chloroplastic photorespiratory bypass increases photosynthesis and biomass production in *Arabidopsis thaliana*.** *Nat Biotechnol.* 2007; **25**(5): 593–9.
PubMed Abstract | Publisher Full Text | F1000 Recommendation

63. Nölke G, Houdelet M, Kreuzaler F, *et al.*: **The expression of a recombinant glycolate dehydrogenase polyprotein in potato (*Solanum tuberosum*) plastids strongly enhances photosynthesis and tuber yield.** *Plant Biotechnol J.* 2014; **12**(6): 734–42.
PubMed Abstract | Publisher Full Text

64. F South PF, Walker BJ, Cavanagh AP, *et al.*: **Bile Acid Sodium Symporter BASS6 Can Transport Glycolate and Is Involved in Photorespiratory Metabolism in *Arabidopsis thaliana*.** *Plant Cell.* 2017; **29**(4): 808–23.
PubMed Abstract | Publisher Full Text | Free Full Text | F1000 Recommendation

65. Maurino VG, Peterhansel C: **Photorespiration: current status and approaches for metabolic engineering.** *Curr Opin Plant Biol.* 2010; **13**(3): 249–56.
PubMed Abstract | Publisher Full Text

66. Xin CP, Tholen D, Devloo V, *et al.*: **The benefits of photorespiratory bypasses: how can they work?** *Plant Physiol.* 2015; **167**(2): 574–85.
PubMed Abstract | Publisher Full Text | Free Full Text

67. Pengelly JJ, Förster B, von Caemmerer S, *et al.*: **Transplastomic integration of a cyanobacterial bicarbonate transporter into tobacco chloroplasts.** *J Exp Bot.* 2014; **65**(12): 3071–80.
PubMed Abstract | Publisher Full Text | Free Full Text

68. F Lieman-Hurwitz J, Rachmilevitch S, Mittler R, *et al.*: **Enhanced photosynthesis and growth of transgenic plants that express *ictB*, a gene involved in HCO_3^- accumulation in cyanobacteria.** *Plant Biotechnol J.* 2003; **1**(1): 43–50.
PubMed Abstract | Publisher Full Text | F1000 Recommendation

69. F Ogawa T, Tamoi M, Kimura A, *et al.*: **Enhancement of photosynthetic capacity in *Euglena gracilis* by expression of cyanobacterial fructose-1,6-/sedoheptulose-1,7-bisphosphatase leads to increases in biomass and wax ester production.** *Biotechnol Biofuels.* 2015; **8**: 80.
PubMed Abstract | Publisher Full Text | Free Full Text | F1000 Recommendation

70. Hay WT, Bihmidine S, Mutlu N, *et al.*: **Enhancing soybean photosynthetic CO_2 assimilation using a cyanobacterial membrane protein, *ictB*.** *J Plant Physiol.* 2017; **212**: 58–68.
PubMed Abstract | Publisher Full Text

71. Gong HY, Li Y, Fang G, *et al.*: **Transgenic Rice Expressing *Ictb* and *FBP*/Sbpase Derived from Cyanobacteria Exhibits Enhanced Photosynthesis and Mesophyll Conductance to CO_2.** *PLoS One.* 2015; **10**(10): e0140928.
PubMed Abstract | Publisher Full Text | Free Full Text

72. Long BM, Rae BD, Rolland V, *et al.*: **Cyanobacterial CO_2-concentrating mechanism components: function and prospects for plant metabolic engineering.** *Curr Opin Plant Biol.* 2016; **31**: 1–8.
PubMed Abstract | Publisher Full Text

73. Driever SM, Simkin AJ, Alotaibi S, *et al.*: **Increased SBPase activity improves photosynthesis and grain yield in wheat grown in greenhouse conditions.** *Philos Trans R Soc Lond B Biol Sci.* 2017; **372**(1730): pii: 20160384.
PubMed Abstract | Publisher Full Text | Free Full Text

74. Köhler IH, Ruiz-Vera UM, VanLoocke A, *et al.*: **Expression of cyanobacterial FBP/SBPase in soybean prevents yield depression under future climate conditions.** *J Exp Bot.* 2017; **68**(3): 715–26.
PubMed Abstract | Publisher Full Text | Free Full Text

75. Stitt M: **Progress in understanding and engineering primary plant metabolism.** *Curr Opin Biotechnol.* 2013; **24**(2): 229–38.
PubMed Abstract | Publisher Full Text

76. F Kromdijk J, Głowacka K, Leonelli L, *et al.*: **Improving photosynthesis and crop productivity by accelerating recovery from photoprotection.** *Science.* 2016; **354**(63): 857–61.
PubMed Abstract | Publisher Full Text | F1000 Recommendation

77. Murchie EH, Niyogi KK: **Manipulation of photoprotection to improve plant photosynthesis.** *Plant Physiol.* 2011; **155**(1): 86–92.
PubMed Abstract | Publisher Full Text | Free Full Text

78. Zhu XG, Ort DR, Whitmarsh J, *et al.*: **The slow reversibility of photosystem II thermal energy dissipation on transfer from high to low light may cause large losses in carbon gain by crop canopies: a theoretical analysis.** *J Exp Bot.* 2004; **55**(400): 1167–75.
PubMed Abstract | Publisher Full Text

79. F Blankenship RE, Tiede DM, Barber J, *et al.*: **Comparing photosynthetic and photovoltaic efficiencies and recognizing the potential for improvement.** *Science.* 2011; **332**(6031): 805–9.
PubMed Abstract | Publisher Full Text | F1000 Recommendation

80. Melis A: **Solar energy conversion efficiencies in photosynthesis: Minimizing the chlorophyll antennae to maximize efficiency.** *Plant Sci.* 2009; **177**(4): 272–80.
Publisher Full Text

81. Ort DR, Melis A: **Optimizing antenna size to maximize photosynthetic efficiency.** *Plant Physiol.* 2011; **155**(1): 79–85.
PubMed Abstract | Publisher Full Text | Free Full Text

82. Kirst H, Gabilly ST, Niyogi KK, *et al.*: **Photosynthetic antenna engineering to improve crop yields.** *Planta.* 2017; **245**(5): 1009–20.
PubMed Abstract | Publisher Full Text

83. Polle JE, Kanakagiri SD, Melis A: **tla1, a DNA insertional transformant of the green alga Chlamydomonas reinhardtii with a truncated light-harvesting chlorophyll antenna size.** *Planta.* 2003; **217**(1): 49–59.
PubMed Abstract

84. Nakajima Y, Tsuzuki M, Ueda R: **Improved productivity by reduction of the content of light-harvesting pigment in *Chlamydomonas perigranulata*.** *J Appl Phycol.* 2001; **13**(2): 95–101.
Publisher Full Text

85. Mussgnug JH, Thomas-Hall S, Rupprecht J, *et al.*: **Engineering photosynthetic light capture: impacts on improved solar energy to biomass conversion.** *Plant Biotechnol J.* 2007; **5**(6): 802–14.
PubMed Abstract | Publisher Full Text

86. Kirst H, Formighieri C, Melis A: **Maximizing photosynthetic efficiency and culture productivity in cyanobacteria upon minimizing the phycobilisome light-harvesting antenna size.** *Biochim Biophys Acta.* 2014; **1837**(10): 1653–64.
PubMed Abstract | Publisher Full Text

87. Gu J, Zhou Z, Li Z, *et al.*: **Rice (*Oryza sativa* L.) with reduced chlorophyll content exhibit higher photosynthetic rate and efficiency, improved canopy light distribution, and greater yields than normally pigmented plants.** *Field Crops Research.* 2017; **200**: 58–70.
Publisher Full Text

88. F Antonovsky N, Gleizer S, Noor E, *et al.*: **Sugar Synthesis from CO_2 in *Escherichia coli*.** *Cell.* 2016; **166**(1): 115–25.
PubMed Abstract | Publisher Full Text | Free Full Text | F1000 Recommendation

89. Antonovsky N, Gleizer S, Milo R: **Engineering carbon fixation in *E. coli*: from heterologous RuBisCO expression to the Calvin-Benson-Bassham cycle.** *Curr Opin Biotechnol.* 2017; **47**: 83–91.
PubMed Abstract | Publisher Full Text

90. F Schwander T, Schada von Borzyskowski L, Burgener S, *et al.*: **A synthetic pathway for the fixation of carbon dioxide *in vitro*.** *Science.* 2016; **354**(6314): 900–4.
PubMed Abstract | Publisher Full Text | F1000 Recommendation

91. Sage RF, Sage TL, Kocacinar F: **Photorespiration and the evolution of C_4 photosynthesis.** *Annu Rev Plant Biol.* 2012; **63**: 19–47.
PubMed Abstract | Publisher Full Text

92. Schlüter U, Bräutigam A, Gowik U, *et al.*: **Photosynthesis in C3-C4 intermediate *Moricandia* species.** *J Exp Bot.* 2017; **68**(2): 191–206.
PubMed Abstract | Publisher Full Text

93. Schlüter U, Weber AP: **The Road to C4 Photosynthesis: Evolution of a Complex Trait via Intermediary States.** *Plant Cell Physiol.* 2016; **57**(5): 881–9.
PubMed Abstract | Publisher Full Text

94. Kennedy RA, Laetsch WM: **Plant species intermediate for c_3, c_4 photosynthesis.** *Science.* 1974; **184**(4141): 1087–9.
PubMed Abstract | Publisher Full Text

95. von Caemmerer S, Quick WP, Furbank RT: **The development of C_4 rice: current progress and future challenges.** *Science.* 2012; **336**(6089): 1671–2.
PubMed Abstract | Publisher Full Text

96. Wang P, Vlad D, Langdale JA: **Finding the genes to build C_4 rice.** *Curr Opin Plant Biol.* 2016; **31**: 44–50.
PubMed Abstract | Publisher Full Text

97. Wang P, Karki S, Biswal AK, *et al.*: **Candidate regulators of Early Leaf Development in Maize Perturb Hormone Signalling and Secondary Cell Wall Formation When Constitutively Expressed in Rice.** *Sci Rep.* 2017; **7**(1): 4535.
PubMed Abstract | Publisher Full Text | Free Full Text

98. Lundgren MR, Christin PA: **Despite phylogenetic effects, C3-C4 lineages bridge the ecological gap to C4 photosynthesis.** *J Exp Bot.* 2017; **68**(2): 241–54.
PubMed Abstract | Publisher Full Text

99. Marshall DM, Muhaidat R, Brown NJ, *et al.*: ***Cleome*, a genus closely related to Arabidopsis, contains species spanning a developmental progression from C_3 to C_4 photosynthesis.** *Plant J.* 2007; **51**(5): 886–96.
PubMed Abstract | Publisher Full Text

100. Aubry S, Smith-Unna RD, Boursnell CM, *et al.*: **Transcript residency on ribosomes reveals a key role for the *Arabidopsis thaliana* bundle sheath in sulfur and glucosinolate metabolism.** *Plant J.* 2014; **78**(4): 659–73.
PubMed Abstract | Publisher Full Text

101. Borland AM, Yang X: **Informing the improvement and biodesign of crassulacean acid metabolism via system dynamics modelling.** *New Phytol.* 2013; **200**(4): 946–9.
PubMed Abstract | Publisher Full Text

102. Yang X, Cushman JC, Borland AM, *et al.*: **A roadmap for research on crassulacean acid metabolism (CAM) to enhance sustainable food and bioenergy production in a hotter, drier world.** *New Phytol.* 2015; **207**(3): 491–504.
PubMed Abstract | Publisher Full Text

103. Borland AM, Hartwell J, Weston DJ, *et al.*: **Engineering crassulacean acid metabolism to improve water-use efficiency.** *Trends Plant Sci.* 2014; **19**(5): 327–38.
PubMed Abstract | Publisher Full Text | Free Full Text

104. F Shivhare D, Mueller-Cajar O: ***In Vitro* Characterization of Thermostable CAM Rubisco Activase Reveals a Rubisco Interacting Surface Loop.** *Plant Physiol.*

2017; **174**(3): 1505–16.
PubMed Abstract | Publisher Full Text | Free Full Text | F1000 Recommendation

105. Meyer MT, McCormick AJ, Griffiths H: **Will an algal CO_2-concentrating mechanism work in higher plants?** *Curr Opin Plant Biol.* 2016; **31**: 181–8.
PubMed Abstract | Publisher Full Text

106. Ma Y, Pollock SV, Xiao Y, *et al.*: **Identification of a novel gene, CIA6, required for normal pyrenoid formation in *Chlamydomonas reinhardtii*.** *Plant Physiol.* 2011; **156**(2): 884–96.
PubMed Abstract | Publisher Full Text | Free Full Text

107. Moroney JV, Ma Y, Frey WD, *et al.*: **The carbonic anhydrase isoforms of *Chlamydomonas reinhardtii*: intracellular location, expression, and physiological roles.** *Photosynth Res.* 2011; **109**(1–3): 133–49.
PubMed Abstract | Publisher Full Text

108. Mackinder LC, Meyer MT, Mettler-Altmann T, *et al.*: **A repeat protein links Rubisco to form the eukaryotic carbon-concentrating organelle.** *Proc Natl Acad Sci U S A.* 2016; **113**(21): 5958–63.
PubMed Abstract | Publisher Full Text | Free Full Text

109. Atkinson N, Feike D, Mackinder LC, *et al.*: **Introducing an algal carbon-concentrating mechanism into higher plants: location and incorporation of key components.** *Plant Biotechnol J.* 2016; **14**(5): 1302–15.
PubMed Abstract | Publisher Full Text | Free Full Text

110. F Hanson MR, Lin MT, Carmo-Silva AE, *et al.*: **Towards engineering carboxysomes into C3 plants.** *Plant J.* 2016; **87**(1): 38–50.
PubMed Abstract | Publisher Full Text | Free Full Text | F1000 Recommendation

111. Lin MT, Occhialini A, Andralojc PJ, *et al.*: **β-Carboxysomal proteins assemble into highly organized structures in *Nicotiana* chloroplasts.** *Plant J.* 2014; **79**(1): 1–12.
PubMed Abstract | Publisher Full Text | Free Full Text

112. F Rae BD, Long BM, Förster B, *et al.*: **Progress and challenges of engineering a biophysical CO2-concentrating mechanism into higher plants.** *J Exp Bot.* 2017; **68**(14): 3717–3737.
PubMed Abstract | Publisher Full Text | F1000 Recommendation

113. F Gonzalez-Esquer CR, Newnham SE, Kerfeld CA: **Bacterial microcompartments as metabolic modules for plant synthetic biology.** *Plant J.* 2016; **87**(1): 66–75.
PubMed Abstract | Publisher Full Text | F1000 Recommendation

114. McGrath JM, Long SP: **Can the cyanobacterial carbon-concentrating mechanism increase photosynthesis in crop species? A theoretical analysis.** *Plant Physiol.* 2014; **164**(4): 2247–61.
PubMed Abstract | Publisher Full Text | Free Full Text

115. F Rolland V, Badger MR, Price GD: **Redirecting the Cyanobacterial Bicarbonate Transporters BicA and SbtA to the Chloroplast Envelope: Soluble and Membrane Cargos Need Different Chloroplast Targeting Signals in Plants.** *Front Plant Sci.* 2016; **7**: 185.
PubMed Abstract | Publisher Full Text | Free Full Text | F1000 Recommendation

116. F Clayton H, Saladié M, Rolland V, *et al.*: **Loss of the Chloroplast Transit Peptide from an Ancestral C_3 Carbonic Anhydrase Is Associated with C_4 Evolution in the Grass Genus *Neurachne*.** *Plant Physiol.* 2017; **173**(3): 1648–58.
PubMed Abstract | Publisher Full Text | Free Full Text | F1000 Recommendation

117. Meyer MT, Genkov T, Skepper JN, *et al.*: **Rubisco small-subunit α-helices control pyrenoid formation in *Chlamydomonas*.** *Proc Natl Acad Sci U S A.* 2012; **109**(47): 19474–9.
PubMed Abstract | Publisher Full Text | Free Full Text

118. Li X, Zhang R, Patena W, *et al.*: **An Indexed, Mapped Mutant Library Enables Reverse Genetics Studies of Biological Processes in *Chlamydomonas reinhardtii*.** *Plant Cell.* 2016; **28**(2): 367–87.
PubMed Abstract | Publisher Full Text | Free Full Text

119. Jin S, Sun J, Wunder T, *et al.*: **Structural insights into the LCIB protein family reveals a new group of β-carbonic anhydrases.** *Proc Natl Acad Sci U S A.* 2016; **113**(51): 14716–21.
PubMed Abstract | Publisher Full Text | Free Full Text

120. Flexas J, Niinemets U, Gallé A, *et al.*: **Diffusional conductances to CO_2 as a target for increasing photosynthesis and photosynthetic water-use efficiency.** *Photosynth Res.* 2013; **117**(1–3): 45–59.
PubMed Abstract | Publisher Full Text

3. CHAPTER II:

Differential metabolic reprogramming in tomato HIGH PIGMENT mutants in response to shading conditions

Differential metabolic reprogramming in tomato HIGH PIGMENT mutants in response to shading conditions

Auderlan M. Pereira[1], Auxiliadora O. Martins[1], William Batista-Silva[1], Jorge A. Condori-Apfata[1], Vitor L. Nascimento[1], Victor F. Silva, Leonardo A. Oliveira[1], David B. Medeiros[2], Samuel C. V. Martins[1], Alisdair R. Fernie[2], Adriano Nunes-Nesi[1] and Wagner L. Araújo[1]*

[1]Departamento de Biologia Vegetal, Universidade Federal de Viçosa, 36570-900, Viçosa, Minas Gerais, Brazil
[2]*Max-Planck-Institute of Molecular Plant Physiology, Am Mühlenberg 1, 14476 Potsdam Golm, Germany*

*To whom correspondence should be addressed.

Wagner L. Araújo

Email: wlaraujo@ufv.br
Tel: +55 (31) 3612-5358

ABSTRACT
High pigment mutations culminated with plants highly responsive to light and high pigmentation, at the same time that these plants produce fruits with high health-beneficial nutrients. This has clearly attracted the attention of breeders and attempts to incorporate these characteristics into commercial crops have been seen over the years. Here, we performed a detailed morphological, physiological and metabolic characterization of *high pigment 1* and *high pigment 2* mutant, respectively, with mutations in the *DDB1* and *DET1* genes, in tomato (*Solanum lycopersicum* L. cv Micro-Tom) plants under different sunlight conditions (natural ligh (NL), shading 50% (S50) and 80% shading (S80)). Our results demonstrate that both mutations affect growth, physiological and metabolic parameters at all stages of plant development. Although the mutants were characterized by higher net photosynthesis (*A*), lower stomatal limitation, higher V_{cmax} and anatomical modifications that favor photosynthesis, we found that carbohydrate levels are not increased. Another conspicuous feature is that shading minimizes the above differences between mutants and WT, or even fully reversed this in the case of certain metabolites. Taken together, our results indicate that the high pigment levels observed in *hp1* and *hp2* mutants may represent an additional energy expenditure for these plants and that extensive physiological and metabolic reprogramming occurs to support increased pigment biosynthesis.

Key-words: high pigment; low luminosity; metabolic profile; photosynthesis; pigments

3.1 INTRODUCTION

Plants are sessile organisms and thus cannot escape from adverse environmental conditions that are a constant throughout their life cycle. However, plants also have the ability to adapt and acclimate to different environmental conditions, regulating both growth and development by extensive signaling pathways, exhibiting an unique developmental flexibility to ever-changing environmental conditions (Wolters and Jürgens, 2009; Vanstraelen and Benková, 2012). Light availability, a highly heterogeneous environmental factor, directly impact plant growth and survival as well as competitive interactions (Valladares and Niinemets, 2008), providing energy to sustain carbon (C) assimilation and information about the constantly changing environment. In fact, the classic effects of variable light environments on plant growth and photosynthesis have been exhaustively investigated. By far, such impact are best understood in the case of sunflecks, in which both the duration and frequency of light modulates photosynthesis and biomass accumulation through an array of physiological and morphological processes (Sims and Pearcy, 1993; Pearcy and Way, 2012; Valladares and Niinemets, 2008). Light is the crucial energy resource for plants that drives photosynthesis, thus governing overall plant growth. Notwithstanding, not only low but also high irradiance can restrict plant performance. Thus, the limitation of key resources, such as light, can compromise growth and survival, and therefore, it is not surprisingly that plants have evolved several biochemical, physiological and structural modification that allow them to cope with specific light conditions.

Tomato (*Solanum lycopersicum* L.), a fleshy fruit bearing species, is one of the main agricultural crops used either for *in natura* consumption or for the production of processed foods. Tomato fruit is a nutritious food that presents substantial amounts of vitamins, minerals and another phytochemicals such as carotenoids that, in turn, attract the attention of consumers due to their beneficial health properties (Abuajah et al., 2015; Perveen et al., 2015). It is not surprisingly, therefore, that significant research efforts have been placed to tomato breeding in attempts to increase the amount of health-beneficial phytochemicals, especially carotenoids and, consequently, their derivatives (Ilahy et al., 2018). Nevertheless, it should be born in mind that deviation of C skeletons to maintain the expensive synthesis of secondary metabolites may account for as much as 30% of the C flow in plants (Huang et

al., 2010). Remarkably, these metabolic adjustments would be anticipated to result in an extensive metabolic reprogramming that remains to be experimentally investigated in tomato.

High pigment tomato mutants, *hp1* and *hp2*, are deficient in the negative regulators of light signal transduction *DAMAGE DNA BINDING PROTEIN 1*(*DDB1*) and *DE-ETIOLATED* (*DET1*), respectively (Levin et al., 2003; Lieberman et al., 2004). Both *hp1* and *hp2* mutations interfere in the light signal transduction pathway, conferring hypersensitivity to light-mediated events, that makes the plants highly responsive to light (Peters et al., 1992; Kendrick et al., 1997; Peters et al., 1998; Mustilli et al., 1999; Levin et al., 2003). Briefly, *high pigment 1* (*hp1*) exhibit a simple transversion of bases (A^{931} by T^{931}) in *the DDB1* gene resulting in a replacement of a conserved asparagine by a tyrosine residue at position 311; and *high pigment 2* (*hp2*), also with a simple transversion of bases (A by T) in the *DET1* gene which cause the deletion of 9 base pair and results in the loss of first three amino acids of exon 11 (Lieberman et al., 2004; Levin et al., 2003). Notably, such modification appears to possibly results in mislocalization of the protein (Mustilli et al., 1999; Levin et al., 2003; Lieberman et al., 2004). It is important to mention that such genes encode, respectively, the DDB1 and DET1 proteins that form a CUL4 (*Cullin4*) protein complex, an E3 (ligase) enzyme conjugating to ubiquitination process (Wang et al., 2008). Furthermore, reductions in the content or poor functionality of DDB1, DET1 or CUL4 proteins results in increased levels of chlorophyll, carotenoids and other pigments in both leaves and fruits since these proteins are negative regulators of photomorphogenesis and the chloroplasts development in plants (Pepper et al., 1994; Mustilli et al., 1999; Lieberman et al., 2004; Tang et al., 2016).

Under high-light conditions (full sun), high levels of photosynthetic pigments in tomato mutants favor the highest carbon assimilation when compared to wild type (WT) (Lieberman et al., 2004; Levin et al., 2003), which could compensate, at least partially, the greater energy expense in the production of these pigments. This fact aside, this exaggerated light response seems to be maintained even under low irradiance levels (150 μmol photons m^{-2} s^{-1}) (Melo et al., 2009). It is important to mention, however, that under low light conditions (shading) the overall efficiency of light interception is greatly minimized, also reducing the production and accumulation of photoassimilates. Under these conditions,

therefore, the competition for assimilated C skeletons among the different metabolic pathway may become even greater, which can lead to drastic consequences and result in impacts on both plant growth and development. Nevertheless, the real impact of *hp* mutations on the overall metabolism and, consequently, on the productivity and quality of these plants is yet incipient.

Although C fixation, a process inherently associated with biomass construction, has been exhaustively investigated, very little research has been based on the subsequent fate of the carbon (C) that is assimilated. Here, we hypothesized that the high pigments levels and other metabolites usually found in the *hp1* and *hp2* mutants may represent an additional energy expense for these plants and that major metabolic adjustments are required to allow maintenance of successful performance of tomato plants grown under different sunlight conditions. Our main goal was to investigate how the metabolic machinery of tomato adjusts itself to varying light supply and whether these adjustments are supported by clear reprogramming of primary and secondary metabolism in leaves. To reach this goal, we assess distinct aspects of the influence of high pigment on plant growth and primary metabolism in leaves through morphological, physiological and biochemical analyses of the tomato *hp* mutant grown under low or high light conditions. Our combined results demonstrate a clear metabolic reprogramming allowing the plant to cope with high light and specifically identified a greater abundance of metabolites likely involved in protection against light-induced oxidative stress. The effect of impaired light signaling in *hp* mutants appears to be fairly specific, particularly on metabolic reprogramming and photosynthetic performance. We compare and contrast our results with those previously published on the impact of the *hp* mutation on tomato fruit and further discuss these data within the context of current models of metabolic adjustments acting not to improve photosynthetic performance *per se* but rather to afford protection associated with energy dissipation and ROS scavenging in leaves.

3.2 MATERIAL AND METHODS

Plant material, growth conditions and experimental design

Seeds of the tomato (*Solanum lycopersicum* L. cv Micro-Tom) wild-type (WT) and *high pigment 1* (*hp1*) and *high pigment 2* (*hp2*) mutants were surface sterilized with 5% sodium hypochlorite solution for 10 min, then washed with running distilled water and subsequently sowed in a tray containing commercial substrate (Plantmax, DDL Agro Indústria). After two weeks of sowing, seedlings were transferred to 2 L pots (one seedling per pot) containing the same substrate used for seedling production but supplemented with 1 g NPK 10-10-10 and 4 g dolomitic limestone (Ca + Mg) per liter of substrate (Pino-Nunes et al., 2018). Plants were grown in a greenhouse located in Viçosa (20°45′S, 42°50′W, 650 m above sea level), southeastern Brazil, with a minimum of 400 μmol photons m^{-2} s^{-1}.

WT, *hp1* and *hp2* plants were grown since the sowing under full (100%) sunlight conditions (NL, natural light) or under two levels of shading (50 and 80%). The shade enclosure was constructed using neutral-density black nylon netting, and the plants were kept in these conditions from the sowing to the analysis. To test the shading effect, a Line Quantum Sensor (The LI-191R) was used to measure Photosynthetic Photon Flux Density (PPFD) expressed in μmol photons m^{-2} s^{-1}. Throughout the experiment, the plants were grown under naturally fluctuating conditions of temperature and air relative humidity, and were fertilized and irrigated as necessary. The pots were randomized periodically to minimize any variation within each light environment. The measurements of PPFD were taken from 06:00 to 18:00 hours in four days throughout the experiment (Supplementary Figure 1). For all samplings and measurements, the second terminal leaflet of the third fully expanded leaf, from the apex to the base, in plants of 4 week after planting, were used. For biochemical analyses, leaf samples were collected in cloudless days at different times during day, prior to flash freezing in liquid nitrogen and subsequent storage at −80°C until analysis. The experiment was arranged in a completely randomized blocks design in subdivided plots scheme (3 x 3), totaling 9 treatments. The plot was formed by 3 light conditions: natural light (NL), shading 1 (S50 ≈ 50% shading) and shading 2 (S80 ≈ 80% shading); while in the subplot were the 3 genotypes studied (WT, *hp1* and *hp2*). The means presented in Tables and

Figures were obtained from six independent replications per treatment of single plant experimental plots (one plant per pot). Data were submitted to analysis of variance (ANOVA) with F test and Duncan test ($P<0.05$).

Determination of biometric parameters

Dry matter accumulation in shoot and roots was determined at 28 days after planting (DAP) and 82 DAP, namely vegetative and reproductive stages, respectively. During these measurements, the plants were harvested in one cut at ground level, separating roots from shoots. The roots, after washing with water to remove soil contamination, and shoots were placed in labelled paper bags and brought to a forced air circulation oven at 70 °C for 5 days, after which the dry weight of roots and shoots (stem, leaves and fruits) was determined. Moreover, plant height, stem diameter, number of leaves, root length, number of flowers, number of fruits, fruit set, leaf area (Li-Cor Model 3100 Area Meter, Lincoln, NE, USA), and total dry weight (= leaves + stem + roots + fruits) were determined. From these characters we determined specific leaf area, relative growth rate and harvest index.

Leaf anatomic analysis

Sections of leaf samples from the third fully expanded leaf were hand cute using a razor blade and fixed in FAA50 (formaldehyde, acetic acid and ethyl alcohol (90:5:5)) for 48 h and then stored in 70% ethanol (Johansen, 1940). Subsequently, the sections were included in methacrylate (Historesin-Leica), following the manufacturer's recommendations, and transversely sectioned on automatic advance rotary microtome (model RM2155, Leica microsystems Inc., Deerfield, USA) with 5 μm thickness, dyed with toluidine blue (O'Brien et al., 1964) and mounted under cover slip. The images were obtained under a light microscope (model AX-70 TRF, Olympus Optical, Tokyo, Japan), coupled to a digital photographic camera (Zeiss AxioCam HRc model, Göttinger, Germany) using the image capture program Axion Vision. Measurements were taken from at least five different fields from each sample using the Image-Pro® Plus software (version 4.1, Media Cybernetics, Inc., Silver Spring, USA). Leaf thickness, palisade and spongy parenchyma, abaxial and adaxial epidermis, stomatal index, epidermal cell density and stomatal density were evaluated.

Measurements of stomatal index and stomatal and cell density leaflets were obtained after a diaphanization process, which consisted of the clarification of the samples using 100% (v/v) methanol for 48 h, followed by a 95% lactic acid incubation at 95 °C for 30 min (Zsögön et al., 2015). Sections were mounted on glass slides and the images of the adaxial and abaxial epidermis were obtained using light microscope (model AX-70 TRF, Olympus Optical, Tokyo, Japan) coupled to a digital camera (Zeiss AxioCam HRc model Göttinger, Germany) and computer with the Axion Vision image capture program. The images were analyzed in the Image-Pro Plus version 4.5 program.

Gas exchange and fluorescence parameters

Gas exchange and chlorophyll *a* fluorescence analysis were performed simultaneously in the third fully expanded leaf from the apex of 4-week-old plants (vegetative stage) using a portable open-flow gas exchange system (Li-6400XT, Li-Cor, Inc., Lincoln, NE, USA) equipped with an integrated fluorescence chamber (LI-6400-40; Li-Cor Inc.). Measurements of the net carbon assimilation rate (A, μmol CO_2 m^{-2} s^{-1}), stomatal conductance (gs, mol H_2O m^{-2} s^{-1}), internal CO_2 concentration (C_i), and transpiration (E, mmol m^{-2} s^{-1}) were conducted from 08:00 to 11:00 h (solar time), which is when A was at its maximum, under an ambient CO_2 concentration (C_a) of 400 μmol mol^{-1} air (CO_2 injected from a cartridge) and a flow rate of 300 μmol s^{-1}. All measurements were conducted under artificial photosynthetic photon flux density (PPFD), saturating light of 1000 μmol photons m^{-2} s^{-1} (from a LED source) with 10% blue light in order to maximize the stomatal opening, at 25 °C and the leaf-to-air vapor pressure deficit was maintained at approximately 1.0 kPa. Dark respiration (R_D) and fluorescence of chlorophyll *a* parameters were measured using the same gas exchange system described above after at least two hours into the dark period in the same leaf previously used to determine gas exchange parameters.

The initial fluorescence (F_0) was measured by illuminating previously dark adapted leaves with weak modulated measuring beams (0.03 μmol m^{-2} s^{-1}). Saturating white light pulses (8000 μmol photons m^{-2} s^{-1}) was applied for 0.8 s to obtain the maximum fluorescence (F_m), from which the variable-to-maximum Chl fluorescence ratio, was then calculated: $F_v/F_m=[(F_m - F_0)/F_m)]$. In light-adapted leaves, the steady-state fluorescence yield (F_s) was measured with the application of a saturating white light pulse (8000 μmol m^{-2} s^{-1}, 0.8 s) to

achieve the light-adapted maximum fluorescence (F_m'). The actinic light was then turned off and a far-red illumination (2 µmol m^{-2} s^{-1}) was applied to measure the light-adapted initial fluorescence (F_0'). The capture efficiency of excitation energy by open photosystem (PS) II reaction centers (F_v'/F_m') was estimated following Logan et al. (2007) and the actual PSII photochemical efficiency (δPSII) was estimated as $\delta PSII = (F_m' - F_s)/F_m'$ (Genty et al., 1989). In addition, the electron transport rate (ETR), were determined as previously described (Martins et al., 2014; Medeiros et al., 2016).

Photosynthetic light-response curves (*A*/PPFD) were obtained by varying the PPFD in 9 steps from 2200 to 0 µmol photons m^{-2} s^{-1} at 25 ºC (Martins et al., 2014). The *A*/PPFD curves were obtained at same conditions described before. From the *A*/PPFD curve, the following variables were determined: net carbon assimilation rate saturated by light (A_{max}), light compensation point (*LCP*), light saturation point (*LSP*) and light use efficiency ($1/\Phi$) (inverse of the apparent quantum yield) (von Caemmerer, 2000).The responses of *A* to C_i were determined at 1000 µmol photons m^{-2} s^{-1}, at 25 ºC, under ambient O_2 following the protocol described by Long and Bernacchi (2003). Briefly, A/C_i curves were initiated at a C_a of 400 µmol mol^{-1} and once the steady state was reached, C_a was decreased stepwise down to 50 µmol mol^{-1} air. Upon completion of the measurements at low C_a, it was returned to 400 µmol mol^{-1} air to restore the original *A*. Next, C_a was increased stepwise to 2000 µmol mol^{-1} air (Martins et al., 2013). The maximum rate of carboxylation (V_{cmax}) and maximum rate of carboxylation limited by electron transport (J_{max}), J_{max}/V_{cmax} ratio and triose phosphate utilization (*TPU*) were then estimated by fitting the mechanistic model of CO_2 assimilation using the Excel spreadsheet provided by Sharkey et al. (2007). Corrections for the leakage of CO_2 into and water vapor out of the leaf chamber of the LI-6400 have been applied to all gas-exchange data, according to Rodeghiero et al. (2007).

Biochemical parameters and metabolic profile

All sampling procedures were carried on the same leaf used for analysis of gas exchange and fluorescence from 4-week-old plants (28 DAP), during vegetative stage. Leaf samples were harvested in different time points along the light/dark cycle (5:30, 12:00; 18:00, 00:00, and 5:30). Leaves were flash-frozen in liquid nitrogen and stored at −80 °C until

further analyses. Metabolite extraction was performed by rapid grinding in liquid nitrogen and immediate addition of the appropriate extraction buffer.

The levels of photosynthetic pigments were determined according to Wellburn (1994) whereas starch, sucrose, glucose and fructose were determined exactly as described previously by Fernie et al. (2001), and total amino acids and total soluble proteins were determined as previously described by Yemm et al. (1955) and Bradford (1976), respectively.

The levels of all other metabolites were quantified by an established gas chromatography associated with mass spectrometry (GCMS) protocol (Roessner et al., 2001; Lisec et al., 2006). Briefly, the extraction (using ~50 mg fresh weight) was performed using 1 mL of methanol and shaking (800 rpm) at 70 °C during 15 min, 60 µL of Ribitol (0.2 mg mL^{-1}) was added as an internal standard. After that, derivatization and sample injection were performed exactly as previously described previously by Lisec et al. (2006). This analysis allowed the determination of 31 different compounds, representing the main classes of compounds (amino acids, organic acids, sugars and others). Chromatograms and generated mass spectra were evaluated using the software TagFinder (Luedemann et al., 2011), using a reference library from the Golm Metabolome Database (Kopka et al., 2005) and the identification and annotation of the detected peaks followed the recommendations for reporting metabolite data described in Fernie et al., (2011).

qRTPCR analysis

Total RNA was isolated from 50 mg of plant material (leaf) using the TRizol reagent (Invitrogen®), according to the manufacturer's instructions. The integrity and amount of RNA were checked on 1% (w/v) agarose gel, and the concentration was measured before and after DNAse I digestion (RQ1 RNase free DNase I, Promega®) using a spectrophotometry (OD_{260}). DNAse-treated RNA (2 µg) was used for cDNA synthesis using the Superscript™ III reverse transcriptase (Invitrogen®, Darmstadt, Germany) according to the manufacturer's recommendations.

Gene expression was accessed using real-time PCR (qRT-PCR) (Step One PlusTMReal Time PCR System, Applied Biosystems, CA, USA) with the SYBR green fluorescence detection (Applied Biosystems®), using the Platinum® SYBR® Green qPCR SuperMix-UDG with ROX kit. The primers used for the *DDB1* gene (Forward:

AAGAGTGGAAGAGTTGACAAGG and Reverse: GGAACTTGTATCACAACCTCAC) and *DET1* (Forward: ATCATAACAGACCCGTAGATGC and Reverse: ACCCATACTAACCGTCTTGGC) were designed using QUANTPRIME software (Arvidsson et al., 2008). Data analyses were performed exactly as described by Caldana et al. (2007). qRT-PCR were performed according with the followed temperature alternations: denaturation of double-stranded DNA and enzyme activation (95°C, 30 seconds, 1x); denaturation of double-stranded DNA (95 °C, 3 seconds, 40x) and finally, primer's annealing and extension of fragment by polymerase enzyme (58 °C, 30 seconds, 40x). Melt curve reaction: 95 °C 15 seconds, 60 °C for 1 minute and 95 °C for 15 seconds (1x). The average CT of the ACTIN (reference control) gene was used for the relative expression analyses. The analyzes were performed in duplicate in each PCR run, using 4 replicates for each genotype, and their mean cycle threshold was used for relative normalized expression analyses.

3.3 RESULTS

HIGH PIGMENT genes are expressed in vegetative tissues and their expression is not reduced in mutant plants

Although the function of *hp* related genes has been extensively demonstrated during tomato fruit development, here we first confirmed that both *DDB1* and *DET1* genes are indeed constitutively expressed also in leaf tissues (Supplementary Figure 2). Given the punctual changes in both *DDB1* and *DET1* genes in *hp1* and *hp2* mutants, respectively, no differences in the expression of *DDB1* and *DET1* genes between WT and *hp* mutants were observed (Table 1).

Morphological changes in *hp* plants during vegetative growth

The expression of both *DDB1* and *DET1* in vegetative tissues of *hp* mutant plants prompted us to investigate the physiological function of those gene in response to shade. Despite of no visible aberrant phenotypes during vegetative and reproductive development of *hp* mutants (Figure 1 and 2) we observed that shading levels did not significantly affect the height of 4-week-old plants of WT, *hp1* and *hp2* (Figure 1A). Notably, *hp1* and *hp2* plants

presented lower height in relation to WT in all light conditions. It was also observed that the *hp1* mutant had a higher stem diameter when compared to the other genotypes, especially under the control condition (Figure 1B).

Although both *hp1* and *hp2* mutants plants presented longer root length than WT under normal light conditions (Figure 1C), this difference was reduced at 50% shading condition (S50), where no difference among the genotypes was observed. Additionally, no difference in root length was observed among genotypes at 80% shading condition (S80); remarkably, under this condition a drastic reduction of root length in relation to the control condition, especially in the mutants plants, was observed.

The total number of leaves was higher in both *hp1* and *hp2* mutant plants than WT under both control and S 50% conditions, and it was virtually invariant among genotypes submitted to S 80%, where the lower number of leaves was observed (Figure 1D). It is important to mention that both *hp1* and *hp2* mutant plants reduced the number of leaves in response to a higher shading, whereas WT plants was virtually irresponsive to fluctuation in light conditions. Leaf area was strongly affected by shading levels (Figure 1E). Under normal light conditions, *hp* mutants plants were characterized by a higher LA relative to WT, mainly *hp1*. Noteworthy, under S50 an increased leaf area was observed for WT plants leading to the absence of differences between WT and *hp1*, with those genotypes showing higher leaf area values than *hp2* (Figure 1E). Total dry weight followed a similar trend to that observed for leaf area, and thus under control conditions the mutants *hp1* and *hp2* showed higher biomass accumulation than WT plants (Figure 1F). When subjected to shading conditions, both *hp1* and *hp2* mutants plants experienced a progressive and significantly reduction of total dry weight, while it was reduced just under S80 for WT plants. Under S80, total dry weight was invariant between genotypes yet large losses of biomass in relation to the control condition was observed (Figure 1F). Notably, at S80 the reduction of leaf area was drastic and not differences between genotypes was observed. As expected, both S50 and S80 culminated with progressive increase in specific leaf area for all genotypes and thus higher specific leaf area were found when genotypes were subjected to S80 (Figure 1G). Interesting, under all light conditions, *hp2* mutant plants display lower specific leaf area than WT and *hp1* plants, which were similar (Figure 1G). We also observed that root/shoot ratio was higher for both *hp1* and *hp2* mutants than in WT plants under control conditions. Under S50 only

hp2 plants maintained higher root/shoot ratio values and no differences were observed among genotypes when they were submitted to S80 (Figure 1H)

hp mutation decreases fruit set and yield without changes in carbon partitioning

We next investigated whether the changes in morphological parameters observed in *hp* plants during the vegetative stage were maintained in the reproductive stage. To this end, morphological and reproductive parameters were evaluated in 12-week-old plants. Overall, regardless the light condition, height was invariant within each genotype. Thus, in 12-week-old plants, height of WT and *hp2* plants was practically similar and higher than that *hp1* plants, regardless of the light environment (Figure 2A). A similar pattern between vegetative and reproductive phases was observed for stem diameter and it was noted that *hp1* mutant plants had a higher stem diameter when compared to the other genotypes, and that stem diameter was reduced in response to shading (Figure 2B). It was observed that regardless of the light condition, root length of WT plants was higher than both *hp1* and *hp2* mutant plants, which showed a similar root length (Figure 2C).

hp1 and hp2 plants significantly outperformed WT genotype in the emission of leaves at NL and S50 condition, and were similar to each other. At S80 there was a reduction on number of leaves to mutant plants which presented similar values to WT plants in the control condition. Plant WT did not vary statistically in relation to the applied shading (Figure 2D).

The total number of leaves was relatively constant between genotypes at reproductive phase (82 DAP) in response to changes in light availability (Figure 2D). *hp2* mutant plants had higher number of leaves than WT and *hp1* mutant plants under both control and S50 conditions, and it was virtually invariant among genotypes submitted to S80 (Figure 2D). Although shading did not modify the leaf area of WT plants at 82 DAP, S80 considerably reduced the leaf area of both *hp1* and *hp2* in comparison to plants cultivated under S50 (Figure 2E). *hp1* mutant plants had lower leaf area when compared to other genotypes under both the control and S80 (Figure 2E). Total dry weight was strongly reduced in response to in all genotypes, especially at S80 (Figure 2F). It is also observed that under all light regimes WT plants were characterized by higher total dry weight (Figure 2F). Specific leaf area increased with increasing shading levels for all genotypes and it was also observed that there

was no difference in specific leaf area under both control condition and S50 when comparing the genotypes (Figure 2G). However, under S80 higher Specific leaf area was observed in WT and *hp1* mutant plants in comparison to *hp2* (Figure 2G). Regarding the root/shoot ratio, whereas WT and *hp1* plants were not negatively affected by shading levels and did not differ statistically, higher root/shoot ratio was observed for *hp2* plants (Figure 2H).

We further observed regardless of light conditions, the highest number of flowers was found in WT plants, which was significantly higher than both *hp1* and *hp2* plants (Figure 3A and Supplementary Figure 3). This also lead to the higher number of fruits observed in WT plants (Figure 3B) and, consequently, to the larger mass allocated to these organs in WT plants (Table 2). Fruit set did was also affected in response to shading and it can be observed that *hp1* plants were able to convert proportionally a greater numbers of flowers into fruits (Figure 3C), and thus fruit set was higher in *hp1* plants than in WT and *hp2* plants. Moreover, fruit set was reduced in all genotypes under S80. In addition, shading levels directly affected fruit yield and fruit mass, reducing the values of these variables as shading increased (Table 2). Interestingly, shading levels delayed the onset of first flower emission in all genotypes, yet for both mutants a greater delay than WT was observed (Figure 3D, E and F). Number of flowers was reduced with the shading application, following the behavior observed for number of flowers, and as such lower values for plants cultivated at S80 were observed. This also led to a similar behavior of fruits dry weight, that are clearly reduced with shading, and were lower in *hp* mutants, especially in *hp2* (Table 2). We did not observe changes on relative growth rate neither in relation to genotypes nor shading levels (Table 2). The harvest index, which reflects the final targeting of photosynthesized products to fruits, was significantly higher in WT and *hp1* plants than in *hp2* mutant plants specially under control and S50 conditions. Remarkably, plant growth at S80 considerably reduced harvest index values although it must be mentioned that *hp1* plants maintained values close to those observed under control condition (Table 2).

Photosynthetic performance is higher in *hp* mutant regardless of light conditions

Given the changes observed in growth related parameters between the genotypes studied and that most of plant biomass is derived from photosynthesis, we next characterized

the photosynthetic performance of *hp* mutants by analyzing gas exchange and chlorophyll fluorescence parameters. Net CO_2 assimilation rate (*A*) and transpiration rates (*E*) were increased in *hp* mutant plants under all growth conditions (Figure 4A and F) yet changes in stomatal conductance (g_s) were only observed under control conditions (higher in *hp* mutants) and g_s was reduced to similar values under S80 (Figure 4C). *Ci* was virtually invariant between genotypes and growth conditions (Figure 4D). Under control conditions, *hp* mutants were characterized by higher R_d, especially *hp1* mutant whereas no differences in R_d were observed between genotypes when submitted to S50. Notably, when the shading level increased to 80%, R_d was higher in WT than in *hp1* and *hp2* mutant plants (Figure 4B). The maximum photochemical efficiency of photosystem II (FSII) (F_v/F_m) was invariant between genotypes and treatments, yet reductions in F_v/F_m at S80 were observed, mainly for WT and *hp1* mutant plants when compared to the control condition (Figure 4F). Similarly to the observed for both *A* (Figure 4A) and *E* (Figure 4F), *hp* mutant plants showed higher *ETR* and *ΦPSIIe* than WT in all three conditions, yet shading levels reduced proportionally the values of those parameters (Figure 4G and H).

We next characterized the photosynthetic performance by analyzing gas exchange under different PPFD (*A*/PPFD curves; Figure 5) and we observed that mutant plants exhibited higher *A* in response to irradiance. From the data obtained by the *A/* PPFD curves we observed that both *hp* mutants (*hp1* and *hp2*), displayed greater *A* than WT, specifically from 500 µmol photons m^{-2} s^{-1} and above in all growth light conditions tested here (Figure 5 A-C). By further analysing gas exchange responses to PPFD that ranged from 0 to 2200 µmol $m^{-2}s^{-1}$, we observed that mutant plants exhibited higher A_{max} than WT plants irrespective of the growth irradiance. Indeed, A_{max} was reduced as long as shading increased (Table 3). There were no differences for light compensation point (*LCP*) between genotypes in any light conditions, yet the shading treatments (S50 and S80) promoted similar reductions in all genotypes (Table 3). Light saturation point (*LSP*) was higher for both *hp1* and *hp2* mutants under control conditions, and at S50 only *hp2* mutant differed from WT plants. At S80 there was no difference among the genotypes, although under this condition all genotypes presented lower *LSP* (Table 3). Light use efficiency (*1/ϕ*) was higher in plants subjected to S80, although no differences among genotypes in all light conditions was observed (Table 3). Additionally, the response of *A* to the leaf internal CO_2 concentration (C_i) (*A/*C_i curves;

Figure 5D-F). Interestingly, under normal light conditions, despite higher *A* higher than WT, the *hp1* mutant plants did not differ in most points of the *A/Ci* curve, whereas from 400 mmol of CO_2 onwards the *hp2* mutant presented values significantly higher than both WT and *hp1* (Figure 5D). Under S50, the difference between *hp* mutants and WT was only observed at the end of the *A/Ci* curve, where the [CO_2] is higher (Figure 5E). Under S80, it was observed that both *hp1* and *hp2* mutants displayed higher *A* than WT (Figure 6F). Altogether, it seems clear that light limitation reduces *A* for all genotypes, although higher values were observed for both *hp1* and *hp2* mutants.

The parameters derived from the *A/Ci* curves (V_{cmax}, J_{max}, J_{max}/V_{cmax} and *TPU*) were generally lower at S80 compared to the other light conditions, except for the J_{max}/V_{cmax} ratio , which was invariant (Table 4). Higher V_{cmax} was observed for *hp1* mutant under control conditions. At S50, both *hp1* and *hp2* mutants had higher V_{cmax} than WT, whereas *hp2* mutant had higher V_{cmax} (88.57 μmol m^{-2} s^{-1}) even under S80 (Table 4). No differences in J_{max} were observed among genotypes under the control condition. Under S80 J_{max} was higher in *hp2* than in *hp1* and WT plants. Higher J_{max}/V_{cmax} ratio was observed for WT in the control and S50 (Table 4). Overall, at S80 higher values of J_{max}/V_{cmax} were observed for all genotypes. Similar values for *TPU* for all genotypes coupled with a significant and gradual decrease following increased shading were observed (Table 4).

Anatomical changes in *hp* mutant in response to shading conditions

Leaf limb anatomical measurements were also investigated and, overall, the highest values were observed at control condition (Figure 6). Overall, the adaxial epidermis thickness was negatively affected by shading in all genotypes, although only at S80 significant changes were observed with smaller values found in WT plants (Figure 6A). This fact aside, no differences were observed in the abaxial epidermis thickness (Figure 6B).Both *hp1* and *hp2* mutants presented larger thickness of the palisade (Figure 6C) and spongy (Figure 6D) parenchyma, even under the influence of shading (S50 and S80), with a relatively small reduction in both parameters following increasing in shading. The consistent pattern between palisade and spongy parenchyma culminated with the lack of difference on SP/PP ratio in all light conditions (Figure 6E). Total leaf thickness followed the same pattern found in the

parenchyma thickness, and as such *hp* mutants displayed a higher thickness than WT in all conditions, yet reductions were observed following increased shading (Figure 6F).

Metabolic reprogramming following shading in *hp* mutants

To enhance our understanding of the consequences of changes in growth and in photosynthetic capacity among the genotypes under different light conditions, we next performed a detailed metabolic analysis in leaves of WT and *hp* plants. First, we determined the levels of some carbon and nitrogen related metabolites in samples harvested at the middle of light period. No effect of shading in both amino acid and protein levels were observed (Figure 7A and B). WT and *hp2* plants were characterized by similar levels of amino acid and protein, while *hp1* mutant plants present higher amino acid levels under control condition and S50, as well as higher protein concentrations only at control condition.

As it should be expected in response to shading, there was an increase in chlorophyll *a* for all genotypes (Figure 7C), and *hp2* mutant had the highest values regardless of light condition. On the other hand, chlorophyll *b* levels did not vary as shading increase (Figure 7D). Total concentration of chlorophylls (chlorophyll *a +b)* follow the same trend observed for the chlorophyll *a* (Figure 7E). Accordingly, chlorophyll a/b ratio was lower for WT than *hp1* and *hp2* mutants plants in the control condition, and was similar between genotypes at S50 and S80 (Figure 7F). In addition, we measured the levels of soluble sugars (glucose, fructose and sucrose) and starch levels were determined throughout the day (Figure 8). We clearly observed that both S50 and S80 reduce sugar levels in both WT plants and *hp* mutant plants (Figure 8A - 8I). Although they presented higher *A*, overall *hp* mutants plants did not show higher sugars accumulation throughout the day, even under the three treatments. It is important to mention that *hp1* and *hp2* were characterized by higher glucose and sucrose levels under the control condition (Figure 8), and *hp2* glucose at S50 (Figure 8). This relatively minor yet significant advantage of *hp* mutants is further reduced as the shading increase, as we observe that low light affects more the *hp* mutants than WT. Similar to the situation observed for soluble sugars, *hp* mutant and WT plants were characterized by similar starch accumulation throughout the day under all conditions (Figure 8J, 8K, 8L). We also

observed that shading reduces starch levels and that differences between genotypes under these conditions are not significant.

To further explore better how and which extension both *hp* mutations and shading can affect primary metabolism, we decided to extend the analysis by studying the major primary metabolic pathways on leaves harvested at the middle of light period. These analyses revealed that among the 30 successfully annotated compounds related to primary metabolism, considerable changes occurred in the levels of a wide range of amino acids, organic acids, and sugars (Figure 9, Supplementary Figure 4, Supplementary Table 2). All comparisons were performed between mutant (*hp1* and *hp2*) and WT plants within each shading level. It should be noted that based on the set of identified amino acids, *hp* mutant plants had higher amino acid content than WT under normal conditions for the majority of amino acids namely alanine, asparagine, glutamine, GABA, isoleucine, phenylalanine, proline, serine, threonine, and valine (Figure 9, Supplementary Figure 4, Supplementary Table 2). This difference was minimized or even reversed by increased shading (S50 and S80). By contrast, lower values of organic acids (e.g. succinate, fumarate, malate, and glycerate) were observed for both *hp1* and *hp2* mutant plants under the control condition and this difference was intensified with shading (Figure 9 and Supplementary Figure 4). Sugars, including sucrose and glucose, generally followed the same pattern observed for organic acids. At S50 and S80, most of the sugars identified were negatively affected in the *hp1* mutant, whereas a drastic reduction on glucose at S80 was observed for *hp2* mutant. For other metabolites, which also had showed altered levels compared to WT, *hp* mutants had higher content, yet such differences were reduced or reversed (e.g., galactinol and guanidine) when plants were cultivated at S80 (Supplementary Figure 4).

3.4 DISCUSSION

Gene expression is not affected by DET1 and DDB1 mutation

The mutations in *DDB1* and *DET1* gene are responsible for the high pigment phenotype (*hp1* and *hp2*, respectively), which promote an exaggerated response to luminosity in these plants, as well as a large amount and size of plastid, and high pigmentation (Peters et al., 1992; Mustilli et al., 1999; Levin et al., 2003; Lieberman et al., 2004; Wang et al., 2008). These mutations were characterized by base transversions that resulted in protein truncation and/or misallocation as well described by Mustilli et al. (1999) e Lieberman et al. (2004). Thus, the expression levels of mutated genes are not greatly altered, however, their proteins lose function or are produced in very low amounts, as found for *hp2/DET1* (Mustilli et al., 1999). This is in agreement with the results obtained here in this work summarized in Table 1, where there was no difference in the expression of *DDB1* and *DET1* genes in the evaluated genotypes; nevertheless, the mutant plants, *hp1* and *hp2*, exhibit the characteristic mutation-related phenotypes, as already described (Mustilli et al., 1999; Levin et al., 2003; Lieberman et al., 2004; Lieberman et al., 2004).

Biometric parameters are affected by both *hp* mutation and shade levels

Although much is known about *hp* mutants, especially their fruits, our current knowledge of the effect of these mutations on growth and metabolism of vegetative parts is quite incipient. To better understand the effects of *hp1* and *hp2* mutations, which make plants highly responsive to light, we evaluated these plants together with their WT under different light levels (natural light-NL, shading 50%-S50 and shading 80%-S80). It is noteworthy that light is one of the most important factors in the first stage of the CO_2 fixation chain, photosynthesis, the process in which biochemical energy is produced, and present a complex influence on crop growth, development and production (Papadopoulos and Hao, 1997; Yamori and Shikanai, 2016).

Up to four weeks after planting, under NL mutants *hp1* and *hp2* showed higher root growth, number of leaves, leaf area, total dry mass and root/shoot ratio than WT (Figure 1C,

D, E, F and H, respectively), highlighting the *hp1* mutant, which also had a larger stem diameter (Figure 1B). Regarding to height growth, WT was the fastest growing genotype (Figure 1A). These results were opposite to those found by Jarret et al. (1984) where these author verified that plants *hp* mutant had lower leaf area and total dry weight. On the other hand, such superiority may be explained by the higher chlorophyll content (Figure 7E) and higher photosynthetic rate (Figure 4A) observed in these plants. Both these parameters may had allowed to the mutant plants to have higher photoassimilates production and, thus, a higher investment on different growth characters, while WT plants concentrated its energy especially on height. This behavior is totally in accordance with the phenotypic pattern of these mutations, which cause plants to over-respond to light (Kendrick et al., 1997; Wang et al., 2008).

Shading levels (S50 and S80) negatively affected the growth characteristics of all plants, except for height growth which remained unchanged (Figure 1A). This result was atypical, once the shading should induce higher plant height due to blanching effects, as reported by Smith et al. (1984). Shading minimized the advantage observed under the number of leaves condition of mutant plants over WT, that is, in S80 the all genotypes presented similar behavior for most growth variables that were evaluated (Figure 1D). This may also be linked to the fact that due to the characteristics of the *hp* mutation, the higher production of chloroplasts and consequently more pigments content, the plants need a higher CO_2 flow to supply these pathways to the detriment of others, which can affect growth and biomass accumulation, and this is evident in conditions where there is a lower flow of photosynthetic energy (shading), since plants that absorbed more light and had higher daily C gain and higher biomass compared to plants grown in low and low light (Vialet-Chabrand et al., 2017).

At 12 weeks after planting, we observed that, in general, at this development stage *hp* mutant plants did not show superiority over WT plants, as expected due to the higher light hypersensitivity conferred by these mutations. Some exception for height (*hp2* under NL), stem diameter (*hp1* in treatments S50), and number of leaves (*hp2* in treatments NL and S50) (Figure 2A, B and D, respectively) which means that lower luminosity minimizes, or even eliminates, the *hp* mutation effects. Micro-Tom plants have a very short stature, which is result from the *d* mutation, which promotes reduction in the internode length and leaves size, which are also, rough and dark green. All these alterations are due to the reduced

brassinosteroids content in these plants (Martí et al., 2006). Here, we verified that *hp1* mutant plants were the ones that grew less in height at S50 and S80, although they maintained their growth identical to the NL condition (Figure 2A). Shading levels mainly affected stem diameter, total dry weight and specific leaf area (Figure 2B, E and F, respectively). WT plants had higher total dry weight than mutants in the three treatments, this is clearly explained due to the higher number of fruits produced and, consequently, the greater accumulated biomass in these organs (Figure 3B, Table 2). However, when considering only the vegetative organs, WT presented higher dry weight accumulation only in the NL condition, not differing from mutants genotypes in the S50 and S80 (data not shown). Kläring and Krumbein (2013) working with solar radiation restriction on tomato plants found significant reductions in leaf, stem, fruit and root dry matter, at the same time, the leaf area of temporarily shaded plants was not reduced compared to non-shaded plants, which resulted in the significant increase in the specific leaf area under shading. Similar result was observed at S80 where all genotypes presented increase of specific leaf area. This leaf behavior, among other traits, is known to contribute to shade tolerance (Björkman, 1981; Ballaré and Pierik, 2017).

In the early phase of growth, mutant plants accumulated more root biomass to the detriment of the shoot in NL condition than WT, this phenotype reversed when subjected to lower light availability (Figure 1H). However, in the reproductive phase, higher root/shoot rate was observed only to *hp2* mutant plants (Figure 2H), which did not suffer S80 level effect. Probably that was a reflex from the low fruit production (Figure 3B). The *hp* mutation reduced the total fruit production in both *hp1* and *hp2* mutants, however, this situation become worse as long as the shade condition increased. This lower total fruit production is due to decrease of flower emission, which drastically has been reduced by *hp* mutation and light restriction combination, and low fruit set. Differently from WT and *hp2* plants, *hp1* showed a distinct strategy to improve its performance on reproductive phase, once it's had the highest fruit set in all light conditions (Figure 3). These results disagree from those found by El-Gizawy et al. (1992), where they verified that number of fruits per plant increased to shading density around 50%, however, over than 50% of light blocked, there were also reduced fruit weight. Similar results were obtained by Cockshull et al. (1992), in addition to the reduction in the number of open flowers. Shading levels also affected the flowering time of all genotypes, delaying the emission and opening of the first flowers (Figure 3D, E and F).

It is interesting to note that the greatest delay in the emission and opening of the first flowers was observed in *hp1* and *hp2*. However, it has been already reported that mutations in *DDB1* and *DET1*, which interact with *CUL4* and *COP1*, result in early flowering (Chen et al., 2010; Pazhouhandeh et al., 2011; Kang et al., 2015; Xu et al., 2016). The differential flowering behaviour observed here can be explained, at least partially, by the growth conditions used here that include photoperiod, light and temperature natural fluctuations.

Gas exchange and fluorescence parameters are modified by higher pigmentation and lower light availability

Here we observed that *hp* mutant plants had higher values than WT for most photosynthetic and fluorescence parameters, a fact noted under all conditions (Figure 4). Certainly, the characteristics of these mutations, which correspond to the greater presence of photosynthetic pigments, due to a larger number and size of plastid compartments (Davuluri *et al*., 2004; Liu *et al*., 2004; Wang *et al*., 2008), and with that higher concentration of Rubisco (Sasanuma, 2001; Spreitzer and Salvucci, 2002), contribute strongly to this higher photosynthesis. Interestingly, *A* was higher in the mutant plants for NL and S80 conditions. The S50 did not provided changes in this parameter, while a reduction was found in all genotypes at S80. Low light availability at S80 also promoted reduction in the *E* and R_d, clearly following what was verified for *gs*, since this parameter can directly influence the CO_2 entry in the plant, the loss of water by transpiration, as well as dark respiration(Liu et al., 2008; Buckley and Mott, 2013; Xiong et al., 2018).

Changes in the F_v/F_m ratio (Figure 4F) were not observed in plants subjected to NL or S50, ranging between 0.81 and 0.82, values close to normal for unstressed leaves (Björkman and Demmig, 1987), indicating that the photosynthetic apparatus under these conditions was not affected. Second Critchley (1998), in sun leaves, typical values of the F_v/F_m ratio are around 0.80 or just below 0.80, while in the shadow leaves, these values are always between 0.83 and 0.85. However, at S80 it was observed that WT and *hp1* plants, compared to NL, had lower F_v/F_m, while *hp2* plants remained stable. It is worth to mention that it was not verified any variation due to mutation. The photosynthetic apparatus responds to changes in the quantity and quality of light with coordinated changes in photosystem light-

gathering complexes (Kunderlikova et al., 2016). Reed *et al*., (2012), working with chlorophyll *a* and *b* content and fluorescence in avocado plants indicated that the photosynthetic apparatus of shaded leaves is more efficient in light capture, although assimilates less CO_2 compared to sun leaves due to other limitations.

Decreasing light intensity results on the reductions in the electron transport rate (*ETR*) (Mauro et al., 2011), which totally agree with ours results (Figure 4G). Differently to F_v/F_m, the *hp* mutation affected *ETR*, once in all conditions, the mutant plants presented higher values than WT. The effective quantum yield of PSII (*ΦPSIIe*) had the same pattern observed for *ETR*, since these two parameters have a direct relationship with each other (Mohammed et al., 1995). *ΦPSIIe* represents the proportion of electrons that are used in the photochemical phase (Campostrini, 2001). The *hp* mutants respond very well to normal light conditions, with high A_{max} and *LSP* values (Table 3), well above those observed for WT.

The advantages observed for the mutant plants in relation to gas exchange and chlorophyll *a* fluorescence parameters are directly related to the higher capacity of antenna complex captivity due to the higher amount of photosynthetic pigments. Another contributing factor is the greater amount of photoprotective pigments (carotenoids), which reduce damage to the photosynthetic apparatus, especially under NL. With a larger number of photosynthetic reaction centers, these mutants have a great advantage in high light environment, taking time to reach the *LSP*, and thus can absorb more light energy to promote the next phases of photosynthesis, which can be limited by Rubisco's maximum carboxylation rate (V_{cmax}) (Quebbeman and Ramirez, 2016; Farquhar et al., 1980). The *hp* mutants showed higher V_{cmax} even under shading, as observed mainly for *hp2* in S80 (Table 4), showing that they are less limited than WT on this factor. This response might be due, at least partially, to the larger number and size of plastids, in addition to increasing the amount of light energy absorbed and consequently higher the *ETR*, that also promotes greater Rubisco concentration in the leaves.

Leaf anatomical changes occur in response to *hp* mutation and shadow increment

Increasing shading up to 80% negatively affected leaf thickness of all genotypes. At the same time, both *hp1* and *hp2* mutant plants had higher parenchymal thickness and total thickness (Figure 6C, D and F). Epidermis thickness in plants is a highly plastic characteristic and has been responsive to different environmental situations to which plants are subjected (Melo et al., 2011). Under NL condition, mutant plants also have higher stomatal index and density than WT on the adaxial face whereas on the abaxial face these parameters hardly differ among WT and *hp* mutant plants (Supplementary Table 1). These result are in agreement with those found by Melo et al. (2011), who further suggested that the behavior observed for *hp* mutants is typical of plants adapted to the sun when compared to shade.

***hp* mutation promotes an extensive metabolic reprogramming in tomato leaves**

Due to the interactive nature of metabolic pathways in plants, pigment metabolism is likely to be modulated or interconnected with other cellular and metabolic processes (Yuan et al., 2016). Therefore, changes in metabolic pathways are expected when evaluating *hp* mutants. Here we found that mutants, as expected, have a higher concentration of photosynthetic pigments than WT, and this concentration tends to increase with the intensification of shading (Figure 7C, D and E). One fact that leads us to believe that the high pigmentation trait may represent an additional metabolic expense for the plant is that, although these mutant plants presented higher *A,* they did not have higher carbohydrate accumulation in leaves (Figure 8A-L), specially at S80. Primary metabolism provides, for all cells, energy, regeneration cofactor and building blocks for biomass and secondary metabolism (Rontein et al., 2002). Thus, pigments can be considered carbon skeletal metabolites, provided by primary metabolism, and of high value to plants. In this context, the higher induction and synthesis of these compounds associated with secondary metabolism clearly affects primary metabolism.

The carbohydrate produced in the photosynthetic process is used for growth , compounds production and energy (ATP), involving glycolysis and TCA cycle. The intermediates of these processes are used not only for respiration, but also, directly or

indirectly, on the biosynthesis of other metabolites such as amino acids (Krahmer et al., 2018) hormones and a secondary compounds range (Araújo et al., 2014). In the present study, we found a large accumulation of amino acids in *hp* mutants under NL conditions, from the 12 amino acids determined via GCMS, the vast majority had high content in the *hp1* and *hp2* plants when compared to WT (Figure 9, Supplementary Figure 2). Krahmer et al. (2018) suggest that one possibility for high amino acid levels is the low rate of protein synthesis. However, we found that the *hp1* mutant presented higher protein level under both NL and S50 (Figure 7A and B). In this case, another possibility is that with the higher rate of CO_2 assimilation, mutants can provide more carbon skeletons for amino acid metabolism. In agreement with this, it is noted that with increasing shading levels the amino acid content decreased in relation to the NL condition, in some cases the mutants have lower amino acid values than WT as glycine and isoleucine in S80 (Supplementary Figure 4).

On the other hand, following this line of reasoning, the content of organic acids and sugars was not higher in the mutant plants when compared to WT, in fact the content of some of these metabolites was lower mainly under the effect of shading (Figure 9, Supplementary Figure 2). Therefore, although the possibility of greater supply of carbon skeletons is viable, somehow some pathway are adequately supplied over than others, possibly by redirection to pigment biosynthesis. Yuan et al. (2016) were able to confirm, through their genomic scale metabolic network model, that under non-stressful conditions, isopentenyl diphosphate (IPP) is synthesized by the methylerythritol phosphate (MEP) chloroplast pathway, which supports that isoprenoids are mainly produced using carbon skeletons directly derived from the Calvin-Benson cycle via the photosynthesis-dependent MEP pathway. Knowing that chlorophylls and carotenoid-related pigments are derived from this chloroplastic pathway (Lichtenthaler et al., 1997), we can suggest that metabolic reprogramming occurs in *hp* mutants to support the increased demand for pigment biosynthesis.

3.5 CONCLUSIONS

In summary, we observed that the increase in the root/shoot ratio as well as the leaf area may be associated with increased photosynthetic rates due to lower stomatal limitation and higher V_{cmax} associated with anatomical modifications. Unfortunately, these changes occurs at the expense of reduction in the number of flowers and fruits and delay in the beginning of flowering, although the harvest index remains similar across genotypes. Such changes are mainly minimized by shading, as the growth of *hp* mutants is similar to WT plants under low light; however, the changes mentioned above are maintained, albeit at lower levels, mainly due to extensive metabolic reprogramming. Collectively, our data suggest that increasing pigment levels have little effect on overall plant growth, although extensive physiological and metabolic changes occur to support the maintenance of pigment biosynthesis.

We additionally postulate that overall changes promoted by the *hp* mutations are most likely involved more in protection against light-induced oxidative stress. Thus, metabolic adjustments that occurs in *hp* mutant plants are not associated with photosynthetic performance *per se*, but are rather associated with energy dissipation and ROS scavenger at the leaf level. Whilst our data provide a clear connection between primary metabolism and pigments biosynthesis, future research efforts are still required to fully elucidate the precise factors underlying this intriguingly metabolic phenotype.

3.6 ACKNOWLEDGEMENTS

The authors would like to acknowledge Professor Dr. Lázaro E. P. Peres (Escola Superior de Agricultura Luiz de Queiroz -ESALQ/USP, Brazil) for sharing the seeds used in this work. This work was supported by funding from the Max Planck Society (to WLA), the National Council for Scientific and Technological Development (CNPq-Brazil, Grant 402511/2016-6 to WLA), and the FAPEMIG (Foundation for Research Assistance of the Minas Gerais State, Brazil, Grant APQ- 01078-15). We also thank the scholarships granted by the Brazilian Federal Agency for Support and Evaluation of Graduate Education (CAPES-

Brazil) to AMP. Research fellowships granted by CNPq-Brazil to ANN and WLA are also gratefully acknowledged.

3.7 REFERENCES

Abuajah CI, Ogbonna AC, Osuji CM (2015) Functional components and medicinal properties of food: a review. Journal of Food Science and Technology **52**: 2522–2529

Araújo WL, Martins AO, Fernie AR, Tohge T (2014) 2-oxoglutarate: Linking TCA cycle function with amino acid, glucosinolate, flavonoid, alkaloid, and gibberellin biosynthesis. Frontiers in Plant Science **5**: 1–6

Arvidsson S, Kwasniewski M, Riaño-Pachón DM, Mueller-Roeber B (2008) QuantPrime - A flexible tool for reliable high-throughput primer design for quantitative PCR. BMC Bioinformatics **9**: 1–15

Ballaré CL, Pierik R (2017) The shade-avoidance syndrome: Multiple signals and ecological consequences. Plant Cell and Environment **40**: 2530–2543

Björkman O (1981) Responses to different quantum flux densities. Physiol Plant Ecol I (eds Lange OL, Nobel PS, Osmond CB Ziegler H), pp 57–107 Springer, Berlin Heidelberg 57–107

Björkman O, Demmig B (1987) Photon yield of O_2 evolution and chlorophyll fluorescence characteristics at 77 K among vascular plants of diverse origins. Planta **170**: 489–504

BRADFORD MM (1976) A rapid and sensitive method for the quantitation of microgram quantities of protein utilizing the principle of protein-dye binding. Analytical Biochemistry **72**: 248–254

Buckley TN, Mott KA (2013) Modelling stomatal conductance in response to environmental factors. Plant, Cell and Environment **36**: 1691–1699

von Caemmerer S (2000) Biochemical models of leaf photosynthesis. CSIRO Publishing, Collingwood

Caldana C, Scheible WR, Mueller-Roeber B, Ruzicic S (2007) A quantitative RT-PCR platform for high-throughput expression profiling of 2500 rice transcription factors. Plant Methods **3**: 1–9

Campostrini E (2001) Fluorescência da clorofila *a*: considerações teóricas e aplicações práticas. Universidade Estadual do Norte Fluminense, Rio de Janeiro, 34p

Chen H, Huang X, Gusmaroli G, Terzaghi W, Lau OS, Yanagawa Y, Zhang Y, Li J, Lee JH, Zhu D, et al (2010) Arabidopsis CULLIN4-damaged DNA binding protein 1 interacts with CONSTITUTIVELY PHOTOMORPHOGENIC1-SUPPRESSOR OF PHYA complexes to regulate photomorphogenesis and flowering time. Plant Cell **22**: 108–123

Cockshull KE, Graves CJ, Cave CRJ (1992) The influence of shading on yield of glasshouse tomatoes. Journal of Horticultural Science **67**: 11–24

Critchley C (1998) Photoinhibition. In: Raghavendra AS. Photosynthesis: A comprehensive treatise. Ed. Cambridge University Press, Cambridge, pp 264–272

Davuluri GR, Van Tuinen A, Mustilli AC, Manfredonia A, Newman R, Burgess D, Brummell DA, King SR, Palys J, Uhlig J, et al (2004) Manipulation of DET1 expression in tomato results in photomorphogenic phenotypes caused by post-transcriptional gene silencing. Plant Journal **40**: 344–354

El-Gizawy AM, Abdallah MMF, Gomaa HM, Mohamed SS (1992) Effect of different shading levels on tomato plants. 2. Yield and fruit quality. Acta Horticuturae **323**: 349–354

Farquhar GD, Caemmerer S Von, Berry JA (1980) A biochemical model of photosynthetic CO_2 assimilation in leaves of C_3 Species. Planta **90**: 78–90

Fernie AR, Aharoni A, Willmitzer L, Stitt M, Tohge T, Kopka J, Carroll AJ, Saito K, Fraser PD, de Luca V (2011) Recommendations for reporting metabolite data. Plant Cell **23**: 2477–2482

Fernie AR, Roscher A, Ratcliffe RG, Kruger NJ (2001) Fructose 2,6-bisphosphate activates pyrophosphate: fructose-6-phos-phate-1 phosphotransferase and increases triose phosphate to hexose phosphate cyclingin heterotrophic cells. Planta **212**: 250–263

Genty B, Briantais J-M, Baker NR (1989) The relationship between the quantum yield of photosynthetic electron transport and quenching of chlorophyll fluorescence. Biochimica et Biophysica Acta (BBA) - General Subjects **990**: 87–92

Gibon Y, Blaesing OE, Hannemann J, Carillo P, Ho M, Palacios N, Cross J, Selbig J, Stitt M (2004) A robot-based platform to measure multiple enzyme activities in arabidopsis using a set of cycling assays : comparison of changes of enzyme activities and transcript levels during diurnal cycles and in prolonged darkness. The Plant Cell **16**: 3304–3325

Huang T, Tohge T, Lytovchenko A, Fernie AR, Jander G (2010) Pleiotropic physiological consequences of feedback-insensitive phenylalanine biosynthesis in *Arabidopsis thaliana*. Plant Journal **63**: 823–835

Ilahy R, Siddiqui MW, Tlili I, Montefusco A, Piro G, Hdider C, Lenucci MS (2018) When color really matters: horticultural performance and functional quality of high-lycopene tomatoes. Critical Reviews in Plant Sciences **37**: 15–53

Jarret R, Sayama H, Tigchelaar E (1984) Pleiotropic effects associated with the chlorophyll intensifier mutations high pigment and dark green in tomato. Journal of the American Society for Horticultural Science **109**: 873–878

Johansen DA (1940) Plant microtechnique. McGraw-Hill Book, New York

Kang JW, Lee NY, Cho KC, Lee MY, Choi DY, Park SH, Kim KP (2015) Analysis of nitrated proteins in *Saccharomyces cerevisiae* involved in mating signal transduction. Proteomics **15**: 580–590

Kendrick RE, Kerckhooffs LHJ, van Tuinen A, Koornneef M (1997) Photomorphogenic mutants of tomato. Plant, Cell and Environment **20**: 746–751

Kläring HP, Krumbein A (2013) The effect of constraining the intensity of solar radiation on the photosynthesis, growth, yield and product quality of tomato. Journal of Agronomy and Crop Science **199**: 351–359

Kopka J, Schauer N, Krueger S, Birkemeyer C, Usadel B, Bergmüller E, Dörmann P, Weckwerth W, Gibon Y, Stitt M, et al (2005) GMD@CSB.DB: The Golm metabolome database. Bioinformatics **21**: 1635–1638

Krahmer J, Ganpudi A, Abbas A, Romanowski A, Halliday KJ (2018) Phytochrome, carbon sensing, metabolism, and plant growth plasticity. Plant Physiology **176**: 1039–1048

Kunderlikova K, Brestic M, Zivcak M, Kusniarova P (2016) Photosynthetic responses of sun- and shade-grown chlorophyll b deficient mutant of wheat. Journal of Central European Agriculture **17**: 950–956

Levin I, Frankel P, Gilboa N, Tanny S, Lalazar A (2003) The tomato dark green mutation is a novel allele of the tomato homolog of the DEETIOLATED1 gene. Theoretical and Applied Genetics **106**: 454–460

Lichtenthaler HK, Schwender J, Disch A, Rohmer M (1997) Biosynthesis of isoprenoids in higher plant chloroplasts proceeds via a mevalonate-independent pathway. FEBS Letters **400**: 271–274

Lieberman M, Segev O, Gilboa N, Lalazar A, Levin I (2004) The tomato homolog of the gene encoding UV-damaged DNA binding protein 1 (DDB1) underlined as the gene that causes the high pigment-1 mutant phenotype. Theoretical and Applied Genetics **108**: 1574–1581

Lisec J, Schauer N, Kopka J, Willmitzer L, Fernie AR (2006) Gas chromatography mass spectrometry-based metabolite profiling in plants. Nature Protocols **1**: 387–396

Liu F, Song R, Zhang X, Shahnazari A, Andersen MN, Plauborg F, Jacobsen SE, Jensen CR (2008) Measurement and modelling of ABA signalling in potato (*Solanum tuberosum* L.) during partial root-zone drying. Environmental and Experimental Botany **63**: 385–391

Liu Y, Roof S, Ye Z, Barry C, van Tuinen A, Vrebalov J, Bowler C, Giovannoni J (2004) Manipulation of light signal transduction as a means of modifying fruit nutritional quality in tomato. Proceedings of the National Academy of Sciences of the United States of America **101**: 9897–902

Logan BA, Adams WW, Demmig-Adams B (2007) Avoiding common pitfalls of chlorophyll fluorescence analysis under field conditions. Functional Plant Biology **34**: 853–859

Long SP, Bernacchi C (2003) Gas exchange measurements, what can they tell us about the underlying limitations to photosynthesis? Procedures and sources of error. Journal of Experimental Botany **54**: 2393–2401

Luedemann A, Malotky L von, Erban A, Kopka J (2011) TagFinder: Preprocessing software for the fingerprinting and the profi ling of gas chromatography–mass spectrometry based metabolome analyses. Plant Metabolomics **860**: 255–286

Martí E, Gisbert C, Bishop GJ, Dixon MS, García-Martínez JL (2006) Genetic and physiological characterization of tomato cv. Micro-Tom. Journal of Experimental Botany **57**: 2037–2047

Martins SC V., Araújo WL, Tohge T, Fernie AR, DaMatta FM (2014) In high-light-acclimated coffee plants the metabolic machinery is adjusted to avoid oxidative stress rather than to benefit from extra light enhancement in photosynthetic yield. PLoS One **9**: e94862

Martins SC V, Galmés J, Molins A, DaMatta FM (2013) Improving the estimation of mesophyll conductance to CO_2: on the role of electron transport rate correction and respiration. Journal of Experimental Botany **64**: 3285–98

Mauro RP, Occhipinti A, Longo AMG, Mauromicale G (2011) Effects of shading on chlorophyll content, chlorophyll fluorescence and photosynthesis of subterranean clover. Journal of Agronomy and Crop Science **197**: 57–66

Medeiros DB, Martins SCV, Cavalcanti JHF, Daloso DM, Martinoia E, Nunes-Nesi A, DaMatta FM, Fernie AR, Araújo WL (2016) Enhanced photosynthesis and growth in atquac1 knockout mutants are due to altered organic acid accumulation and an increase in both stomatal and mesophyll conductance. Plant Physiology **170**: 86–101

Melo HC, de Castro EM, Alves E, Perina FJ (2011) Leaf anatomy of micro-tomato phytochrome-mutants and chloroplast ultra-structure. Ciencia e Agrotecnologia **35**: 11–18

Melo HC, Castro EM, SOARES AM, Oliveira C, RAMOS SJ (2009) Micro-tomato phytochrome-mutants. Ciência e Agrotecnologia **33**: 1213–1219

Mohammed GH, Binder WD, Gillies SL (1995) Chlorophyll fluorescence: A review of its practical forestry applications and instrumentation. Scandinavian Journal of Forest Research **10**: 383–410

Mustilli AC, F. F, CILIENTO R, ALFONSO F, BOWLER C (1999) Phenotype of the Tomato *high pigment-2* mutant is caused by a mutation in the tomato homolog of *DEETIOLATED1*. Plant Cell Online **11**: 145–158

O'Brien TP, Feder N, McCully ME (1964) Polychromatic staining of plant cell walls by toluidine blue O. Protoplasma **59**: 368–373

Papadopoulos AP, Hao X (1997) Effects of three greenhouse cover materials on tomato growth, productivity, and energy use. Scientia Horticulturae **70**: 165–178

Pazhouhandeh M, Molinier J, Berr A, Genschik P (2011) MSI4/FVE interacts with CUL4-DDB1 and a PRC2-like complex to control epigenetic regulation of flowering time in *Arabidopsis*. Proceedings of the National Academy of Sciences of the United States of America **108**: 3430–3435

Pearcy RW, Way DA (2012) Two decades of sunfleck research: Looking back to move forward. Tree Physiology **32**: 1059–1061

Pepper A, Delaney T, Washburnt T, Poole D, Chory J (1994) *DET1*, a negative regulator of light-mediated development and gene expression in arabidopsis, encodes a novel nuclear-localized protein. Cell **78**: 109–116

Perveen R, Suleria HAR, Anjum FM, Butt MS, Pasha I, Ahmad S (2015) Tomato (*Solanum lycopersicum*) Carotenoids and lycopenes chemistry; metabolism, absorption, nutrition, and allied health claims—A Comprehensive Review. Critical Reviews in Food Science and Nutrition **55**: 919–929

Peters JL, Schreuder MEL, Verduin SJW, Kendrick RE (1992) Physiological characterization of a high-pigment mutant of tomato. Photochemistry and Photobiology **56**: 75–82

Peters JL, Széll M, Kendrick RE (1998) The Expression of light-regulated genes in the high-pigment-1 mutant of tomato. Plant Physiology **117**: 797–807

Pino-Nunes LE, Lattarulo M, P Peres LE (2010) Manual do modelo vegetal micro-tom capitulo 2: plantio, irrigação e adubação nas canaletas/vasos e cultivo no canteiro. Laboratory of hormonal control of plant development (ESALQ), Piracicaba 7p

Quebbeman JA, Ramirez JA (2016) Optimal allocation of leaf-level nitrogen: Implications for covariation of V_{cmax} and J_{max} and photosynthetic downregulation. Journal of Geophysical Research: Biogeosciences **121**: 2464–2475

Reed S, Schnell R, Moore JM, Dunn C (2012) Chlorophyll a + b Content and Chlorophyll Fluorescence in Avocado. Journal of Agricultural Science **4**: 29–36

Rodeghiero M, Niinemets Ü, Cescatti A (2007) Major diffusion leaks of clamp-on leaf cuvettes still unaccounted: How erroneous are the estimates of Farquhar et al. model parameters? Plant, Cell and Environment **30**: 1006–1022

Roessner U, Luedemann A, Brust D, Fiehn O, Linke T, Willmitzer L, Fernie AR (2001) Metabolic profiling allows comprehensive phenotyping of genetically or environmentally modified plant systems. Plant Cell **13**: 11–29

Rontein D, Dieuaide-Noubhani M, Dufourc EJ, Raymond P, Rolin D (2002) The metabolic architecture of plant cells: Stability of central metabolism and flexibility of anabolic pathways during the growth cycle of tomato cells. Journal of Biological Chemistry **277**: 43948–43960

Sasanuma T (2001) Characterization of the rbcS multigene family in wheat: Subfamily classification, determination of chromosomal location and evolutionary analysis. Molecular and General Genetics **265**: 161–171

Sharkey TD, Bernacchi CJ, Farquhar GD, Singsaas EL (2007) Fitting photosynthetic carbon dioxide response curves for C 3 leaves. Plant, Cell and Environment **30**: 1035–1040

Sims DA, Pearcy RW (1993) Sunfleck frequency and duration affects growth rate of the understorey plant , alocasia macrorrhiza. Functional Ecology **7**: 683–689

Smith IE, Savage MJ, Mills P (1984) Shading effects on greenhouse tomatoes and cucumbers. Acta Horticulturae **148**: 491–500

Spreitzer RJ, Salvucci ME (2002) RUBISCO: Structure, regulatory interactions, and possibilities for a better enzyme. Annual Review of Plant Biology **53**: 449–475

Tang X, Miao M, Niu X, Zhang D, Cao X, Jin X, Zhu Y, Fan Y, Wang H, Liu Y, et al (2016) Ubiquitin-conjugated degradation of golden 2-like transcription factor is mediated by CUL4-DDB1-based E3 ligase complex in tomato. New Phytologist **209**: 1028–1039

Valladares F, Niinemets Ü (2008) Shade tolerance, a key plant feature of complex nature and consequences. Annual Review of Ecology, Evolution, and Systematics **39**: 237–257

Vanstraelen M, Benková E (2012) Hormonal interactions in the regulation of plant development. Annual Review of Cell and Developmental Biology **28**: 463–487

Vialet-Chabrand S, Matthews JSA, Simkin AJ, Raines CA, Lawson T (2017) Importance of fluctuations in light on plant photosynthetic acclimation. Plant Physiology **173**: 2163–2179

Wang S, Liu J, Feng Y, Niu X, Giovannoni J, Liu Y (2008) Altered plastid levels and potential for improved fruit nutrient content by downregulation of the tomato DDB1-interacting protein CUL4. Plant Journal **55**: 89–103

Wellburn AR (1994) The spectral determination of chlorophylls *a* and *b*, as well as total carotenoids, using various solvents with spectrophotometers of different resolution. Journal of Plant Physiology **144**: 307–313

Wolters H, Jürgens G (2009) Survival of the flexible: Hormonal growth control and adaptation in plant development. Nature Reviews Genetics **10**: 305–317

Xiong D, Douthe C, Flexas J (2018) Differential coordination of stomatal conductance, mesophyll conductance, and leaf hydraulic conductance in response to changing light across species. Plant Cell and Environment **41**: 436–450

Xu D, Zhu D, Deng XW (2016) The role of COP1 in repression of photoperiodic flowering. F1000Research **5**: 1–5

Yamori W, Shikanai T (2016) Physiological functions of cyclic electron transport around photosystem i in sustaining photosynthesis and plant growth. Annual Review of Plant Biology **67**: 81–106

Yemm EW, Cocking EC, Ricketts RE (1955) The determination of amino-acids with ninhydrin. Analyst 80: 209–214

Yuan H, Cheung CYM, Poolman MG, Hilbers PAJ, Van Riel NAW (2016) A genome-scale metabolic network reconstruction of tomato (*Solanum lycopersicum* L.) and its application to photorespiratory metabolism. Plant Journal **85**: 289–304

Zsögön A, Alves Negrini AC, Peres LEP, Nguyen HT, Ball MC (2015) A mutation that eliminates bundle sheath extensions reduces leaf hydraulic conductance, stomatal conductance and assimilation rates in tomato (*Solanum lycopersicum*). New Phytologist **205**: 618–626

3.8 FIGURES AND TABLES

Table 1 - Relative expression of *DDB1* and *DET1* genes in WT plants and *hp1* and *hp2* mutants. Means followed by the same letter in vertical did not differ (P <0.05) significantly from WT plants by the Duncan test. Values are presented as means ± standard error (n = 4).

	DDB1	*DET1*
WT	1.02 ± 0.12 a	1.01 ± 0.10 a
hp1	1.03 ± 0.14 a	1.00 ± 0.26 a
hp2	1.25 ± 0.20 a	1.43 ± 0.34 a

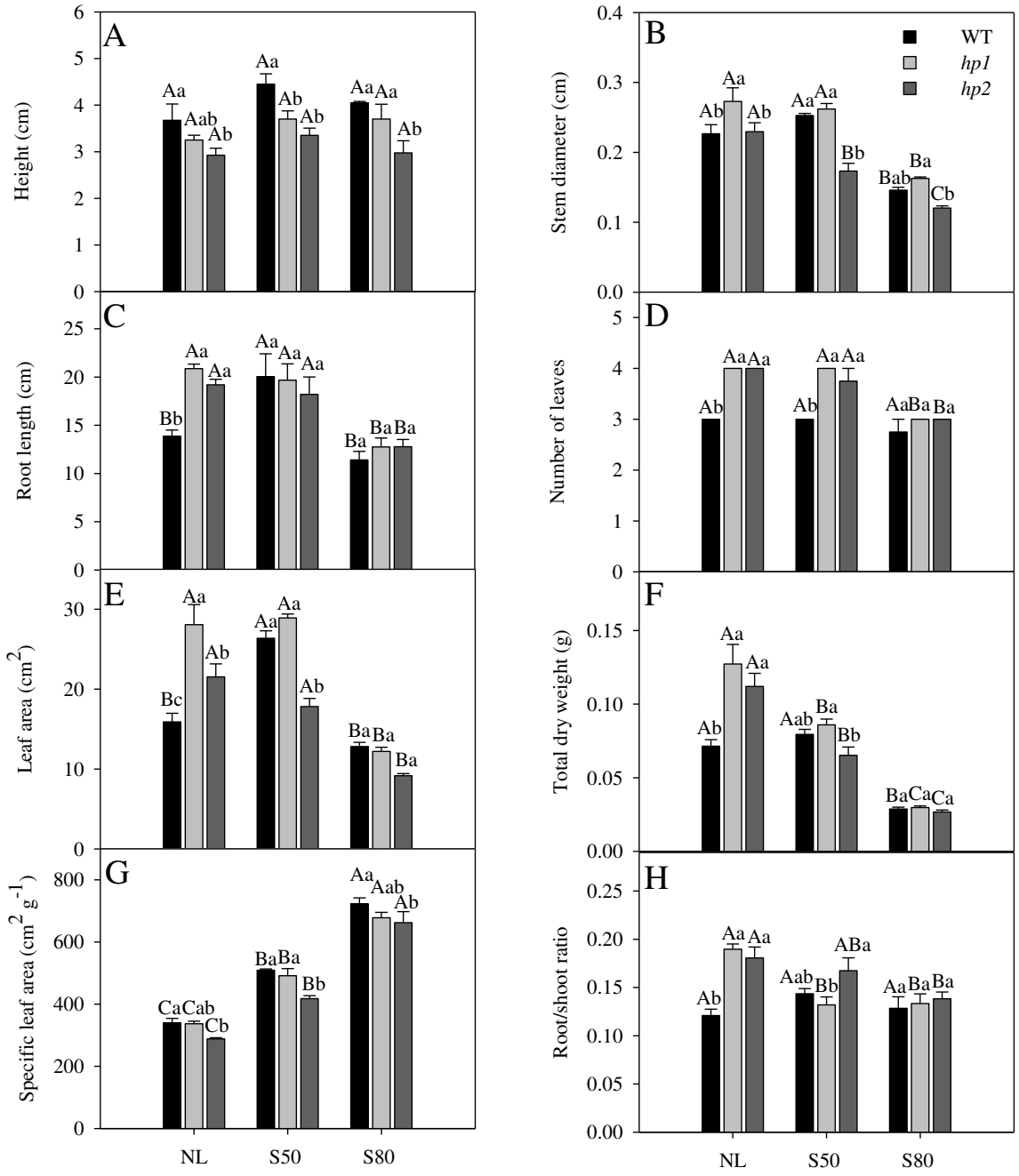

Figure 1 – Morphological changes in response to shading in *hp* mutant plants at vegetative stage. Changes were observed in Micro-Tom (WT) plants and *hp1* and *hp2* mutants growing under natural light conditions (NL) and two levels of shading (S50 and S80)). Evaluations were carried out on four-week-old plants (28 DAP). (A) Heigth; (B) Stem diameter; (C) Root length; (D) Number of leaves; (E) Leaf area; (F) Total dry weight; (G) Specific leaf area; (H) Root/Shoot ratio. Means followed by the same letter do not differ from each other (P <0.05) by the Duncan test. Capital letters compare the same genotype in different treatments; lower case letters compare the different genotypes within each treatment. Values are presented as means ± standard error (n = 4).

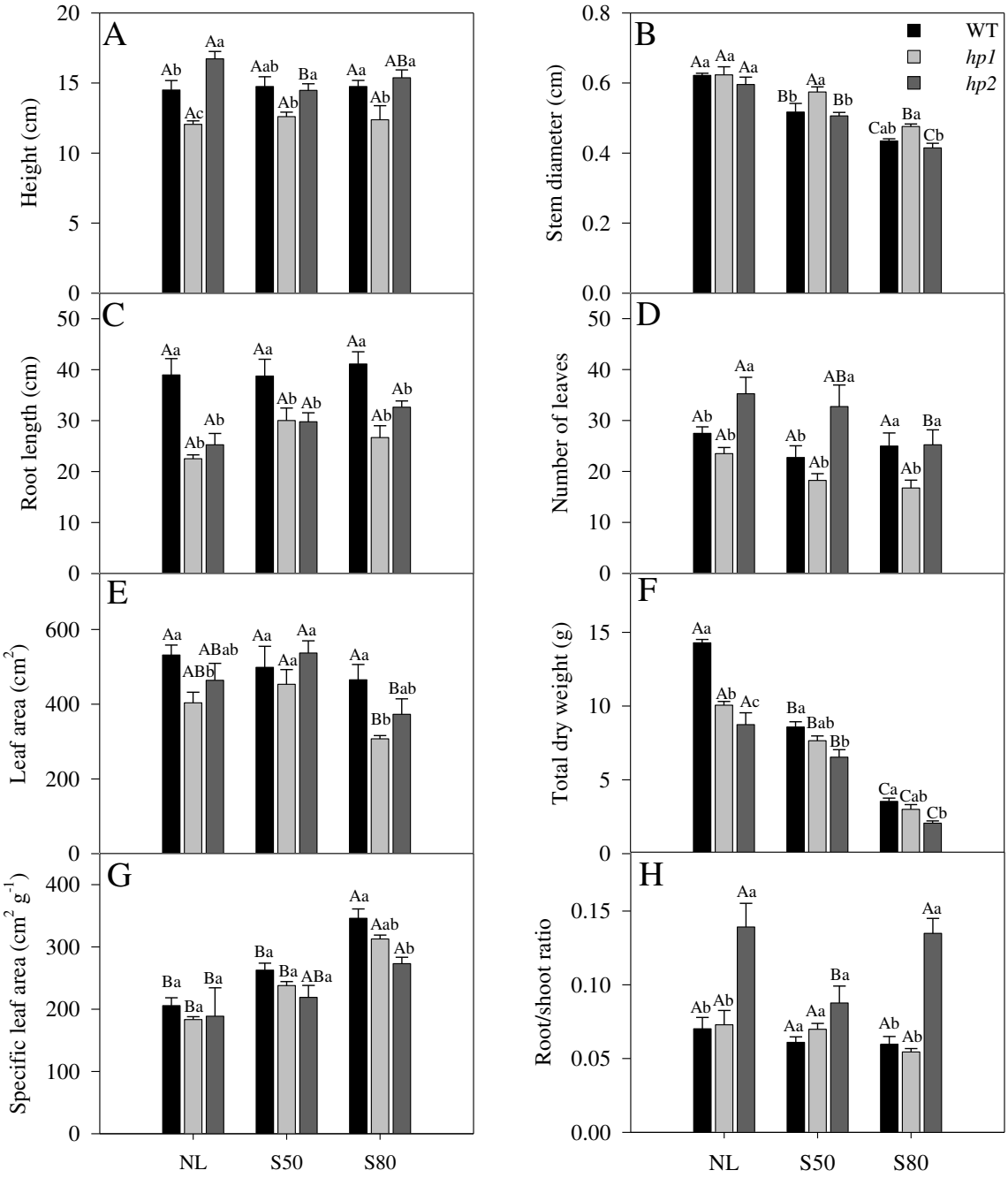

Figure 2 – Morphological changes in response to shading in *hp* mutant plants at reproductive stage. Changes were analysed in Micro-Tom (WT) plants and *hp1* and *hp2* mutants grown under natural light conditions (NL) and two levels of shading (S50 and S80). Evaluations were carried out on twelve-week-old plants (82 DAP). (A) Height; (B) Stem diameter; (C) Root length; (D) Number of leaves; (E) Leaf area; (F) Total dry weight; (G) Specific leaf area; (H) Root/Shoot ratio. Means followed by the same letter do not differ from each other (P <0.05) by the Duncan test. Capital letters compare the same genotype in different treatments; lower case letters compare the different genotypes within each treatment. Values are presented as means ± standard error (n = 4).

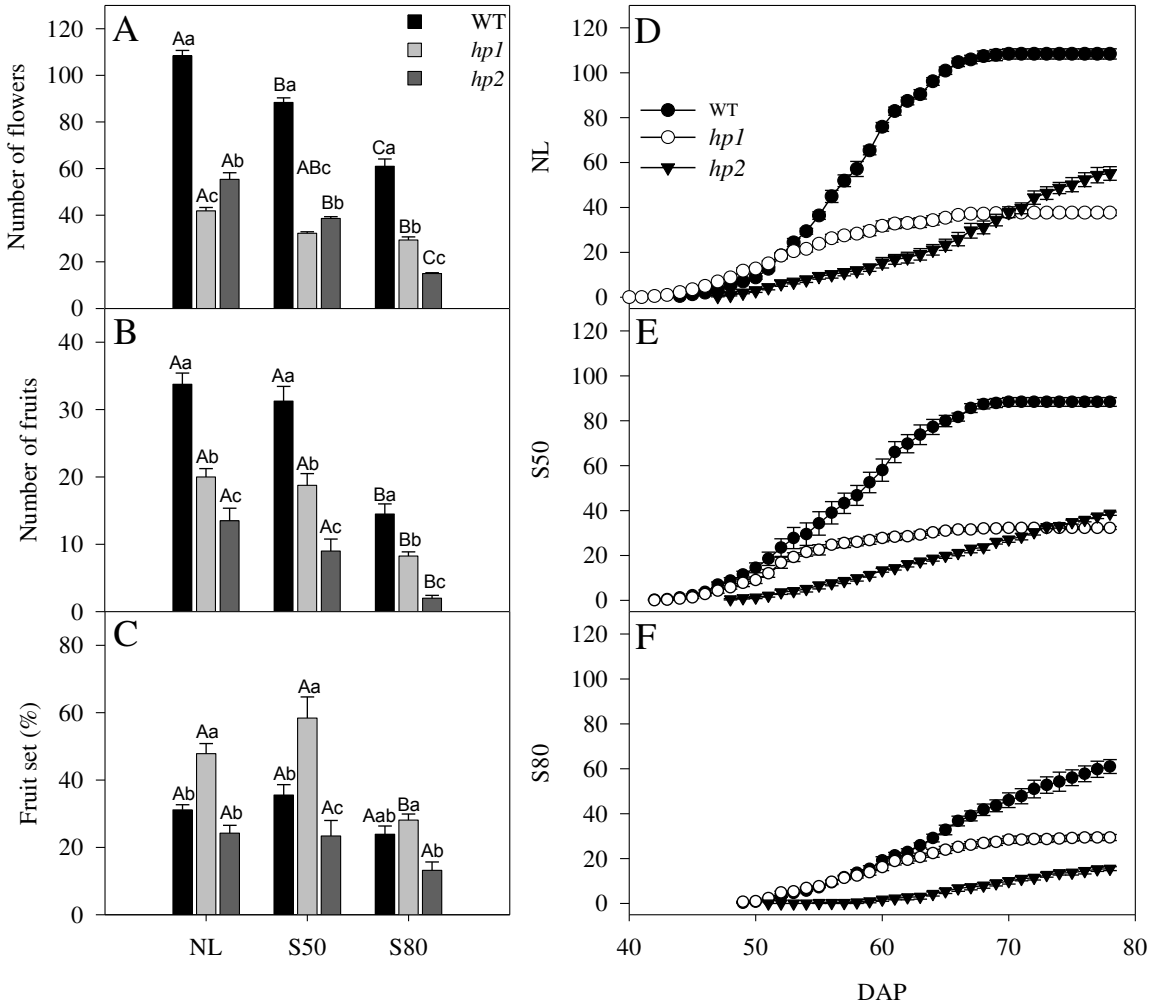

Figure 3 - Changes in yield of Micro-Tom (WT) and *hp1* and *hp2* mutants grown under natural light conditions (NL) and two levels of shading (S50 and S80). Evaluations were carried out on twelve-week-old plants (82 DAP). (A) Number of flowers; (B) number of fruits; (C) Fruit set; (D, E and F) Cumulative number of flowers. Means followed by the same letter do not differ ($P < 0.05$) by the Duncan test. Capital letters compare the same genotype in different treatments; lower case letters compare the different genotypes within each treatment. Values are presented as means ± standard error (n = 4).

Table 2 - Changes in growth rates and yield of Micro-Tom (WT) plants and *hp1* and *hp2* mutants grown under natural light conditions (NL) and two levels of shading (S50 and S80). Evaluations were carried out on four twelve old plants (82 DAP). (FDW) Fruit dry weight; (RGR) Relative growth rate; (HI) Harvest index. Means followed by the same letter do not differ (P <0.05) by the Duncan test. Capital letters, vertically, compare the same genotype in different treatments; lower case letters compare the different genotypes within each treatment. Values are presented as means ± standard error (n = 4).

		FDW	RGR	HI
NL	WT	7.47 ± 0.27 Aa	18.43 ± 0.01 Aa	52.24 ± 1.46 Aa
	hp1	5.76 ± 0.11 Ab	18.29 ± 0.02 Aa	57.37 ± 1.80 Aa
	hp2	2.90 ± 0.77 Ac	18.27 ± 0.03 Aa	32.98 ± 8.58 Ab
S50	WT	4.55 ± 0.12 Ba	18.35 ± 0.01 Aa	53.21 ± 2.35 Aa
	hp1	4.26 ± 0.17 Ba	18.31 ± 0.01 Aa	55.66 ± 1.19 Aa
	hp2	2.50 ± 0.41 Ab	18.33 ± 0.02 Aa	38.14 ± 6.14 Ab
S80	WT	1.30 ± 0.20 Ca	18.36 ± 0.02 Aa	32.63 ± 5.76 Bb
	hp1	1.42 ± 0.21 Ca	18.32 ± 0.03 Aa	46.51 ± 2.40 Aa
	hp2	0.03 ± 0.00 Bb	18.27 ± 0.02 Aa	1.23 ± 0.04 Bc

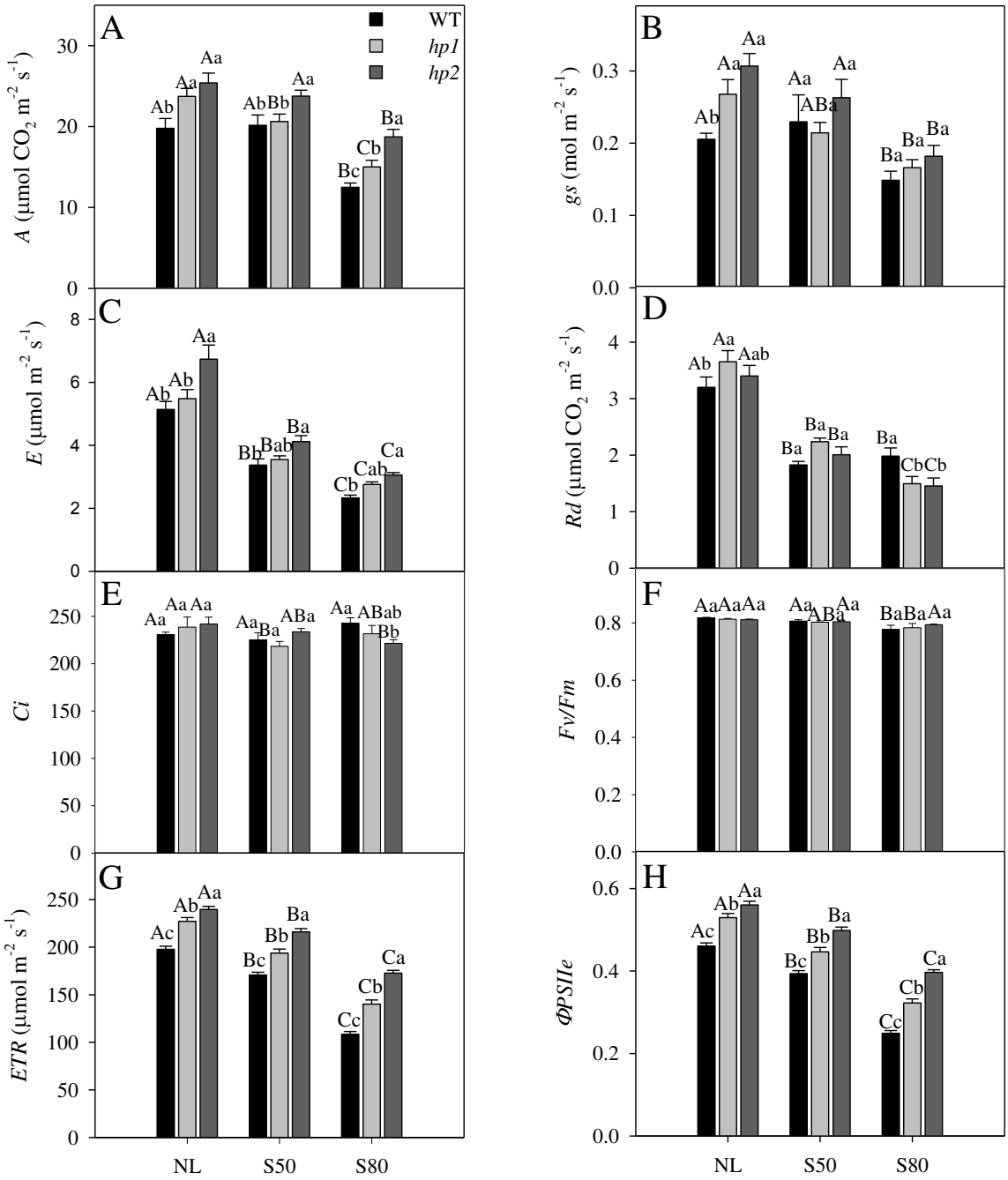

Figure 4 - Changes in gas exchange and fluorescence parameters of Micro-Tom (WT) and *hp1* and *hp2* mutants grown under natural light conditions (NL) and two levels of shading (S50 and S80). Evaluations were carried out on four-week-old plants (28 DAP). (A) *A*: Photosynthesis; (B) *Rd*: Dark respiration; (C) *gs*: Stomatal conductance; (D) *Ci*: Internal CO_2 concentration; (E) *Fv/Fm* ratio; (F) *E*: transpiration; (G) *ETR*: electron transport rate; (H) *ΦFSII*: effective quantum yield of Photosystem II. Means followed by the same letter do not differ (P <0.05) by the Duncan test. Capital letters compare the same genotype in different treatments; lower case letters compare the different genotypes within each treatment. Values are presented as means ± standard error (n = 6).

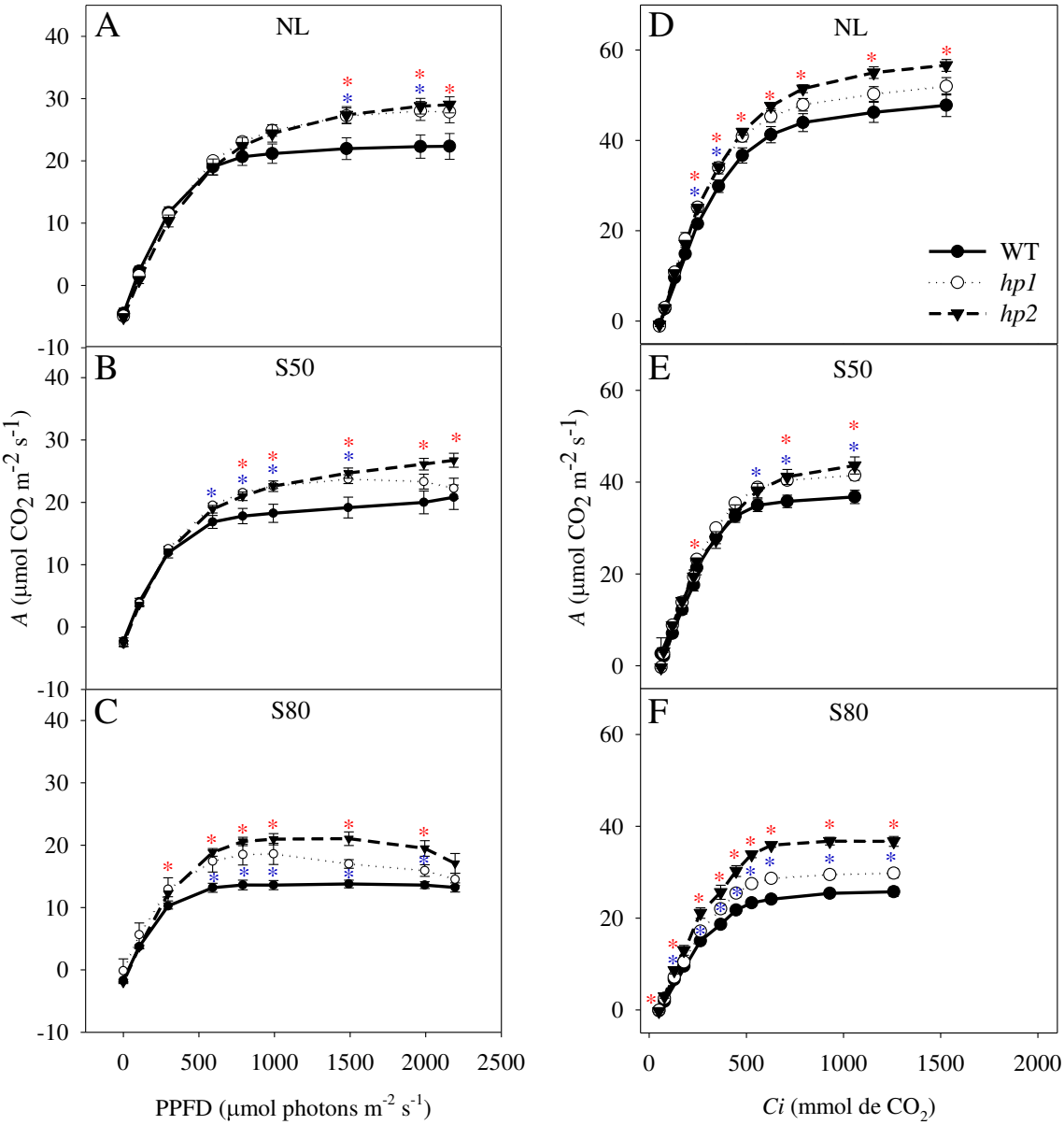

Figure 5 - Photosynthesis curves (*A*) in response to changes in both photosynthetic photon flux density (PPFD) and internal CO_2 concentration (*Ci*) of Micro-Tom plants (WT) and *hp1* and *hp2* mutants grown under natural light conditions (NL) and two levels of shading (S50 and S80). Evaluations were carried out on four-week-old plants (28 DAP). AsAterisks indicate at which point in the curve the mutants were significantly different to WT according to Student's t-test (P <0.05); *hp1* blue asterisk, *hp2* red asterisk. Values are presented as means ± standard error (n = 6).

Table 3 - Photosynthetic parameters derived from light curves (*A*/PPFD) for Micro-Tom (WT) plants and *hp1* and *hp2* mutants grown under natural light conditions (NL) and two levels of shading (S50 and S80). Evaluations were carried out on four-week-old plants (28 DAP). DAP). A_{max}: net assimilation rate of carbon saturated by light; *LCP*: light compensation point; *LSP*: light saturation point; $1/\Phi$: light use efficiency. Means followed by the same letter do not differ (P <0.05) by the Duncan test. Capital letters compare, vertically, the same genotype in different treatments; lower case letters compare the different genotypes within each treatment. Values are presented as means ± standard error (n = 6).

		A_{max} (µmol CO_2 m^{-2} s^{-1})	*LCP* (mmol m^{-2} s^{-1})	*LSP* (mmol m^{-2} s^{-1})	$1/\phi$ (µmol photons mol^{-1} CO_2)
NL	WT	26.42 ± 1.36 Ac	83.85 ± 6.59 Aa	632.27 ± 50.09 ABb	16.48 ± 0.49 Ba
	hp1	34.21 ± 1.58 Ab	82.88 ± 6.04 Aa	1030.41 ± 39.64 Aa	15.27 ± 0.32 Ca
	hp2	38.75 ± 0.6 Aa	95.65 ± 8.31 Aa	1085.74 ± 23.99 Aa	15.60 ± 0.70 Ba
S50	WT	22.83 ± 1.79 Bc	41.62 ± 8.69 Ba	739.79 ± 75.22 Ab	14.46 ± 0.88 Cb
	hp1	26.11 ± 1.00 Bb	48.18 ± 5.98 Ba	712.38 ± 63.50 Bb	17.68 ± 0.56 Ba
	hp2	31.94 ± 0.80 Ba	44.50 ± 5.27 Ba	1064.24 ± 29.36 Aa	13.93 ± 0.36 Bb
S80	WT	15.31 ± 0.47 Cc	33.76 ± 2.08 Ba	559.13 ± 56.81 Ba	20.07 ± 0.39 Aa
	hp1	18.36 ± 0.88 Cb	35.91 ± 3.32 Ba	509.63 ± 45.40 Ca	21.15 ± 0.35 Aa
	hp2	22.66 ± 1.06 Ca	35.38 ± 2.52 Ba	566.88 ± 21.83 Ba	19.76 ± 0.30 Aa

Table 4 - Photosynthetic parameters derived from the *A/Ci* curve for Micro-Tom (WT) plants and *hp1* and *hp2* mutants grown under natural light conditions (NL) and two levels of shading (S50 and S80). Evaluations were carried out on four-week-old plants (28 DAP). V_{cmax}: maximum carboxylation rate; J_{max}: maximum carboxylation rate limited by electron transport; J_{max}/V_{cmax} ratio; *TPU*: triose phosphate utilization. Means followed by the same letter do not differ (P <0.05) by the Duncan test. Capital letters compare, vertically, the same genotype in different treatments; lower case letters compare the different genotypes within each treatment. Values are presented as means ± standard error (n = 6).

		Vc_{max} (µmol m^{-2} s^{-1})	J_{max} (µmol m^{-2} s^{-1})	J_{max}/V_{cmax}	*TPU* (mmol m^{-2} s^{-1})
NL	WT	96.21 ± 1.33 Ab	180.15 ± 3.64 Aa	1.87 ± 0.03 Aa	13.67 ± 0.19 Ab
	hp1	109.89 ± 2.27 Aa	186.33 ± 5.65 Aa	1.69 ± 0.03 Bb	14.50 ± 0.26 Aab
	hp2	104.40 ± 5.05 Aab	192.06 ± 6.51 Aa	1.85 ± 0.09 ABab	15.30 ± 0.36 Aa
S50	WT	88.75 ± v1.65 Ab	166.67 ± 3.16 Ab	1.88 ± 0.41 Aa	11.20 ± 0.16 Bb
	hp1	101.48 ± 1.23 Aa	186.01 ± 5.16 Aa	1.83 ± 0.05 Bab	12.12 ± 0.37 Bab
	hp2	100.79 ± 4.44 Aa	169.04 ± 9.72 Ab	1.68 ± 0.07 Bb	13.02 ± 0.60 Ba
S80	WT	59.79 ± 1.40 Bb	120.33 ± 1.25 Bc	2.02 ± 0.06 Aab	8.30 ± 0.21 Cc
	hp1	67.11 ± 2.55 Bb	140.91 ± 2.54 Bb	2.11 ± 0.08 Aa	9.86 ± 0.16 Cb
	hp2	88.57 ± 1.28 Ba	169.35 ± 2.77 Ba	1.91 ± 0.02 Ab	11.69 ± 0.25 Ca

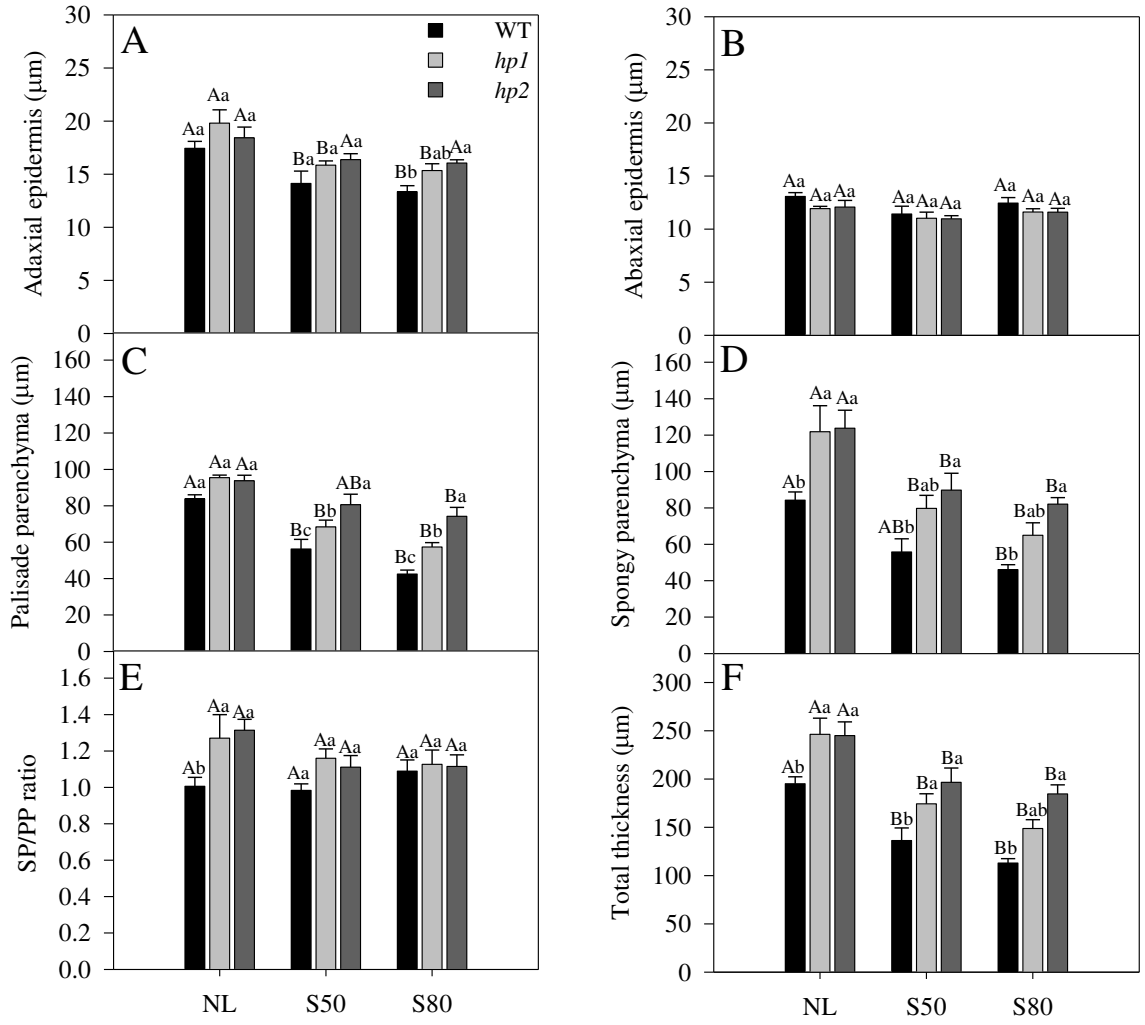

Figure 6 - Leaf limb measurements of Micro-Tom (WT) plants and *hp1* and *hp2* mutants grown under natural light conditions (NL) and two levels of shading (S50 and S80). Evaluations were carried out on four-week-old plants (28 DAP). (A) Adaxial epidermis; (B) Abaxial epidermis; (C) Palisade parenchyma; (D) Spongy parenchyma; (E) SP/PP ratio; (F) Total thickness. Means followed by the same letter do not differ (P <0.05) by the Duncan test. Capital letters compare the same genotype in different treatments; lower case letters compare the different genotypes within each treatment. Values are presented as means ± standard error (n = 4).

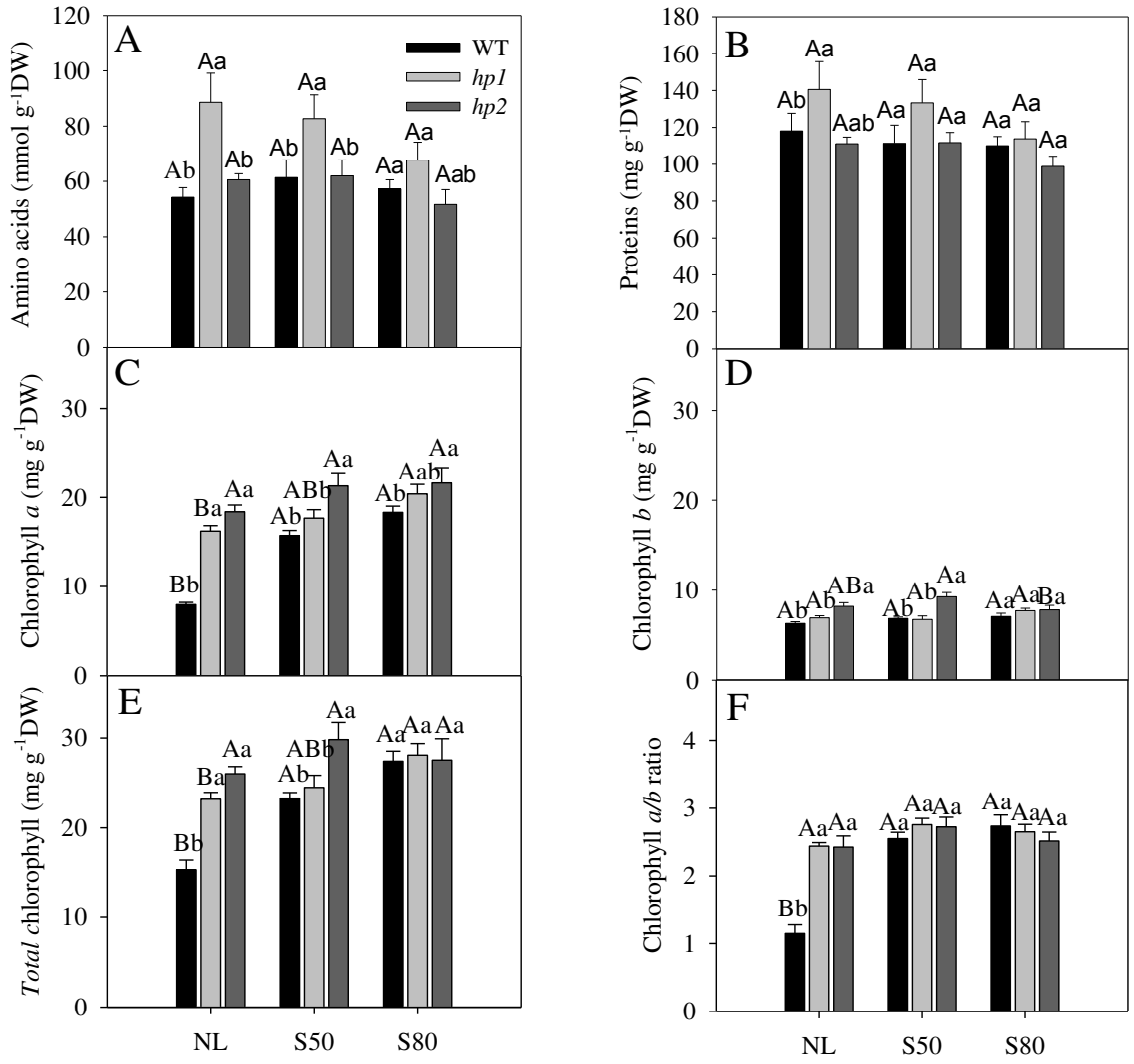

Figure 7 - Comparison of metabolite and pigment levels for Micro-Tom (WT) and *hp1* and *hp2* mutants grown under natural light conditions (NL) and two levels of shading (S50 and S80). Evaluations were carried out on four-week-old plants (28 DAP). (A) Amino acids; (B) Proteins; (C) Chlorophyll *a*; (D) Chlorophyll *b*; (E) Total chlorophyll; (F) Chlorophyll *a/b* ratio. Means followed by the same letter do not differ (P <0.05) by the Duncan test. Capital letters compare the same genotype in different treatments; lower case letters compare the different genotypes within each treatment. Values are presented as means ± standard error (n = 5).

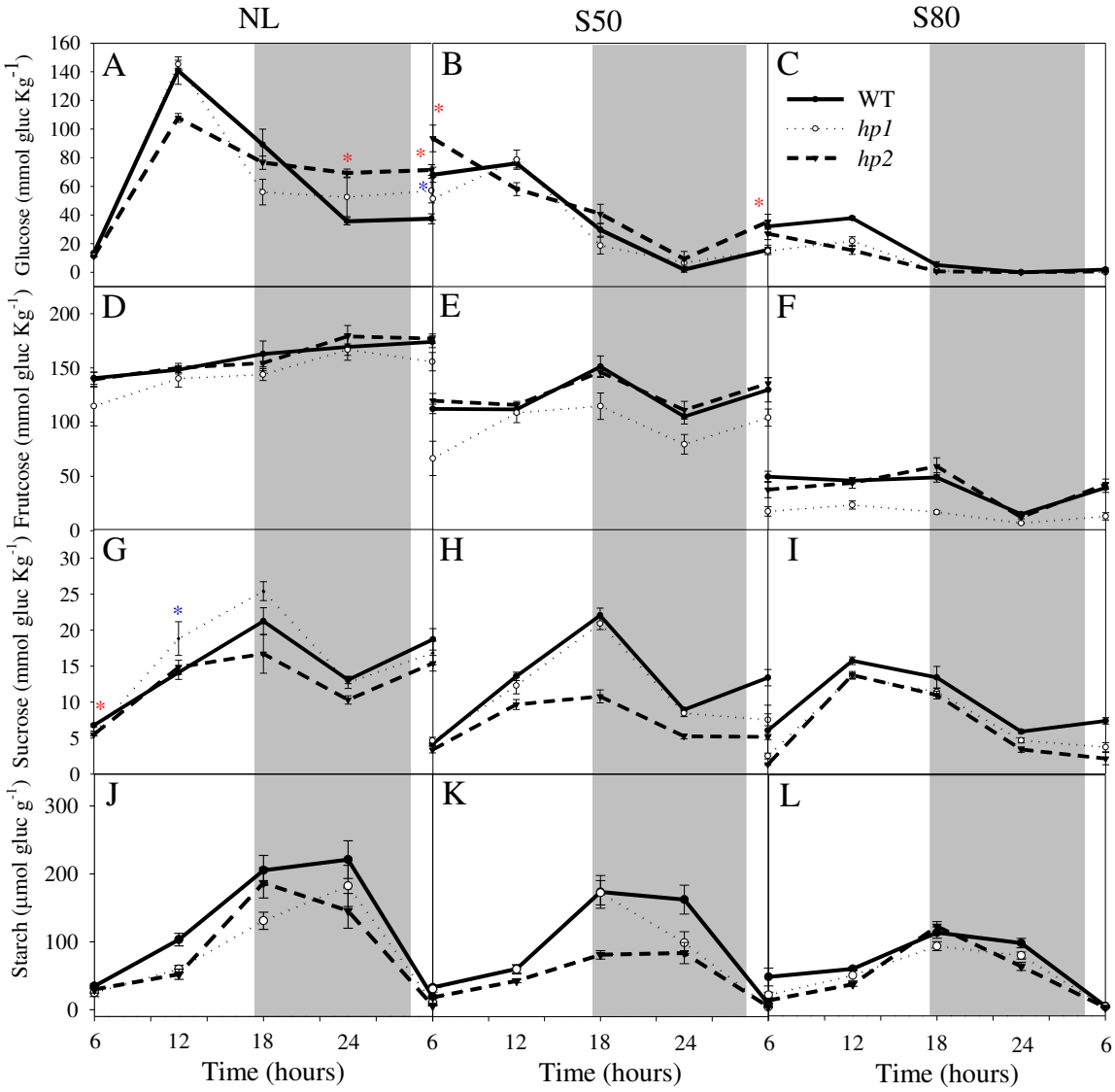

Figure 8 - Variation in carbohydrate contents of Micro-Tom (WT) and *hp1* and *hp2* mutants grown under natural light conditions (NL) and two levels of shading (S50 and S80). Evaluations were carried out on-four-week old plants (28 DAP). (A, B and C) Glucose; (D, E and F) Fructose; (G, H and I) Sucrose; (J, K and L) Starch. Asterisks indicate at which point in the curve the mutants were significantly different to WT according to Student's t-test ($P < 0.05$); *hp1* blue asterisk, *hp2* red asterisk. Values are presented as means ± standard error ($n = 5$).

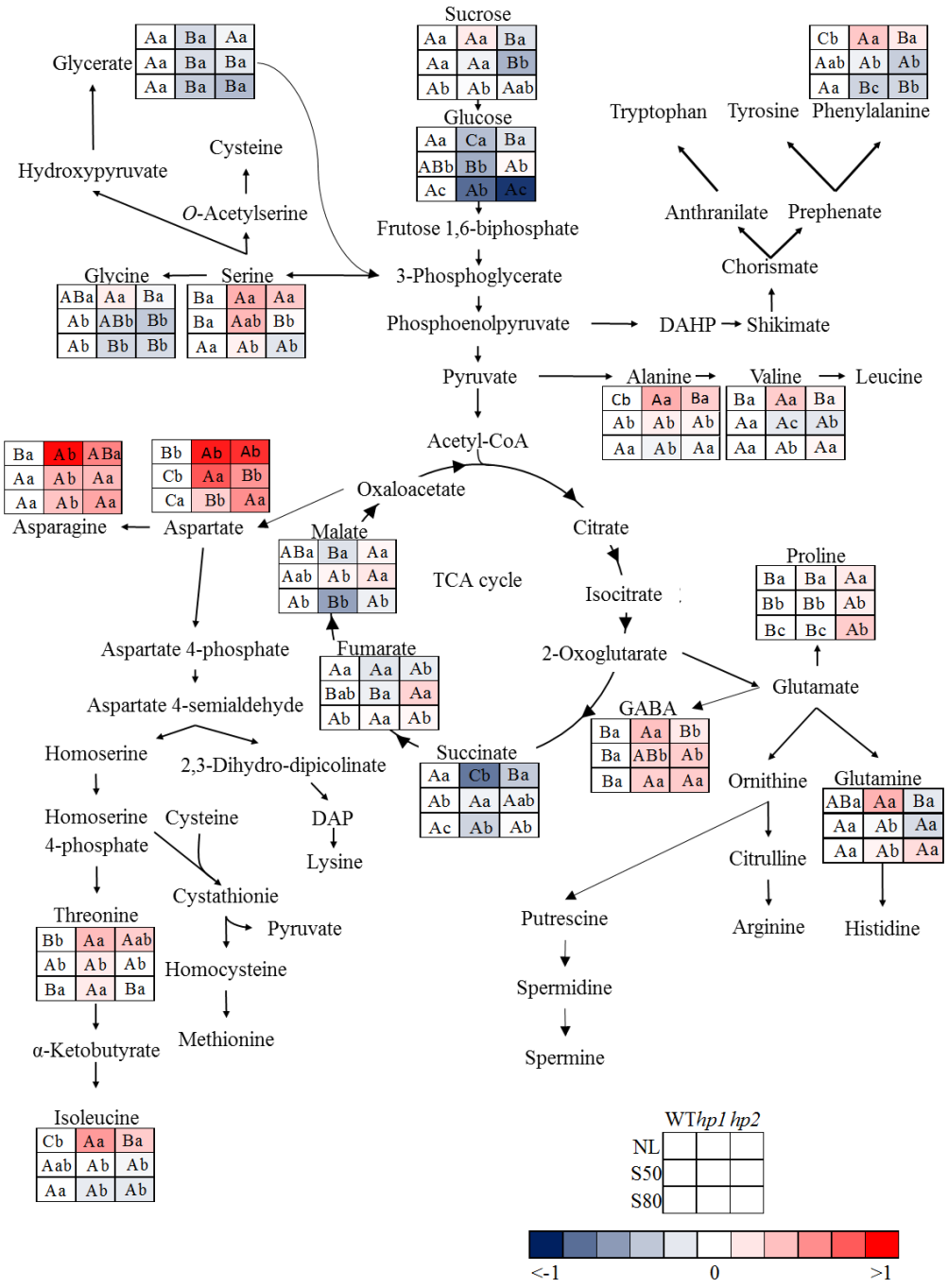

Figure 9 - Metabolic pathway summarizing changes in relative metabolite content of Micro-Tom (WT) plants and *hp1* and *hp2* mutants grown under natural light conditions (NL) and two levels of shading (S50 and S80). Evaluations were carried out on four-week-old plants (28 DAP). Shades other than blue and red represent the levels of metabolite change according to the scale (control log2 ratio). Data were normalized to the mean wild type response calculated for each treatment. Means followed by the same letter do not differ ($P < 0.05$) by the Duncan test. Capital letters compare the same genotype in different treatments; lower case letters compare the different genotypes within each treatment. Values are presented as means ± standard error (n = 4).

3.9 SUPPLEMENTARY DATA

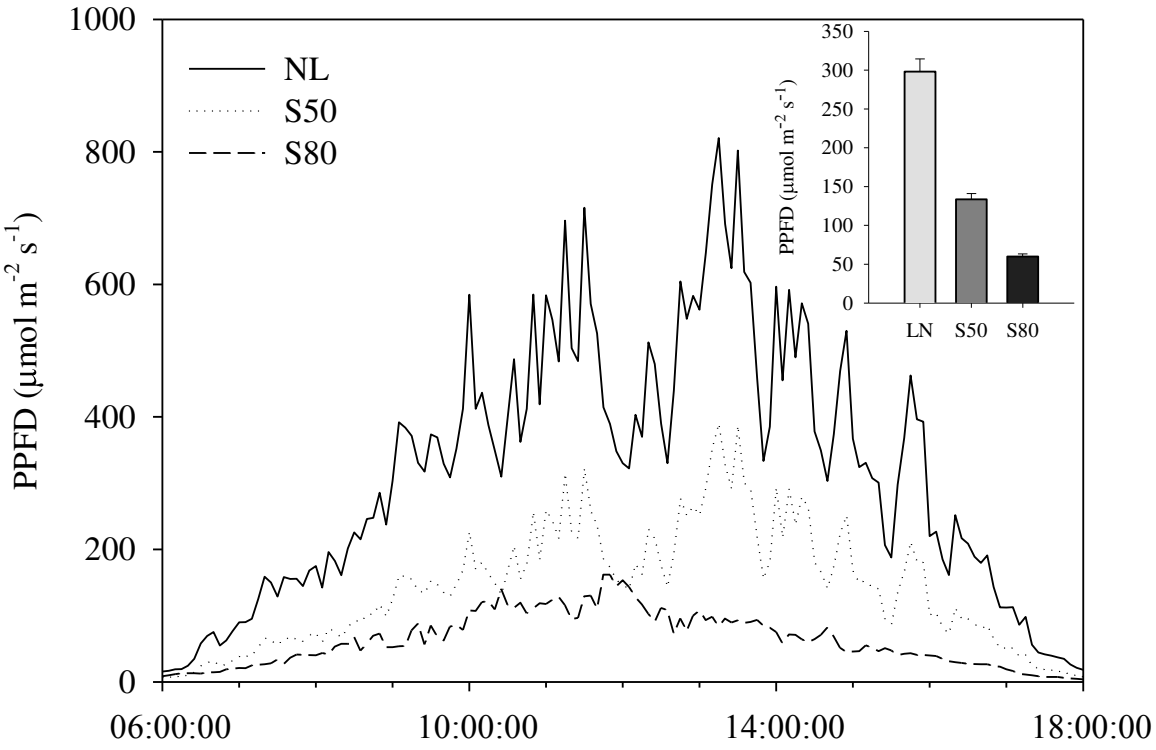

Supplementary Figure 1 - Time course of photosynthetic photon flux density (PPFD) throughout the day for WT and *hp* mutants. Plants were grown in greenhouse under natural light conditions (NL) and two shading levels (S50 ≈ 50% shading, S80 ≈ 80% shading). Lines represent the PPFD throughout the day in different light conditions and the inset bars represent the means of PPFD measured from 6:00 to 18:00 hours in four days throughout the experiment.

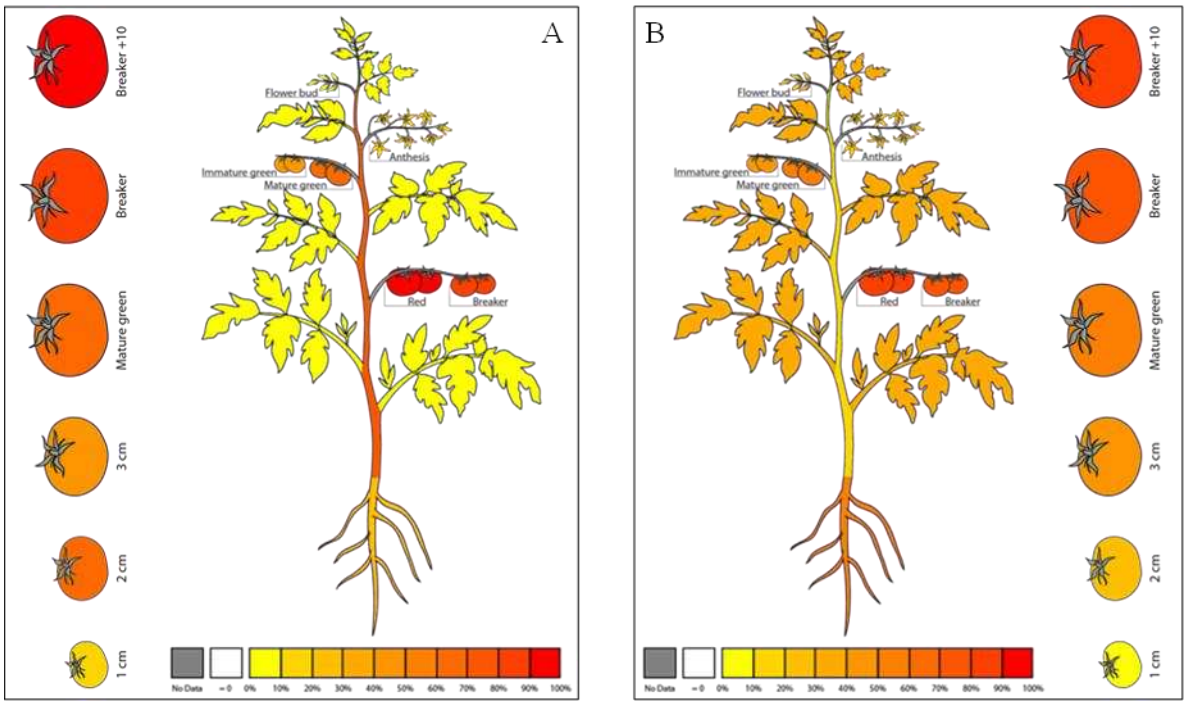

Supplementary Figure 2 - Expression levels of genes *DAMAGE DNA BINDING PROTEIN 1*(*DDB1*) (A) and *DE-ETIOLATED 1* (*DET1*) (B) in different tissues of tomato (*Solanum lycopersicum* L). Font: TomExpress.

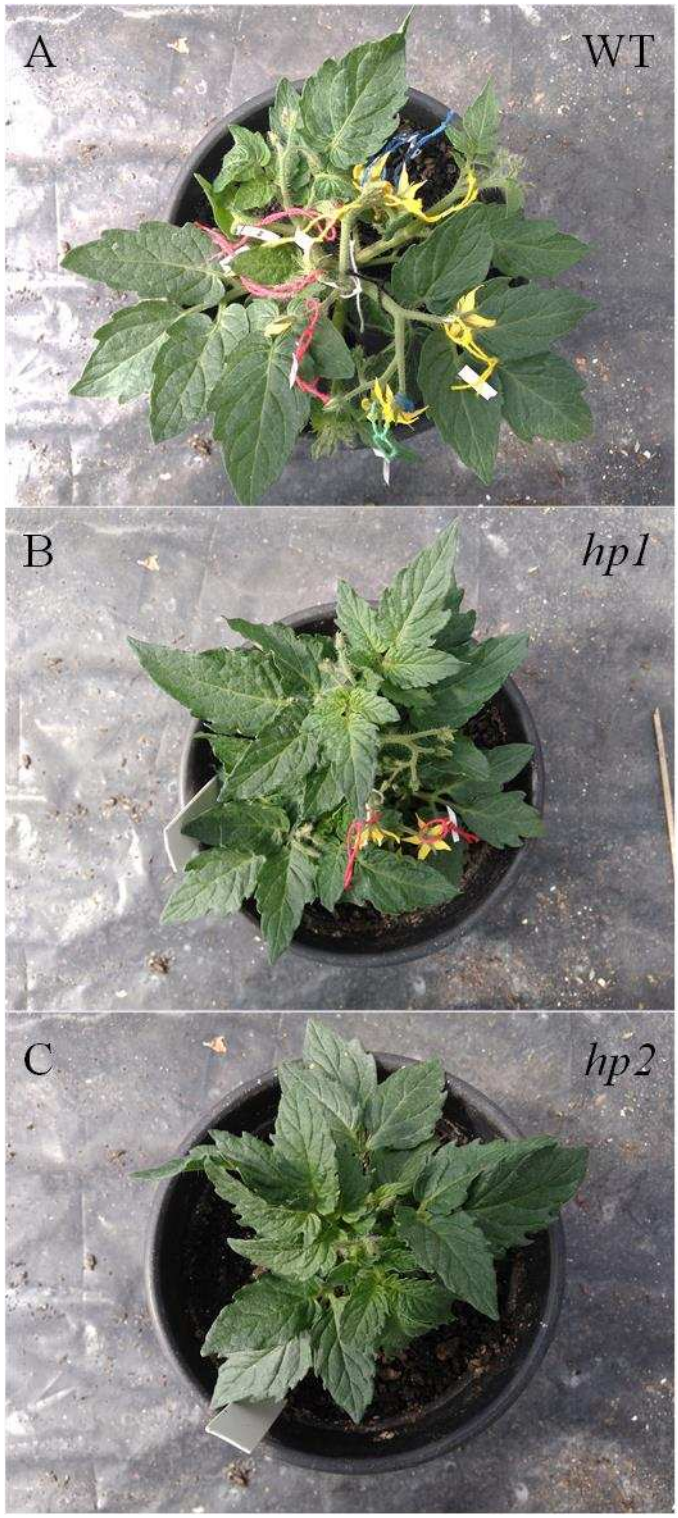

Supplementary Figure 3 – Difference in emission and number of flowers for plants WT (A), *hp1* (B) and *hp2* (C). Plants with six-weeks-old under natural light (LN).

Supplementary Table 1 - Changes in stomatical indexes of Micro-Tom (WT) plants and *hp1* and *hp2* mutants grown under natural light conditions (NL) and two levels of shading (S50 and S80). Evaluations were carried out on four-old-plants (28 DAP). (SI) Stomatal idex; (SD) Stomatal density; (CD) Cells density. Means followed by the same letter do not differ (P <0.05) by the Duncan test. Capital letters compare, vertically, the same genotype in different treatments; lower case letters compare the different genotypes within each treatment. Values are presented as means ± standard error (n = 4).

ADAXIAL EPPIDERMIS				
		SI (%)	SD (n° mm^{-2})	CD (n° mm^{-2})
NL	WT	1.76 ± 1.06 Ab	11.56 ± 10.01 Ab	695.58 ± 48.60 Aa
	hp1	7.67 ± 2.58 Aa	46.36 ± 22.16 Aa	545.70 ± 31.35 Ab
	hp2	10.08 ± 3.18 Aa	53.45 ± 24.91 Aa	462.98 ± 14.66 Bc
S50	WT	2.43 ± 0.42 Aa	16.54 ± 3.61 Aa	650.10 ± 25.96 Aa
	hp1	4.94 ± 0.23 Aba	25.35 ± 1.96 Aba	485.32 ± 15.55 Ab
	hp2	5.09± 1.42 Aba	30.80 ± 9.49 Aba	562.71 ± 5.56 Ab
S80	WT	0 ± 0.00 Aa	0 ± 0.00 Aa	624.42 ± 13.91 Aa
	hp1	0.58 ± 0.58 Ba	3.34 ± 3.33 Ba	532.02 ± 14.73 Ab
	hp2	1.05 ± 0.65 Ba	5.00 ± 3.19 Ba	482.49 ± 89 Abb
ABAXIAL EPPIDERMIS				
		SI	SD (n° mm^{-2})	CD (n° mm^{-2})
NL	WT	23.64 ± 0.75 Aa	206.92 ± 10.02 Aa	668.56 ± 26.02 Aa
	hp1	24.06 ± 0.61 Aa	183.68 ± 10.78 Aab	579.94 ± 30.07 Ab
	hp2	23.29 ± 1.16ABa	177.01 ± 10.71 Bb	581.72 ± 7.49 Bb
S50	WT	20.14 ± 0.55 Bb	187.79 ± 4.47 Ab	748.17 ± 39.94 Aa
	hp1	24.93 ± 0.65 Aa	199.97 ± 14.00 Ab	599.57 ± 23.41 Ab
	hp2	25.64 ± 0.59 Aa	233.49 ± 12.74 Aa	679.12 ± 46.27 Aab
S80	WT	20.23 ± 0.51 Ba	135.65 ± 6.48 Ba	534.13 ± 12.03 Ba
	hp1	20.92 ± 1.22 Ba	142.09 ± 5.24 Ba	540.36 ± 24.10 Aa
	hp2	22.55 ± 0.18 Ba	164.55 ± 4.76 Ba	564.82 ± 12.58 Ba

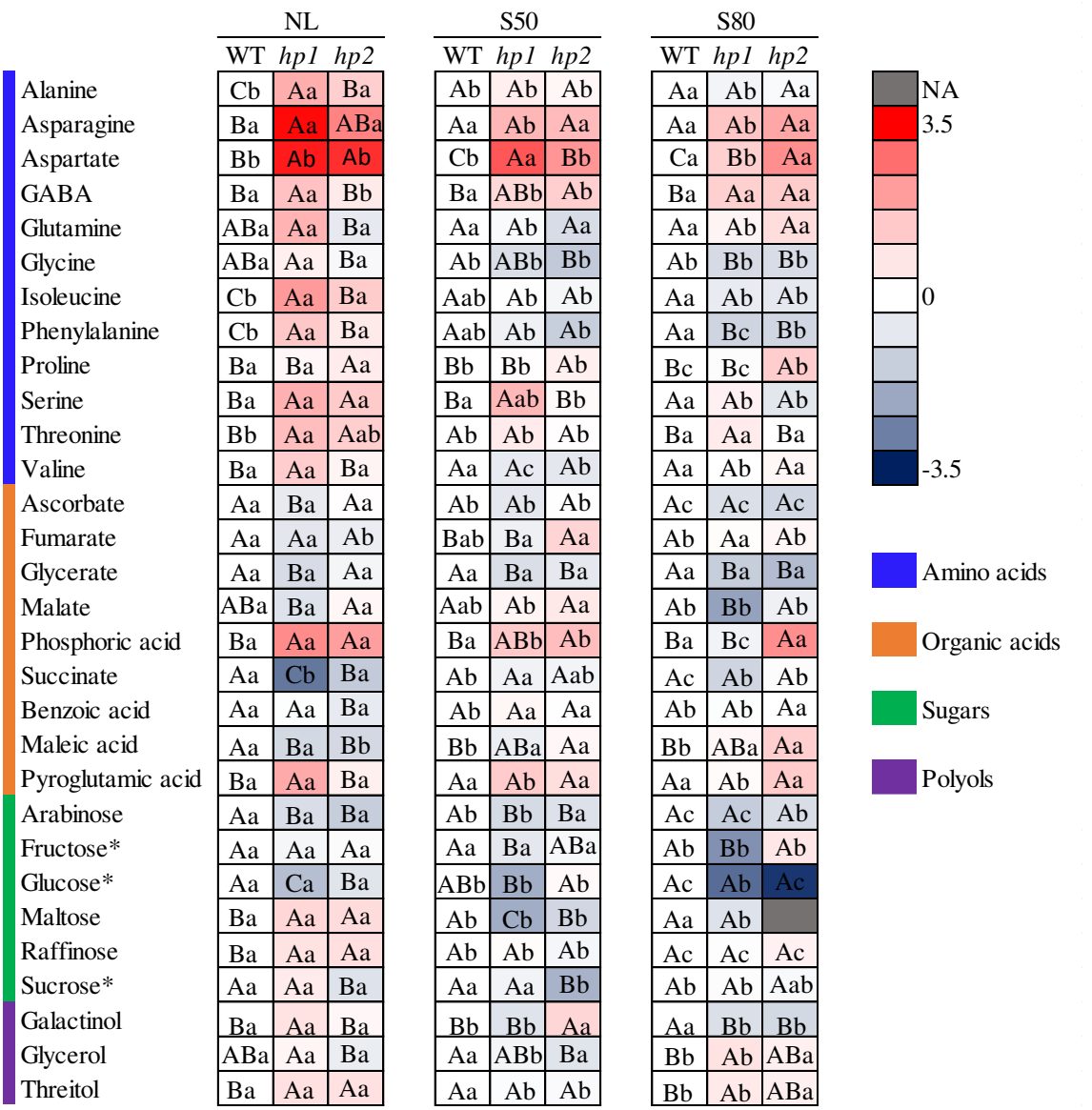

Supplementary Figure 4 - Heat map representing metabolic changes of Micro-Tom (WT) plants and *hp1* and *hp2* mutants grown under natural light conditions (NL) and two levels of shading (S50 and S80). Evaluations were carried out on four-week-old plants (28 DAP). Shades other than blue and red represent the levels of metabolite change according to the scale (control log2 ratio). Data were normalized to the mean wild type response calculated for each treatment. Asterisk indicates that relative metabolite values were obtained by enzymatic method as described in the methodology. NA indicates unmeasured metabolite. Squares followed by the same letter do not differ (P <0.05) by the Duncan test. Capital letters compare the different genotypes within each treatment; lower case letters compare the same genotype in different treatments. Values are presented as means ± standard error (n = 4).

Supplementary Table 2 - Mean values for metabolites Micro-Tom plants (WT) and mutant *hp1* and *hp2* grown natural light conditions (NL) and two levels of shading (S50 and S80). Evaluations were carried out on four-week-old plants (28 DAP). The data presented were obtained by gas chromatography coupled to mass spectrometry (GC-MS) and normalized by standard (Ribitol) and mass (g). Means followed by the same letter of not differ (P <0.05) by the Duncan test. Capital letters compare the different genotypes within each treatment; lower case letters compare the same genotype in different treatments. Values are presented as means ± standard error (n = 4).

Compounds	NL			S50			S80		
	WT	*hp1*	*hp2*	WT	*hp1*	*hp2*	WT	*hp1*	*hp2*
Alanine	12.58 ± 0.54 Cb	27.28 ± 02.46 Aa	20.11 ± 1.05 Ba	14.64 ± 1.12 Ab	17.09 ± 1.31 Ab	15.97 ± 0.39 Ab	22.37 ± 0.65 Aa	19.92 ± 0.85 Ab	21.28 ± 0.74 Aa
Asparagine	1.69 ± 0.12 Ba	17.63 ± 8.35 Ab	5.50 ± 0.67 ABa	1.89 ± 0.25 Aa	3.81 ± 1.09 Ab	3.64 ± 0.36 Aa	1.91 ± 043 Aa	3.35 ± 0.54 Ab	4.49 ± 1.06 Aa
Aspartate	26.95 ± 5.13 Bb	236.62 ± 21.14 Ab	195.57 ± 3.25 Ab	65.80 ± 7.53 Cb	326.65 ± 22.55 Aa	181.11 ± 13.75 Bb	125.53 1.20 Ca	197.36 ± 25.11 Bb	369.97 ± 24.87 Aa
GABA	74.16 ± 2.19 Ba	133.82 ± 15.28 Aa	90.58 ± 5.15 Bb	58.91 ± 2.84 Ba	85.43 ± 3.10 ABb	94.53 ± 4.28 Ab	75.01 ± 7.52 Ba	117.44 ± 8.20 Aa	122.04 ± 4.72 Aa
Glutamine	10.86 ± 0.56 ABa	22.38 ± 0.90 Aa	8.58 ± 0.83 Ba	4.37 ± 0.48 Aa	4.14 ± 0.50 Ab	3.01 ± 0.30 Aa	1.99 ± 0.30 Aa	2.23 ± 0.32 Ab	2.76 ± 0.59 Aa
Glycine	58.60 ± 4.51 ABa	68.31 ± 4.40 Aa	54.84 ± 1.04 Ba	36.34 ± 0.85 Ab	25.50 ± 0.88 ABb	20.46 ± 0.54 Bb	39.29 ± 20.50 Ab	26.41 ± 0.57 Bb	27.10 ± 1.63 Bb
Isoleucine	10.69 ± 0.48 Cb	28.21 ± 3.41 Aa	17.44 ± 0.35 Ba	12.28 ± 0.40 Aab	12.27 ± Ab	11.18 ± 0.27 Ab	15.87 ± 1.08 Aa	12.86 ± 0.67 Ab	12.51 ± 0.74 Ab
Phenylalanine	9.48 ± 0.19 Cb	16.10 ± 0.72 Aa	11.60 ± 0.29 Ba	11.02 ± 0.54 Aab	9.55 ± 0.08 Ab	6.51 ± 0.30 Bb	12.27 ± 0.50 Aa	7.71 ± 0.66 Bc	7.96 ± 0.42 Bb
Proline	7118.77 ± 282.72 Ba	7687.61 ± 45.46 Ba	8625.55 ± 258.42 Aa	5901.91 ± 66.24 Bb	6058.88 ± 100.62 Bb	6907.69 ± 202.70 Ab	4084.03 ± 84.59 Bc	3976.49 ± 125.37 Bc	6632.79 ± 141.44 Ab
Serine	117.95 ± 1.17 Ba	252.36 ± 18.02 Aa	196.55 ± 17.10 Aa	116.07 ± 16.64 Ba	229.94 ± 17.65 Aab	122.06 ± 4.94 Bb	162.85 ± 2.20 Aa	187.46 ± 16.09 Ab	124.70 ± 17.13 Ab
Threonine	58.11 ± 2.71 Bb	109.15 ± 6.47 Aa	92.62 ± 1.55 Aab	74.82 ± 4.43 Ab	91.18 ± 4.11 Ab	76.57 2.82 Ab	100.78 ± 2.45 Ba	122.38 ± 2.94 Aa	100.85 ± 8.77 Ba
Valine	30.32 ± 1.83 Ba	49.15 ± 5.09 Aa	33.80 ± 0.85 Ba	30.20 ± 0.49 Aa	24.21 ± 1.18 Ac	23.41 ± 0.35 Ab	33.60 ± 2.09 Aa	33.88 ± 0.74 Ab	36.81 ± 1.37 Aa
Ascorbate	11.90 ± 0.91 Aa	9.57 ± 0.79 Ba	12.15 ± 0.24 Aa	7.74 ± 0.21 Ab	6.02 ± 0.42 Ab	7.85 ± 0.25 Ab	3.38 ± 0.33 Ac	2.41 ± 0.22 Ac	2.20 ± 0.11 Ac
Fumarate	8.27 ± 0.83 Aa	6.37 ± 0.28 Aa	6.84 ± 0.81 Ab	6.88 ± 0.51 Bab	5.86 ± 0.50 Ba	10.43 ± 1.09 Aa	5.25 ± 0.21 Ab	5.41 ± 0.43 Aa	5.70 ± 0.59 Ab
Glycerate	181.66 ± 8.72 Aa	124.13 ± 8.03 Ba	163.06 ± 3.69 Aa	183.39 ± 6.75 Aa	129.10 ± 14.48 Ba	144.51 ± 3.82 Ba	159.51 ± 2.97 Aa	93.25 ± 8.51 Ba	76.95 ± 4.54 Ba
Malate	1089.41 ± 42.02 ABa	801.55 ± 151.87 Ba	1188.30 ± 60.42 Aa	965.12 ± 43.65 Aab	1064.88 ± 74.24 Aa	1206.61 ± 16.70 Aa	781.55 ± 26.00 Ab	286.50 ± 69.21 Bb	667.61 ± 105.56 Ab
Phosphoric acid	263.20 ± 21.23 Ba	795.46 ± 48.46 Aa	668.02 ± 59.09 Aa	249.76 ± 37.13 Ba	421.39 ± 57.70 ABb	470.69 ± 83.09 Ab	241.11 ± 24.19 Ba	213.44 ± 2.03 Bc	706.00 ± 30.20 Aa
Succinate	1151.17 ± 94.10 Aa	265.89 ± 12.08 Cb	650.69 ± 33.34 Ba	585.05 ±70.74 Ab	511.55 ± 25.43 Aa	521.08 ± 29.64 Aab	385.80 ±6.52 Ac	242.28 ±18.21 Ab	377.21 ± 16.01 Ab
Benzoic acid	3.39 ± 010 Aa	3.32 ± 0.06 Aa	2.72 ± 0.14 Ba	2.93 ± 0.08 Ab	3.21 ± 0.08 Aa	2.99 ± 0.07 Aa	2.88 ± 0.07 Ab	2.83 ± 0.19 Ab	2.89 ± 0.10 Aa
Maleic acid	135.36 ± 7.52 Aa	89.58 ± 7.06 Ba	89.31 ± 6.32 Bb	110.38 ± 7.67 Bb	91.88 ± 8.38 ABa	119.47 ± 17.70 Aa	84.83 ± 5.00 Bb	91.65 ± 5.71 ABa	134.76 ± 15.85 Aa
Pyroglutamic acid	147.38 ± 9.46 Ba	331.91 ± 54.01 Aa	171.03 ± 10.87 Ba	86.49 ± 50.9 Aa	142.75 13.43 Ab	119.06 ± 8.56 Aa	79.08 ± 5.14 Aa	82.46 ± 3.37 Ab	130.44 ± 9.28 Aa
Arabinose	62.04 ± 5.36 Aa	43.22 ± 3.70 Ba	36.12 ± 0.61 Ba	40.11 ± 1.16 Ab	27.15 ± 1.77 Bb	29.24 ± 1.28 Ba	14.90 ± 0.60 Ac	8.60 ± 0.90 Ac	10.30 ± 0.84 Ab
Fructose*	153.26 ± 8.96 Aa	139.75 ± 4.68 Aa	147.69 ± 2.46 Aa	159.22 ± 6.93 Aa	123.31 ± 10.60 Ba	148.92 ± 3.16 ABa	52.69 ± 3.20 Ab	16.07 ± 1.43 Bb	66.67 ± 3.67 Ab
Glucose*	96.72 ± 9.88 Aa	48.70 ± 6.65 Ca	72.32 ± 2.45 Ba	33.62 ± 2.64 ABb	13.99 ± 4.75 Bb	35.71 ± 5.77 Ab	6.27 ± 2.63 Ac	1.28 ± 1.28 Ab	0.71 ± 0.71 Ac
Maltose	6.53 ± 0.22 Ba	9.64 ± 0.53 Aa	9.15 ± 0.14 Aa	4.59 ± 0.05 Ab	1.89 ± 0.07 Cb	2.97 ± 0.10 Bb	1.55 ± 0.14 Ac	1.13 ± 0.06 Ac	NA
Raffinose	3.99 ± 0.26 Ba	5.26 ± 0.40 Aa	5.43 ± 0.21 Aa	3.02 ± 0.09 Ab	3.13 ± 0.12 Ab	2.77 ± 0.15 Ab	1.73 ± 0.10 Ac	1.71 ± 0.15 Ac	1.98 ± 0.07 Ac
Sucrose*	20.04 ±1.86 Aa	24.35 ± 0.98 Aa	14.70 ± 2.32 Ba	22.89 ± 0.68 Aa	20.24 ± 0.68 Aa	10.10 ± 0.74 Bb	12.13 ± 1.03 Ab	11.85 ± 0.43 Ab	11.42 ± 0.41 Aab
Galactinol	3.39 ± 0.21 Ba	4.48 ± 0.08 Aa	3.68 ± 0.16 Ba	2.54 ± 0.24 Bb	1.88 ± 0.21 Bb	3.78 ± 0.23 Aa	3.26 ± 0.11 Aa	2.32 ± 0.09 Bb	2.16 ± 0.14 Bb
Glycerol	31.04 ± 1.04 ABa	34.27 ± 1.20 Aa	25.56 ± 2.00 Ba	29.19 ± 0.37 Aa	26.20 ± 1.31 ABb	21.78 ± 1.59 Ba	22.38 ± 0.96 Bb	29.22 0.31 Ab	26.05 ± 1.95 ABa
Threitol	1.56 ± 0.11 Ba	2.09 ± 0.07 Aa	2.09 ± 0.06 Aa	1.64 ± 0.03 Aa	1.59 ± 0.02 Ab	1.57 ± 0.05 Ab	1.27 ± 0.04 Bb	1.57 ± 0.03 Ab	1.46 ± 0.02 ABb

Amino acids Organic acids Sugars Polyols

4. CHAPTER III:

Differential leaf pigmentation in tomato culminate in a complex metabolic reprogramming without growth impacts

Differential leaf pigmentation in tomato culminate in a complex metabolic reprogramming without growth impacts

Auderlan M. Pereira[1], Auxiliadora O. Martins[1], William Batista-Silva[1], Jorge A. Condori-Apfata[1], Vitor L. Nascimento[1], Victor F. silva, Leonardo A. Oliveira[1], Samuel C. V. Martins[1], David B. Medeiros, Alisdair R. Fernie, Adriano Nunes-Nesi[1] and Wagner L. Araújo[1]*

[1]Departamento de Biologia Vegetal, Universidade Federal de Viçosa, 36570-900, Viçosa, Minas Gerais, Brazil

* Correspondence author.

Wagner L. Araújo

Email: wlaraujo@ufv.br
Tel: +55 (31) 3612-5358

ABSTRACT

Although significant efforts to produce carotenoid-enriched foods either by biotechnology or traditional breeding strategies have been carried out, our understanding of how increased carotenoid biosynthesis might affect overall plant performance remains limited. Here, we investigate how the metabolic machinery of well characterized tomato carotenoid mutant plants [namely *crimson* (*old gold-og*), *Delta carotene* (*Del*) and *tangerine* (*t*)] adjusts itself to varying carotenoid biosynthesis and whether these adjustments are supported by clear reprogramming of photosynthetic and primary metabolism. We observed that mutations *og*, *Del* and *t* did not greatly affect vegetative growth, leaf anatomy and gas exchange parameters. However, an exquisite metabolic reprogramming was recorded. Taken together, our results show that despite minor impacts on growth and gas exchange, carbon flux is extensively affected, leading to adjustments in tomato metabolism to support changes in carotenoid biosynthesis. We discuss these data in the context of our current understanding of metabolic adjustments and carotenoid biosynthesis as well as regarding to improving human nutrition.

Key-words: carotenoids; metabolic adjusts; photosynthesis; pigments

4.1 INTRODUCTION

Carotenoids, isoprenoid molecules widespread in nature and present in all photosynthetic organisms (Fraser and Bramley, 2004), are the second most abundant natural pigment group on earth, with more than 750 compounds already described (Nisar et al., 2015). Notably, carotenoids are synthesized by all photosynthetic organisms (bacteria, algae and plants), as well as in some non-photosynthetic bacteria and fungi (Nisar et al., 2015). It is important to mention that they are pigments responsible for the yellow, orange and red colors of flowers and fruits, egg yolks, fish (e.g. salmon and trout), birds and crustacea (Maldonade et al., 2008; Nisar et al., 2015), which clearly contribute to their economic and biological value to attract insects and animals for pollination and seed dispersal (Rolland et al., 2012; Hou et al., 2016). In plant, these pigments are involved in a wide range of physiological processes, including growth, development and responses to environmental stimuli. In addition, oxidative cleavage of carotenoids produces apocarotenoids and the phytohormone abscisic acid (ABA), the most well-known apocarotenoid derivative, that regulates a wide range of biological processes in plants (Lu and Li, 2008; Rolland et al., 2012). As accessory pigment to harvest light for photosynthesis, carotenoids increase the light uptake by absorbing light at wavelengths that chlorophyll cannot (450-570 nm), and act structurally in the assembly and stabilization of the antenna complex (Nisar et al., 2015; Hashimoto et al., 2016).

Highly reactive intermediates and by-products are inevitably generated during photosynthesis and it can culminate with oxidative damage to the photosynthetic apparatus decreasing the efficiency of photosynthesis (Niyogi, 1999). Briefly, reactive oxygen species (ROS) are generated during photosynthesis and, under stress conditions, it can lead to photooxidative stress (Barber and Andersson, 1992). Overall, both abiotic and biotic stress lead to a generalized response known as oxidative stress that occurs due to an imbalance between the production and the dissipation of ROS (Demidchik, 2015). It is important to mention that ROS namely superoxide (O_2^-), hydrogen peroxide (H_2O_2) and hydroxyl radical (R-OH), which are highly reactive oxidant molecules and by-product of intracellular metabolic processes, also act as signaling molecules (Janků et al., 2019). However, when there is an excessive accumulation of ROS, substantial damage to DNA, RNA, proteins and

lipids may occur, eventually leading to cell death (Bhattacharjee, 2012). In this case, carotenoids play a crucial role allowing energy dissipation (Young and Frank, 1996; Kloz et al., 2011), minimizing or even avoiding the damages caused by ROS. In fact, it has been demonstrated that genetically modified algae and plants that are unable to synthesize carotenoid are characterized by bleached phenotypes (Baroli et al., 2000; Dong et al., 2007; Qin et al., 2007; Avendaño-Vázquez et al., 2014). Furthermore, by using different Arabidopsis mutants with changes in the composition of xanthophyll it was possible to demonstrate that main determinant of photoprotective efficiency in such plants are indeed the carotenoids (Niyogi et al., 2001; Dall'Osto et al., 2007; Cazzaniga et al., 2012).

Carotenoids are essential components of the human diet providing precursors for vitamin A biosynthesis (Krinsky and Johnson, 2005). Lycopene, the most abundant carotenoid in most ripe fruits, is a bioactive component used in both the treatment of chronic diseases and reduction risk of cancer and cardiovascular diseases (Sandmann et al., 2006; Ford and Erdman, 2012). In addition to their functions as pigments and nutrients, carotenoids are also the precursors of many important volatile compounds related to taste, conferring a sensory attribute that can be detected by consumers (Vogel et al., 2010). It is not surprising therefore that carotenoids attract great interest not only given their positive economic impact but also because of their benefits to human health. Indeed, there is an increased effort in the development of new plant varieties rich in phytochemicals beneficial to health, through breeding programs (Goldman, 2011).

In this context, tomato (*Solanum lycopersicum* L.), a fleshy fruit bearing species largely produced and consumed worldwide, presents itself as an excellent model for studding the impacts of changes in carotenoids. Accordingly, in tomato, a climacteric fruit, ripening is characterized by colour de-greening and accumulation of carotenoids which is associated with a chloroplast-to-chromoplast transition (Egea et al., 2011; Batista-Silva et al., 2018). Although significant efforts to produce carotenoid-enriched foods either by biotechnology or traditional breeding strategies have been carried out not only in tomato but also in other plant species (*e.g.* rice, tobacco and sweet potatoes) (Kim et al., 2018), highly variable results are usually observed. Nevertheless, these alterations are successfully followed by increased carotenoid levels coupled with enhanced tolerance to water stress, saline and moderate

increase in resistance to some herbicides (Ye et al., 2000; Apel and Bock, 2009; Park et al., 2015; Ke et al., 2019).

Given the aforementioned facts, we postulate that this metabolic cross-talk that led to changes in carotenoid biosynthesis and stress responses might affect overall plant performance, yet a better understanding of the accumulation of these metabolites rely on our current ability to decipher the complexity of the isoprenoid metabolic network. To this end, senescence and ripening-related tomato mutants represent potentially excellent models, since they provide a means to study metabolic fluxes between these pathways. Our main goal was to investigate how the metabolic machinery of tomato adjusts itself to varying carotenoid biosynthesis and whether these adjustments are supported by clear reprogramming of photosynthetic and primary metabolism. To reach this goal, we compared well characterized tomato carotenoid mutant plants [namely *crimson* (*old gold-og*), *Delta carotene* (*Del*) and *tangerine* (*t*)] grown under natural fluctuation conditions by analyzing photosynthetic traits, antioxidant capacity, as well as primary metabolite profiles. Our combined results demonstrate that in response to changes in carotenoid biosynthesis an exquisite metabolic reprogramming takes place allowing the plant to cope with a highly energetic cost without significant growth impacts. We further discuss these data in the context of metabolic adjustments acting not to enhance energy dissipation and ROS scavenging *per se* but rather to afford improvements of photosynthetic performance supporting the maintenance of growth.

4.2 MATERIAL AND METHODS

Plant material, growth conditions and experimental design

We used three mutants involved in the biosynthesis of carotenoids. Briefly, the *crimson* mutant carries a recessive mutation that leads to loss of function of the enzyme LICOPENO β-CYCLASE (CYC-B) (RONEN et al., 2000). As such, the conversion of lycopene to ß-carotene is abolished, resulting in fruits with high lycopene content and intense red coloration and flowers with orange petals (hereafter called *og* from *old gold*) (Thompson et al., 1967). Second, we used the *Delta carotene* (*Del*) mutant which harbors a dominant

mutation that increases the expression of the *Lcy-e* gene encoding the enzyme LICOPENO ε-CICLASE (LCY-E), favoring the conversion of trans-lycopene to δ-carotene. The orange fruit phenotype resulting from this modification observed in ripe fruits is due to the accumulation of δ-carotene (Ronen et al., 1999). Last, the *tangerine* (*t*) mutant, which are characterized by an orange ripe fruits due to the substantial accumulation of pro-lycopene occurs along with other carotenoids, carries a mutation in the gene encoding the CAROTENOID cis-trans ISOMERASE (CRTISO), responsible for the isomerization of tetra-cis-lycopene (pro-lycopene) in trans-lycopene (Isaacson et al., 2002).

Seeds of the tomato (*Solanum Lycopersicon* Micro-Tom) wild-type (WT) and the mutants *og*, *Del* and *t* were surface sterilized with 5% sodium hypochlorite solution for 10 min, then washed with running distilled water and subsequently sowed in a tray containing commercial substrate (Plantmax, DDL Agro Indústria). After two weeks of sowing, seedlings were transferred to 2 L pots (one seedling per pot) containing the same substrate used for seedling production but supplemented with 1 g NPK 10-10-10 and 4 g dolomitic limestone (Ca + Mg) per liter of substrate (Pino-Nunes et al., 2010). Plants were grown in a greenhouse located in Viçosa (20°45′S, 42°50′W, 650 m above sea level), southeastern Brazil, with a minimum of 400 μmol photons m^{-2} s^{-1}. Throughout the entire experiment, the plants were grown under naturally fluctuating conditions of temperature and air relative humidity, and sunlight (Supplementary Figure 1), and were fertilized and irrigated as necessary. The pots were randomized periodically to minimize any variation within each light environment. For all samplings and measurements, the second terminal leaflet of the third fully expanded leaf, from the apex to the base, in plants of 4 week after planting, were used. For biochemical analyses, leaf samples were collected in cloudless days at different times during day, prior to flash freezing in liquid nitrogen and subsequent storage at −80 °C until analysis. The experiment was arranged in a completely randomized design with four genotypes (WT, *Del*, *og* and *t*). The means presented in Tables and Figures were obtained from, at least, four independent replications per treatment of single plant experimental plots (one plant per pot). Data were submitted to analysis of variance (ANOVA) with *F* test and Duncan test ($P<0.05$).

Determination of biometric parameters

Dry matter accumulation in shoot and roots was determined at 28 days after planting (DAP). During these measurements, the plants were harvested in one cut at ground level, separating roots from shoots. The roots, after washing with water to remove soil contamination, and shoots were placed in labelled paper bags and brought to a forced air circulation oven at 70 °C for 5 days, after which the dry weight of roots and shoots (stem and leaves) was determined. Moreover, plant height, stem diameter, number of leaves, root length, leaf area (Li-Cor Model 3100 Area Meter, Lincoln, NE, USA), and total dry weight (= leaves + stem + roots) were determined. From these characters we determined specific leaf area and root/shoot ratio.

Leaf anatomic analysis

Sections of leaf samples from the third fully expanded leaf were hand cute using a razor blade and fixed in FAA50 (formaldehyde, acetic acid and ethyl alcohol (90:5:5)) for 48 h and then stored in 70% ethanol (Johansen, 1940). Subsequently, the sections were included in methacrylate (Historesin-Leica), following the manufacturer's recommendations, and transversely sectioned on automatic advance rotary microtome (model RM2155, Leica microsystems Inc., Deerfield, USA) with 5 μm thickness, dyed with toluidine blue (O'Brien et al., 1964) and mounted under cover slip. The images were obtained under a light microscope (model AX-70 TRF, Olympus Optical, Tokyo, Japan), coupled to a digital photographic camera (Zeiss AxioCam HRc model, Göttinger, Germany) using the image capture program Axion Vision. Measurements were taken from at least five different fields from each sample using the Image-Pro® Plus software (version 4.1, Media Cybernetics, Inc., Silver Spring, USA). Leaf thickness, palisade and spongy parenchyma, abaxial and adaxial epidermis, stomatal index, epidermal cell density and stomatal density were evaluated.

Measurements of stomatal and cells density and stomatal index were obtained after a diaphanization process, which consisted of the clarification of the samples using 100% (v/v) methanol for 48 h, followed by a 95% lactic acid incubation at 95 °C for 30 min (Zsögön et al., 2015). Sections were mounted on glass slides and the images of the adaxial and abaxial

epidermis were obtained using light microscope (model AX-70 TRF, Olympus Optical, Tokyo, Japan) coupled to a digital camera (Zeiss AxioCam HRc model Göttinger, Germany) and computer with the Axion Vision image capture program. The images were analyzed in the Image-Pro Plus version 4.5 program.

Gas exchange and fluorescence parameters

Gas exchange and chlorophyll *a* fluorescence analysis were performed simultaneously in the third fully expanded leaf from the apex of 4-week-old plants (vegetative stage) using a portable open-flow gas exchange system (Li-6400XT, Li-Cor, Inc., Lincoln, NE, USA) equipped with an integrated fluorescence chamber (LI-6400-40; Li-Cor Inc.). Measurements of the net carbon assimilation rate (A, μmol CO_2 m^{-2} s^{-1}), stomatal conductance (g_s, mol H_2O m^{-2} s^{-1}), internal CO_2 concentration (C_i), and transpiration (E, mmol m^{-2} s^{-1}) were conducted from 08:00 to 11:00 h (solar time), which is when A was at its maximum, under an ambient CO_2 concentration (C_a) of 400 μmol mol^{-1} air (CO_2 injected from a cartridge) and a flow rate of 300 μmol s^{-1}. All measurements were conducted under artificial photosynthetic photon flux density (PPFD), saturating light of 1000 μmol photons m^{-2} s^{-1} (from a LED source) with 10% blue light in order to maximize the stomatal opening, at 25 °C and the leaf-to-air vapor pressure deficit was maintained at approximately 1.0 kPa. Dark respiration (R_D) and fluorescence of chlorophyll *a* parameters were measured using the same gas exchange system described above after at least two hours into the dark period in the same leaf previously used to determine gas exchange parameters.

The initial fluorescence (F_0) was measured by illuminating previously dark-adapted leaves with weak modulated measuring beams (0.03 μmol m^{-2} s^{-1}). Saturating white light pulses (8000 μmol photons m^{-2} s^{-1}) was applied for 0.8 s to obtain the maximum fluorescence (F_m), from which the variable-to-maximum chlorophyll fluorescence ratio, was then calculated: $F_v/F_m=[(F_m - F_0)/F_m)]$. In light-adapted leaves, the steady-state fluorescence yield (F_s) was measured with the application of a saturating white light pulse (8000 μmol m^{-2} s^{-1}, 0.8 s) to achieve the light-adapted maximum fluorescence (F_m'). The actinic light was then turned off and a far-red illumination (2 μmol m^{-2} s^{-1}) was applied to measure the light-adapted initial fluorescence (F_0'). The capture efficiency of excitation energy by open

photosystem (PS) II reaction centers (F_v'/F_m') was estimated following Logan et al. (2007) and the actual PSII photochemical efficiency (δPSII) was estimated as $\delta PSII = (F_m' - F_s)/F_m'$ (Genty et al., 1989). In addition, the electron transport rate (ETR), were determined as previously described (Martins et al., 2014a; Medeiros et al., 2016).

Photosynthetic light-response curves (*A*/PPFD) were obtained by varying the PPFD in 9 steps from 2200 to 0 µmol photons m^{-2} s^{-1} at 25 ºC (Martins et al., 2014a). The *A*/PPFD curves were obtained at same conditions described before. From the *A*/PPFD curve, the following variables were determined: net carbon assimilation rate saturated by light (A_{max}), light compensation point (*LCP*), light saturation point (*LSP*) and light use efficiency ($1/\Phi$) (inverse of the apparent quantum yield) (von Caemmerer, 2000).The responses of *A* to C_i were determined at 1000 µmol photons m^{-2} s^{-1}, at 25 ºC, under ambient O_2 following the protocol described by Long and Bernacchi (2003). Briefly, A/C_i curves were initiated at a C_a of 400 µmol mol^{-1} and once the steady state was reached, C_a was decreased stepwise down to 50 µmol mol^{-1} air. Upon completion of the measurements at low C_a, it was returned to 400 µmol mol^{-1} air to restore the original *A*. Next, C_a was increased stepwise to 2000 µmol mol^{-1} air (Martins et al., 2013). The maximum rate of carboxylation (V_{cmax}) and maximum rate of carboxylation limited by electron transport (J_{max}), J_{max}/V_{cmax} ratio and triose phosphate utilization (*TPU*) were then estimated by fitting the mechanistic model of CO_2 assimilation using the Excel spreadsheet provided by Sharkey et al. (2007). Corrections for the leakage of CO_2 into and water vapor out of the leaf chamber of the LI-6400 have been applied to all gas-exchange data, according to Rodeghiero et al. (2007).

Biochemical parameters and metabolic profile

All sampling procedures were carried on the same leaf used for analysis of gas exchange and fluorescence from four-week-old plants (28 DAP), during vegetative stage. Leaves were flash-frozen in liquid nitrogen and stored at −80 °C until further analyses. Metabolite extraction was performed by rapid grinding in liquid nitrogen and immediate addition of the appropriate extraction buffer.

The levels of photosynthetic pigment were determined according to Wellburn (1994) whereas starch, sucrose, glucose and fructose were determined exactly as described

previously by Fernie et al. (2001), and total amino acids and total soluble proteins were determined as previously described by Yemm et al. (1955) and Bradford (1976), respectively.

The levels of all other metabolites were quantified by an established gas chromatography associated with mass spectrometry (GCMS) protocol (Roessner et al., 2001; Lisec et al., 2006). Briefly, the extraction (using ~50 mg fresh weight) was performed using 1 mL of methanol and shaking (800 rpm) at 70 °C during 15 min, 60 µL of Ribitol (0.2 mg mL^{-1}) was added as an internal standard. After that, derivatization and sample injection were performed exactly as previously described previously by Lisec et al. (2006). This analysis allowed the determination of 31 different compounds, representing the main classes of compounds (amino acids, organic acids, sugars and others). Chromatograms and generated mass spectra were evaluated using the software TagFinder (Luedemann et al., 2011), using a reference library from the Golm Metabolome Database (Kopka et al., 2005) and the identification and annotation of the detected peaks followed the recommendations for reporting metabolite (Fernie et al., 2011).

qRTPCR analysis

Total RNA was isolated from 50 mg of plant material (leaf) using the TRizol reagent (Invitrogen®), according to the manufacturer's instructions. The integrity and amount of RNA were checked on 1% (w/v) agarose gel, and the concentration was measured before and after DNAse I digestion (RQ1 RNase free DNase I, Promega®) using a spectrophotometry (OD_{260}). DNAse-treated RNA (2 µg) was used for cDNA synthesis using the Superscript™ III reverse transcriptase (Invitrogen®, Darmstadt, Germany) according to the manufacturer's recommendations.

Gene expression was accessed using real-time PCR (qRT-PCR) (Step One PlusTMReal Time PCR System, Applied Biosystems, CA, USA) with the SYBR green fluorescence detection (Applied Biosystems®), using the Platinum® SYBR® Green qPCR SuperMix-UDG with ROX kit. The primers used (Supplementary Table 1) were designed using QUANTPRIME software (Arvidsson et al., 2008). Data analyses were performed exactly as described by Caldana et al. (2007). qRT-PCR were performed according with the followed temperature alternations: denaturation of double-stranded DNA and enzyme

activation (95 °C, 30 seconds, 1x); denaturation of double-stranded DNA (95 °C, 3 seconds, 40x) and finally, primer's annealing and extension of fragment by polymerase enzyme (58°C, 30 seconds, 40x). Melt curve reaction: 95 °C 15 seconds, 60 °C for 1 minute e 95 °C for 15 seconds (1x). The average CT of the ACTIN (reference control) gene was used for the relative expression analyses. The analyzes were performed in duplicate in each PCR run, using 4 replicates for each genotype, and their mean cycle threshold was used for relative normalized expression analyses.

4.3 RESULTS

Leaf expression of genes involved in carotenoid biosynthesis are not reduced in mutant plants

The function of the three mutated genes, namely *Lcy-e*, *Cyc-B* and *CrtISO* have been extensively demonstrated during tomato fruit development, and are responsible for the *Del*, *og* and *t* phenotype, respectively (Ronen et al., 1999; Ronen et al., 2000; Isaacson et al., 2002). Nevertheless, the expression pattern of these genes in leaf samples of the Micro-Tom (WT) background has not been investigated (Supplementary Figure 2). Thus, we first confirmed that all genes are indeed constitutively expressed also in leaf tissues (Table 1). Next, we observed that the *t* mutant is characterized by a higher expression of the *Lcy-e* gene than the other genotypes. Surprisingly, no difference was observed between genotypes in the expression of the *Cyc-B* gene. The *Del* mutant displayed a higher expression of the *CrtISO* gene whereas WT plants and the other mutants (*og* and *t*) did not show any difference (Table 1).

Vegetative growth parameters are not affected in carotenoid mutant plants

The changes in the expression of carotenoid related genes of carotenoid mutant plants prompted us to investigate the physiological function of those gene during vegetative growth. Despite of no visible aberrant phenotypes during vegetative development of carotenoids mutants, closed inspection of growth parameters revealed that plant height (Supplementary

Figure 3), root length, specific leaf area and root/shoot area (Figure 1A, C, G and H, respectively) did not differ among genotypes investigated here. Notably, *t* mutant plants were characterized by the thickest stem diameter (0.49 cm), while *og* plants had the smallest (0.44 cm) (Figure 1B), although they did not differ from WT plants. Similarly, it was observed that *Del* mutant plants presented the lowest values of number of leaves, total leaf area and total dry weight (Figure 1D, E and F, respectively) in comparison to WT plants whilst both *og* and *t* mutant plants did not differ from WT.

Changes in carotenoid biosynthesis do not modify leaf anatomy

Similarly to what we have observed for growth parameters (Figure 1), there were overall no variation in leaf blade thickness among genotypes (Figure 2). Thus, we only observed that adaxial epidermis of the *og* mutant plants was lower than that of WT plants (Figure 2A). However, the stomatal indices were modified and we observed that *Del* plants had higher stomatal index, together with mutant *t*, higher stomata and cell density on the abaxial face (Supplementary Table 2).

Photosynthetic performance is not affected in carotenoid related mutant

Given the absence of great changes in both growth and anatomy related parameters between the genotypes studied, we next investigated the photosynthetic performance of carotenoid related mutants. By analyzing gas exchange parameters, we observed that there were few differences among the genotypes (Table 2). Although both g_s and C_i were lower in *Del* mutant plants than in the other genotypes, virtually no differences were observed for *A,* R_D and *E* between genotypes (Table 2). Similarly, only relatively minor variations were verified in chlorophyll *a* fluorescence parameters between WT and mutant plants. Notably, *t* mutant plants presented higher *ΦPSIIe* and *qN* when compared to the other genotypes, whereas *og* plants were characterized by lower *qP* in relation to WT, *Del* and *t* plants, that did not differ between then.

We next characterized the photosynthetic performance by analyzing gas exchange under different photosynthetic photon flux density (PPFD) (*A*/PPFD curves and g_s/PPFD

curves; Figure 3A and Supplementary Figure 4) and we observed that mutant plants exhibited unaltered *A* and g_s irrespective of the irradiance, except for the mutant *Del* that showed low values of g_s (Supplementary Figure 4). Thus, no changes in light saturation point (*LCP*), maximum net assimilation rate light saturated (A_{max}), light compensation point (*LCP*) and light use efficiency ($1/\Phi$) were observed between WT and mutant plants (Table 3). Additionally, the response of *A* to the leaf internal CO_2 concentration (C_i) (*A*/C_i curves; Figure 3C) was obtained. Both WT and mutant plants were characterized by higher *A* with increments in CO_2 (Figure 3C), and we further noticed that the maximum carboxylation velocity (V_{cmax}) was higher in all mutant plants whereas the lower J_{max}:V_{cmax} ratios observed in carotenoid related mutants (Table 4) suggest that differences in *A* were more likely related to higher carboxylation than electron transport rates (Table 3). No differences were observed for the maximum capacity for electron transport rate (J_{max}) and triose phosphate utilization (TPU) in carotenoid related plants (Table 4).

Modification in the metabolic profile of carotenoid related mutants

To enhance our understanding of the consequences of alterations in carotenoid biosynthesis that culminated with minor changes in growth and in photosynthetic capacity among the genotypes we next performed a detailed metabolic analysis in leaves of WT and mutant plants. First, we determined the levels of some carbon and nitrogen related metabolites in samples harvested at the middle of light period (Figure 4). The levels of total amino acids were lowest in the *t* mutant plants, while both *Del* and *og* mutants were characterized by similar levels found in WT plants (Figure 4A). Despite this relatively minor variation in total amino acids, it did not reflect in the total soluble protein, which were similar between WT and mutant plants (Figure 4B). This fact aside, significant variation was verified for the carbohydrates metabolism (Figure 4C). Thus, the pattern of glucose and fructose was the same behavior among the genotypes, where *Del* mutant plants presented highest amount, followed by both *t* and *og*, respectively, that did not differ from WT plants. Regarding the sucrose content, *og* mutant presented the lowest content, similar to observed for other sugars, followed by *Del* mutant plants (Figure 4C). Interestingly, *Del* mutant plants presented higher levels of glucose and fructose and lower sucrose levels. Similarly to sucrose, starch data

presented the same behavior to all genotypes (Figure 4D). All mutant plants showed a trend to present reduced levels of starch (significant only for *og*) in comparison to WT plants.

By contrast to the situation observed for carbohydrates, the variation in chlorophyll *a* content was higher in both *og* and *t* mutant plants whereas *Del* mutant showed reduced content of chlorophyll *a* in comparison to WT plants (Figure 4E). Similar behavior was observed in the chlorophyll *b* for both *og* and *t* mutant plants, which clearly reflected in higher levels of total chlorophyll. The chlorophyll *a/b* ratio was only modified in the *t* mutant which showed a significantly higher values than WT and other mutant plants.

To further explore the consequences of alterations in carotenoid biosynthesis on primary metabolism, we next performed a detailed metabolic profile on leaves harvested at the middle of light period. This analysis allowed the identification of at least 30 metabolites revealing considerable variations in the levels of various amino acids (Figure 5), organic acids (Figure 6), sugars and polyols (Figure 7). The full data set from these metabolic profiling studies are additionally available in Supplemental Figure 5 and Supplemental Table 3. Overall, in relation to WT plants, mutant plants were characterized by considerable increases for amino acids such as asparagine, aspartate, GABA, glycine, isoleucine, proline, serine and threonine (Figure 5). Notably, *og* mutant displayed higher levels of asparagine, GABA and serine than the other genotypes (Figure 5B, D and J). The mutant plants, which did not differ from each other, presented higher levels of aspartate and threonine than WT (Figure 5C and K). Taken together, these data indicate that nitrogen metabolism is likely to be constrained by an increased availability of carotenoids.

Considerable variation was additionally observed for organic acids (Figure 6). Thus, ascorbate levels were higher for both *Del* and *t* mutants, and were similar between *og* and WT plants (Figure 6 A). Moreover, *og* mutant were characterized by lower fumarate values than WT, *Del* and *t* plants, which were virtually invariant (Figure 6B). Both *Del* and *og* mutants had lower levels of malate than WT and *t*, which did not differ from each other (Figure 6D). Increased content of glycerate in *t* mutant (Figure 6C) and phosphoric acid in *Del* mutant (Figure 6E) compared to other genotypes was observed. Higher levels of succinate were observed in WT compared to all other mutants (Figure 6 F). Both *og* and *t* mutant had lower levels of benzoate than WT whereas *Del* did not differ from WT (Figure 6G). As for maleate levels, both *Del* and *og* mutants presented the lowest levels, but these

mutants had the highest values of pyroglutamate, although *Del* mutant did not differ from WT for pyroglutamate; for both metabolites *t* mutant did not differ from WT (Figure 6H and I).

Del mutant had higher levels of arabinose, fructose and glucose than WT and the other mutants (Figure 7 A, B and C), consistent with the results of the biochemical analyzes showed in Figure 4C. Moreover, *t* mutant had the highest maltose content (Figure 7D), while raffinose levels were higher for the *Del* mutant compared to the other mutants (Figure 7E). Sucrose levels were higher for WT and *t* (Figure 7F). Both *Del* and *og* mutants had lower galactinol content than WT (Figure 7G); on the other hand, *og* had higher glycerol levels than WT (Figure 7H) whereas Threitol levels did not vary between genotypes (Figure 7I).

4.4 DISCUSSION

Tomato is a well-established important model for climacteric fruit development and has therefore been studied intensively with respect to fruit genetics, physiology and biochemistry (Isaacson et al., 2002; Park et al., 2002; Tian et al., 2004). Moreover, in tomato, a leading vegetable crop and the main model system for fleshy fruits, enhanced production of carotenoids contributes to visual changes in color during ripening. Accordingly, the function of carotenoids during fruit ripening has been extensively demonstrated in tomato (Kachanovsky et al., 2012; McQuinn et al., 2015; Yoo et al., 2017). However, the importance of enhanced carotenoid biosynthesis on leaf metabolism and its connection to plant growth is poorly understood. It is equally important to mention that our knowledge is relatively limited on how exactly and to which extent the metabolic flux is seemingly distributed among different branches of the general isoprenoid biosynthetic pathway. Here, we hypothesize that changes in carotenoid biosynthesis might affect overall plant performance, by using senescence and ripening-related tomato mutants we investigate how the metabolic machinery of tomato adjusts itself to varying carotenoid biosynthesis. Interestingly, despite relatively minor changes in photosynthetic traits, a clear reprogramming of primary metabolism was observed in carotenoid related mutants with no growth penalty. By comparing well characterized tomato carotenoid mutant plants [namely *crimson* (*old gold*), *Delta carotene* (*Del*) and *tangerine* (*t*)] grown under natural fluctuation conditions we demonstrate that in

response to changes in carotenoid biosynthesis an exquisite metabolic reprogramming takes place allowing the plant to cope with an highly energetic cost without significant growth impacts.

Expression of *Lcy-e*, *Cyc-B* and *CrtISO* are not modified in leaves

First, we confirm that mutated genes are constitutively expressed in leaf tissue (Table 1). *Del*, *og* e *t* mutations are characterized by enhanced *Lcy-e* gene expression levels and reductions in *Cyc-B* and *CrtISO* in fruits, respectively, promoting the characteristic phenotype of each mutation, especially during fruit ripening (Ronen et al., 1999; Ronen et al., 2000; Isaacson et al., 2002). Our results showed a different expression pattern in leaves of mutants at 28 DAP. It seems reasonable to suggest that without any (a) biotic stress the leaf expression does not occur as for fruits or at least with the same intensity during this developmental phase of plants. According to Ronen et al. (2000), in mutations that lead to nullity of locus *B*, as in the case of mutant *og*, there is no phenotypic manifestation of mutation, either biochemical or developmental, in leaves and stems, indicating that the locus *B* does not play an indispensable role in vegetative tissues, at least under "optimal growth conditions". Thus, it seems reasonable to anticipate that such changes in carotenoid biosynthesis would be more important under stress conditions.

Leaf anatomy and growth are not drastically affected in carotenoid related mutants

Although we postulated that increased carotenoid biosynthesis would impact overall plant performance, under optimal growth conditions only few variations were observed in *Del*, *og* and *t* mutants. These changes occurred mainly with the *Del* mutant, which, compared to WT, was characterized by lower number of leaves, leaf area and total dry weight (Figure 1D, E and F), suggesting that the *Del* mutation has some negative effect on leaf growth and biomass accumulation. Significant efforts have been placed to better understand the carotenoid biosynthesis pathway, and therefore numerous transgenic or natural cultures with modified carotenoid levels have been studied, including tomato (Apel and Bock, 2009), rice (Ye et al., 2000), potatoes (Diretto et al., 2007) and maize (Yan et al., 2010). Accordingly, it

has been noted that changes in carotenogenesis flow may increase or decrease metabolic flow in other concurrent pathways, leading to unexpected phenotypic changes (Kim et al., 2018). In this context, Fray et al. (1995) observed that the constitutive expression of *PSY-1* in tomato resulted in stunted growth most likely due to the high precursor geranylgeranyl diphosphate (GGPP) consumption of gibberellin biosynthesis. In another case, even though it is possible to take advantage of the positive effects, *hp* mutations with changes in light signaling genes culminate with negative effects including reduced growth and retarded development in tomato, at least during early stages of growth (Kendrick et al., 1997; Mustilli et al., 1999; Azari et al., 2010). Another important fact is that carotenoid metabolic turnover not only helps maintain constant levels of carotenoids in plants, but also produces important signaling molecules and accessory apocarotenoids such as ABA phytohormones and strigolactones (Kim et al., 2018). In good agreement, mutations in the carotenoid biosynthesis pathway did not impact the leaf blade thickness parameters of the evaluated genotypes (Figure 3). Given this, it is tempting to speculate that, at least under optimal conditions, a mutation that culminates in changes in carotenoid biosynthesis, a compound with a clear function associated with stress response in plants, may also act as sustaining growth. Since it remains unclear whether this response will be maintained under field conditions and therefore care should be taken in interpreting the results presented here in the context of improving tomato growth with biotechnological applications.

Gas exchange and fluorescence parameters

Despite the relatively few differences observed among genotypes, we observed that the *Del* mutant had lower g_s values, and consequently both C_i and A were also reduced in relation to WT or the other mutants (Table 2). According to the g_s/PPFD curve data we found that the g_s observed for *Del* plants is significantly lower than that observed for WT up to 600 µmol photons m^{-2} s^{-1}, and remains virtually, though not statistically, below that recorded for the other genotypes up to 1800 µmol photons m^{-2} s^{-1}; while *og* and t did not differ from WT (Supplementary Figure 4). It seems reasonable to suggest that increased carotenoid biosynthesis in *Del* mutant plants occurs at the expense of changes in photosynthetic performance with no direct growth impact.

Carotenoids are assumedly essential isoprenoid compounds to protect the photosynthetic apparatus against excess light. In fruits of the *Del* mutant, the main carotenoid that begins to accumulate in the breaker stage is δ-carotene, which makes up 65% of the total carotenoids in the mature phase, while lycopene is only 25%, and β-carotene appears in these fruits only in small quantities (Ronen et al., 1999). Ronen et al. (1999), proposes that regulation of ε-cyclase activity, possibly by controlling *CtrL-e* expression, determines the composition of xanthophyll in leaves and other plant tissues. The relative activities of ε-cyclase versus β-cyclase may determine the flow of carotenoids from lycopene to α-carotene or β-carotene (Ronen et al., 1999). Thus the *CtrL-e* mutation found in *Del* plants converts most of lycopene to δ-carotene, which leads to α-carotene, reducing precursor pool for the synthesis of β-carotene, carotenoid precursor of xanthophyll cycle carotenoids (Liu et al., 2015), and the latter in turn are indispensable for the protection of the photosynthetic apparatus. Thus, changes in F_v/F_m ratio and *qN* were expected indicating damage to the photosynthetic apparatus due to the probable low carotenoid content of the xanthophyll cycle, which was not observed here and indeed F_v/F_m values for *Del* plants are within normal range for non-stressed plants (Björkman and Demmig, 1987).

Metabolic reprogramming in carotenoid related mutants

The terpenoid or isoprenoid are necessary to produce a variety of important compounds such as chlorophylls, carotenoids and plant hormones. Isoprenoid biosynthesis depends on the availability of reduced carbon, ATP and NADPH, which are provided by photosynthesis in non-stressed plants (Yuan et al., 2016). It is important to mention that our knowledge is relatively limited on how exactly and to what extent metabolic flow is apparently distributed among the different branches of the general isoprenoid biosynthetic pathway. However, due to the interactive nature of metabolic pathways in plants, carotenoid metabolism is likely to be modulated or interconnected with other cellular and metabolic processes (Yuan et al., 2015).

Carotenoid biosynthesis is generally controlled by light in green tissues (Lang and Hunter, 1994; Simkin et al., 2003; Römer and Fraser, 2005). In addition, compelling evidence

indicates that primary and secondary metabolism are reprogrammed in response to changing light availability (Martins et al., 2014b). However, how light (and excess of light) modulates this process remains uncertain. It should be borne in mind that the final carotenoid accumulation is a net result of biosynthesis, turnover and ultimately stable storage of the end products. Although we have not measured carotenoid levels in leaf samples, there is compelling evidence using different tomato mutants that increased storage capacity may have a profound influence on carotenoid accumulation (Li et al., 2006; Wurbs et al., 2007; Kilambi et al., 2013; Li and Van Eck, 2007). Concomitant increase of sink capacity and the catalytic activity of the carotenoid biosynthetic pathway may therefore represent a promising strategy for improving carotenoid content in crops. It seems reasonable to anticipate that such changes in carotenoid biosynthesis would be more important under stress conditions. This fact aside, it should be emphasized that many amino acids that accumulate in mutant plants, concomitantly with the accumulation of sugar alcohols and polyamines, are apparently involved in multiple stress responses (Obata and Fernie, 2012).

The changes observed in sugars and organic acids might, at least partially, explain the absence of growth changes observed in carotenoid-related mutants. It seems plausible that there is an interaction between carotenoid metabolism and these compounds, and it will be important to further establish the functional significance of this connection in future studies.

4.5 CONCLUSIONS

We believe that, for species such as tomatoes, which can grow successfully under full sunlight, the increase in energy expenditure through the metabolic reprogramming can be critical to the growth and sustained fitness when the biosynthesis of carotenoids is altered. Although interactions between the carotenoid biosynthetic pathway and other metabolic pathways and how these interactions influence plant growth and development remain rather unclear, it is tempting to speculate that the pathways of energy metabolism and carotenoid biosynthesis are tightly regulated at leaf level in a suitable manner, allowing the plant to prioritize aerial growth, especially under optimal conditions.

Despite the maintenance of vegetative growth observed in carotenoid related mutants, our results demonstrated that carbon flux is apparently altered by changes in carotenoid biosynthesis, and it seems reasonable to suggest that such changes should be even greater under stress conditions. The precise connection between energy metabolism and carotenoid-mediated growth control is only beginning to be revealed.

4.6 ACKNOWLEDGEMENTS

The authors would like to acknowledge Professor Dr. Lázaro E. P. Peres (Escola Superior de Agricultura Luiz de Queiroz -ESALQ/USP, Brazil) for sharing seeds used in this work. This work was supported by funding from the Max Planck Society (to WLA), the National Council for Scientific and Technological Development (CNPq-Brazil, Grant 402511/2016-6 to WLA), and the FAPEMIG (Foundation for Research Assistance of the Minas Gerais State, Brazil, Grant APQ- 01078-15 and APQ-01357-14 to WLA). We also thank the scholarships granted by the Brazilian Federal Agency for Support and Evaluation of Graduate Education (CAPES-Brazil) to AMP. Research fellowships granted by CNPq-Brazil to ANN and WLA are also gratefully acknowledged.

4.7 REFERENCES

Apel W, Bock R (2009) Enhancement of carotenoid biosynthesis in transplastomic tomatoes by induced lycopene-to-provitamin a conversion. Plant Physiology **151**: 59–66

Arvidsson S, Kwasniewski M, Riaño-Pachón DM, Mueller-Roeber B (2008) QuantPrime - A flexible tool for reliable high-throughput primer design for quantitative PCR. BMC Bioinformatics **9**: 1–15

Avendaño-Vázquez AO, Cordoba E, Llamas E, San Román C, Nisar N, De la Torre S, Ramos-Vega M, de la Luz Gutiérrez-Nava M, Cazzonelli CI, Pogson BJ, et al (2014) An uncharacterized apocarotenoid-derived signal generated in ζ-carotene desaturase mutants regulates leaf development and the expression of chloroplast and nuclear genes in Arabidopsis. Plant Cell **26**: 2524–2537

Azari R, Reuveni M, Evenor D, Nahon S, Shlomo H, Chen L, Levin I (2010) Overexpression of UV-DAMAGED DNA BINDING PROTEIN 1 links plant development and phytonutrient accumulation in high pigment-1 tomato. Journal of Experimental Botany **61**: 3627–3637

Barber J, Andersson B (1992) Too much of a good thing: light can be bad for photosynthesis. Trends in Biochemical Sciences **17**: 61–66

Baroli I, Niyogi KK, Barber J, Heifetz P (2000) Molecular genetics of xanthophyll-dependent photoprotection in green algae and plants. Philosophical Transactions of the Royal Society B: Biological Sciences **355**: 1385–1394

Batista-Silva W, Nascimento VL, Medeiros DB, Nunes-Nesi A, Ribeiro DM, Zsögön A, Araújo WL (2018) Modifications in organic acid profiles during fruit development and ripening: Correlation or causation? Frontiers in Plant Science **871**: 1-20

Bhattacharjee S (2012) The language of reactive oxygen species signaling in plants. Journal of Botany **2012**: 1–22

Björkman O, Demmig B (1987) Photon yield of O_2 evolution and chlorophyll fluorescence characteristics at 77 K among vascular plants of diverse origins. Planta **170**: 489–504

BRADFORD MM (1976) A rapid and sensitive method for the quantitation of microgram quantities of protein utilizing the principle of protein-dye binding. Analytical Biochemistry **72**: 248–254

von Caemmerer S (2000) Biochemical models of leaf photosynthesis. CSIRO Publishing, Collingwood

Caldana C, Scheible WR, Mueller-Roeber B, Ruzicic S (2007) A quantitative RT-PCR platform for high-throughput expression profiling of 2500 rice transcription factors. Plant Methods **3**: 1–9

Cazzaniga S, Li Z, Niyogi KK, Bassi R, Dall'Osto L (2012) The Arabidopsis szl1 mutant reveals a critical role of β-carotene in photosystem I photoprotection. Plant Physiology **159**: 1745–1758

Dall'Osto L, Fiore A, Cazzaniga S, Giuliano G, Bassi R (2007) Different roles of α- and β-branch xanthophylls in photosystem assembly and photoprotection. Journal of Biological Chemistry **282**: 35056–35068

Demidchik V (2015) Mechanisms of oxidative stress in plants: From classical chemistry to cell biology. Environmental and Experimental Botany **109**: 212–228

Diretto G, Al-babili S, Tavazza R, Papacchioli V, Beyer P, Giuliano G (2007) Metabolic engineering of potato carotenoid content through tuber-specific overexpression of a bacterial. PLoS ONE 1–8

Dong H, Deng Y, Mu J, Lu Q, Wang Y, Xu Y, Chu C, Chong K, Lu C, Zuo J (2007) The Arabidopsis Spontaneous Cell Death1 gene, encoding a ζ-carotene desaturase essential for carotenoid biosynthesis, is involved in chloroplast development, photoprotection and retrograde signalling. Cell Research **17**: 458–470

Egea I, Bian W, Barsan C, Jauneau A, Pech JC, Latché A, Li Z, Chervin C (2011) Chloroplast to chromoplast transition in tomato fruit: Spectral confocal microscopy analyses of carotenoids and chlorophylls in isolated plastids and time-lapse recording on intact live tissue. Annals of Botany **108**: 291–297

Fernie AR, Aharoni A, Willmitzer L, Stitt M, Tohge T, Kopka J, Carroll AJ, Saito K, Fraser PD, de Luca V (2011) Recommendations for reporting metabolite data. Plant Cell **23**: 2477–2482

Fernie AR, Roscher A, Ratcliffe RG, Kruger NJ (2001) Fructose 2,6-bisphosphate activates pyrophosphate: fructose-6-phos-phate 1-phosphotransferase and increases triose phosphate to hexose phosphate cyclingin heterotrophic cells. Planta **212**: 250–263

Ford NA, Erdman JW (2012) Are lycopene metabolites metabolically active? Acta Biochimica Polonica **59**: 1–4

Fraser PD, Bramley PM (2004) The biosynthesis and nutritional uses of carotenoids. Progress in Lipid Research **43**: 228–265

Fray RG, Wallace A, Fraser PD, Valero D, Hedden P, Bramley PM, Grierson D (1995) Constitutive expression of a fruit phytoene synthase gene in transgenic tomatoes causes dwarfism by redirecting metabolites from the gibberellin pathway. The Plant Journal **8**: 693–701

Genty B, Briantais J-M, Baker NR (1989) The relationship between the quantum yield of photosynthetic electron transport and quenching of chlorophyll fluorescence. Biochimica et Biophysica Acta (BBA) - General Subjects **990**: 87–92

Gibon Y, Blaesing OE, Hannemann J, Carillo P, Ho M, Palacios N, Cross J, Selbig J, Stitt M (2004) A robot-based platform to measure multiple enzyme activities in arabidopsis using a set of cycling assays: Comparison of changes of enzyme activities and transcript levels during diurnal cycles and in prolonged darkness. The Plant Cell **16**: 3304–3325

Goldman IL (2011) Molecular breeding of healthy vegetables. EMBO Reports **12**: 96–102

Hashimoto H, Uragami C, Cogdell RJ (2016) Carotenoids and photosynthesis. Subcell Biochem **79**: 111–139

Hou X, Rivers J, León P, McQuinn RP, Pogson BJ (2016) Synthesis and function of apocarotenoid signals in plants. Trends in Plant Science **21**: 792–803

Isaacson T, Ronen G, Zamir D, Hirschberg J (2002) Cloning of tangerine from tomato reveals a carotenoid isomerase essential for the production of ?-Carotene and xanthophylls in plants. Plant Cell **14**: 333–342

Janků, Luhová, Petřivalský (2019) On the origin and fate of reactive oxygen species in plant cell compartments. Antioxidants **8**: 105

Johansen DA (1940) Plant microtechnique. McGraw-Hill Book, New York

Kachanovsky DE, Filler S, Isaacson T, Hirschberg J (2012) Epistasis in tomato color mutations involves regulation of phytoene synthase 1 expression by cis-carotenoids. Proceedings of the National Academy of Sciences of the United States of America **109**:19021-19026

Ke Q, Kang L, Kim HS, Xie T, Liu C, Ji CY, Kim SH, Park WS, Ahn MJ, Wang S, et al (2019) Down-regulation of lycopene ε-cyclase expression in transgenic sweetpotato plants increases the carotenoid content and tolerance to abiotic stress. Plant Science **281**: 52–60

Kendrick RE, Kerckhooffs LHJ, van Tuinen A, Koornneef M (1997) Photomorphogenic mutants of tomato. Plant, Cell and Environment **20**: 746–751

Kilambi H V., Kumar R, Sharma R, Sreelakshmi Y (2013) Chromoplast-specific carotenoid-associated protein appears to be important for enhanced accumulation of carotenoids in hp1 tomato fruits. Plant Physiology **161**: 2085–2101

Kim HS, Ji CY, Chan-Lee J, So-Kim E, Sung-Park C, Sang A, -Soo, Kwak (2018) Orange : A target gene for regulating carotenoid homeostasis and increasing plant tolerance to environmental stress in marginal lands. Journal Experimental Botany 1–8

Kloz M, Pillai S, Kodis G, Gust D, Moore TA, Moore AL, Van Grondelle R, Kennis JTM (2011) Carotenoid photoprotection in artificial photosynthetic antennas. Journal of the American Chemical Society **133**: 7007–7015

Kopka J, Schauer N, Krueger S, Birkemeyer C, Usadel B, Bergmüller E, Dörmann P, Weckwerth W, Gibon Y, Stitt M, et al (2005) GMD@CSB.DB: The Golm metabolome database. Bioinformatics **21**: 1635–1638

Krinsky NI, Johnson EJ (2005) Carotenoid actions and their relation to health and disease. Molecular Aspects of Medicine **26**: 459–516

Lang HP, Hunter CN (1994) The relationship between carotenoid biosynthesis and the assembly of the light-harvesting LH2 complex in *Rhodobacter sphaeroides*. Biochemical Journal **298**: 197–205

Li L, Van Eck J (2007) Metabolic engineering of carotenoid accumulation by creating a metabolic sink. Transgenic Research **16**: 581–585

Li L, Lu S, Cosman KM, Earle ED, Garvin DF, O'Neill J (2006) β-Carotene accumulation induced by the cauliflower Or gene is not due to an increased capacity of biosynthesis. Phytochemistry **67**: 1177–1184

Lisec J, Schauer N, Kopka J, Willmitzer L, Fernie AR (2006) Gas chromatography mass spectrometry-based metabolite profiling in plants. Nature Protocols **1**: 387–396

Liu L, Shao Z, Zhang M, Wang Q (2015) Regulation of carotenoid metabolism in tomato. Molecular Plant **8**: 28–39

Logan BA, Adams WW, Demmig-Adams B (2007) Avoiding common pitfalls of chlorophyll fluorescence analysis under field conditions. Functional Plant Biology **34**: 853–859

Long SP, Bernacchi C (2003) Gas exchange measurements, what can they tell us about the underlying limitations to photosynthesis? Procedures and sources of error. Journal of Experimental Botany **54**: 2393–2401

Lu S, Li L (2008) Carotenoid metabolism: Biosynthesis, regulation, and beyond. Journal of Integrative Plant Biology **50**: 778–785

Luedemann A, Malotky L von, Erban A, Kopka J (2011) TagFinder: Preprocessing software for the fingerprinting and the profi ling of gas chromatography–mass spectrometry based metabolome analyses. Plant Metabolomics **860**: 255–286

Maldonade IR, Rodriguez-Amaya DB, Scamparini ARP (2008) Carotenoids of yeasts isolated from the Brazilian ecosystem. Food Chemistry **107**: 145–150

Martins SCV, Araújo WL, Tohge T, Fernie AR, DaMatta FM (2014) In high-light-acclimated coffee plants the metabolic machinery is adjusted to avoid oxidative stress rather than to benefit from extra light enhancement in photosynthetic yield. PLoS One **9**: 1–11

Martins SC V, Galmés J, Molins A, DaMatta FM (2013) Improving the estimation of mesophyll conductance to CO2: On the role of electron transport rate correction and respiration. Journal of experimental botany **64**: 3285–98

McQuinn RP, Giovannoni JJ, Pogson BJ (2015) More than meets the eye: From carotenoid biosynthesis, to new insights into apocarotenoid signaling. Current Opinion in Plant Biology **27**: 172–179

Medeiros DB, Martins SCV, Cavalcanti JHF, Daloso DM, Martinoia E, Nunes-Nesi A, DaMatta FM, Fernie AR, Araújo WL (2016) Enhanced photosynthesis and growth in atquac1 knockout mutants are due to altered organic acid accumulation and an increase in both stomatal and mesophyll conductance. Plant Physiology **170**: 86–101

Mustilli AC, F. F, CILIENTO R, ALFONSO F, BOWLER C (1999) Phenotype of the tomato high pigment-2 mutant is caused by a mutation in the tomato homolog of DEETIOLATED1. Plant Cell Online **11**: 145–158

Nisar N, Li L, Lu S, Khin NC, Pogson BJ (2015) Carotenoid metabolism in plants. Molecular Plant **8**: 68–82

Niyogi K, Shih C, Soon Chow W, Pogson B, DellaPenna D, Björkman O (2001) Photoprotection in a zeaxanthin- and lutein-deficient double mutant of Arabidopsis. Photosynthesis Research **67**: 139–145

Niyogi KK (1999) Photoprotection revisited: Genetic and molecular approaches. Annual Review of Plant Physiology and Plant Molecular Biology **50**: 333–359

O'Brien TP, Feder N, McCully ME (1964) Polychromatic staining of plant cell walls by toluidine blue O. Protoplasma **59**: 368–373

Obata T, Fernie AR (2012) The use of metabolomics to dissect plant responses to abiotic stresses. Cellular and Molecular Life Sciences **69**: 3225–3243

Park H, Kreunen SS, Cuttriss AJ, DellaPenna D, Pogson BJ (2002) Identification of the carotenoid isomerase provides insight into carotenoid biosynthesis, prolamellar body formation, and photomorphogenesis. Plant Cell **14**: 321–332

Park SC, Kim SH, Park S, Lee HU, Lee JS, Park WS, Ahn MJ, Kim YH, Jeong JC, Lee HS, et al (2015) Enhanced accumulation of carotenoids in sweet potato plants overexpressing IbOr-Ins gene in purple-fleshed sweetpotato cultivar. Plant Physiology and Biochemistry **86**: 82–90

Pino-Nunes LE, Lattarulo M, P Peres LE (2010) Manual do modelo vegetal micro-tom capitulo 2: plantio, irrigação e adubação nas canaletas/vasos e cultivo no canteiro. Laboratory of hormonal control of plant development (ESALQ), Piracicaba 7p

Qin G, Gu H, Ma L, Peng Y, Deng XW, Chen Z, Qu LJ (2007) Disruption of phytoene desaturase gene results in albino and dwarf phenotypes in Arabidopsis by impairing chlorophyll, carotenoid, and gibberellin biosynthesis. Cell Research **17**: 471–482

Rodeghiero M, Niinemets Ü, Cescatti A (2007) Major diffusion leaks of clamp-on leaf cuvettes still unaccounted: How erroneous are the estimates of Farquhar et al. model parameters? Plant, Cell and Environment **30**: 1006–1022

Roessner U, Luedemann A, Brust D, Fiehn O, Linke T, Willmitzer L, Fernie AR (2001) Metabolic profiling allows comprehensive phenotyping of genetically or environmentally modified plant systems. Plant Cell **13**: 11–29

Rolland N, Curien G, Finazzi G, Kuntz M, Maréchal E, Matringe M, Ravanel S, Seigneurin-Berny D (2012) The biosynthetic capacities of the plastids and integration between cytoplasmic and chloroplast processes. Annual Review of Genetics **46**: 233–264

Römer S, Fraser PD (2005) Recent advances in carotenoid biosynthesis, regulation and manipulation. Planta **221**: 305–308

Ronen G, Carmel-Goren L, Zamir D, Hirschberg J (2000) An alternative pathway to beta-carotene formation in plant chromoplasts discovered by map-based cloning of Beta and old-gold color mutations in tomato. Proceedings of the National Academy of Sciences **97**: 11102–11107

Ronen G, Cohen M, Zamir D, Hirschberg J (1999) Regulation of carotenoid biosynthesis during tomato fruit development: expression of the gene for lycopene epsilon cyclase is down- regulated during ripening and is elevated in the mutant Delta. The Plant Journal **17**: 341–351

Sandmann G, Römer S, Fraser PD (2006) Understanding carotenoid metabolism as a necessity for genetic engineering of crop plants. Metabolic Engineering **8**: 291–302

Sharkey TD, Bernacchi CJ, Farquhar GD, Singsaas EL (2007) Fitting photosynthetic carbon dioxide response curves for C_3 leaves. Plant, Cell and Environment **30**: 1035–1040

Simkin AJ, Zhu C, Kuntz M, Sandmann G (2003) Light-dark regulation of carotenoid biosynthesis in pepper (*Capsicum annuum*) leaves. Journal of Plant Physiology **160**: 439–443

Thompson AE, Tomes ML, Erickson HT, Wann EV, Armstrong RJ (1967) Inheritance of crimson fruit color in tomatoes. Proceedings of the American Society for Horticultural Science **91**: 495–504

Tian L, Musetti V, Kim J, Magallanes-Lundback M, DellaPenna D (2004) The Arabidopsis LUT1 locus encodes a member of the cytochrome P450 family that is required for carotenoid ε-ring hydroxylation activity. Proceedings of the National Academy of Sciences of the United States of America **101**: 402–407

Vogel JT, Tieman DM, Sims CA, Odabasi AZ, Clark DG, Klee HJ (2010) Carotenoid content impacts flavor acceptability in tomato (*Solanum lycopersicum*). Journal of the Science of Food and Agriculture **90**: 2233–2240

Wellburn AR (1994) The spectral determination of chlorophylls a and b, as well as total carotenoids, using various solvents with spectrophotometers of different resolution. Journal of Plant Physiology **144**: 307–313

Wurbs D, Ruf S, Bock R (2007) Contained metabolic engineering in tomatoes by expression of carotenoid biosynthesis genes from the plastid genome. Plant Journal **49**: 276–288

Yan J, Kandianis CB, Harjes CE, Bai L, Kim E, Yang X, Skinner DJ, Fu Z, Mitchell S, Li Q, et al (2010) Rare genetic variation at *Zea mays* crtRB1 increases β-carotene in maize grain. Nature Publishing Group **42**: 322–327

Ye X, Al-babili S, Klöti A, Zhang J, Lucca P, Beyer P, Endosperm R, Ye X, Al-babili S, Kloti A, et al (2000) Engineering provitamin A (b-carotene) biosynthesis pathway into (carotenoid-free) rice endosperm. Science **287**: 303–305

Yemm EW, Cocking EC, Ricketts RE (1955) The determination of amino-acids with ninhydrin. Analyst 80: 209–214

Yoo HJ, Park WJ, Lee GM, Oh CS, Yeam I, Won DC, Kim CK, Lee JM (2017) Inferring the genetic determinants of fruit colors in tomato by carotenoid profiling. Molecules **22**: 1–14

Young AJ, Frank HA (1996) Energy transfer reactions involving carotenoids: Quenching of chlorophyll fluorescence. Journal of Photochemistry and Photobiology B: Biology **36**: 3–15

Yuan H, Cheung CYM, Poolman MG, Hilbers PAJ, Van Riel NAW (2016) A genome-scale metabolic network reconstruction of tomato (*Solanum lycopersicum* L.) and its application to photorespiratory metabolism. Plant Journal **85**: 289–304

Yuan H, Zhang J, Nageswaran D, Li L (2015) Carotenoid metabolism and regulation in horticultural crops. Horticulture Research **2**: 1-11

Zsögön A, Alves Negrini AC, Peres LEP, Nguyen HT, Ball MC (2015) A mutation that eliminates bundle sheath extensions reduces leaf hydraulic conductance, stomatal conductance and assimilation rates in tomato (*Solanum lycopersicum*). New Phytologist **205**: 618–626

4.8 FIGURES AND TABLES

Table 1 - Relative expression on *Lcy-e*, *Cyc-B* and *CrtISO* genes in Micro-Tom plants (WT) and *Del*, *og* and *t* mutants. Means followed by the same letter on the vertical did not differ (P <0.05) significantly from WT plants by the Duncan's test. Values are presented as means ± standard error (n = 4).

	Lcy-e	*Cyc-B*	*CrtISO*
WT	1.01 ± 0.009 b	1.14 ± 0.35 a	1.05 ± 0.21 b
Del	1.48 ± 0.60 b	1.93 ± 0.41 a	3.49 ± 0.62 a
og	1.33 ± 0.26 b	0.84 ± 0.19 a	2.46 ± 0.27 ab
t	3.10 ± 0.90 a	0.50 ± 0.23 a	1.59 ± 0.32 ab

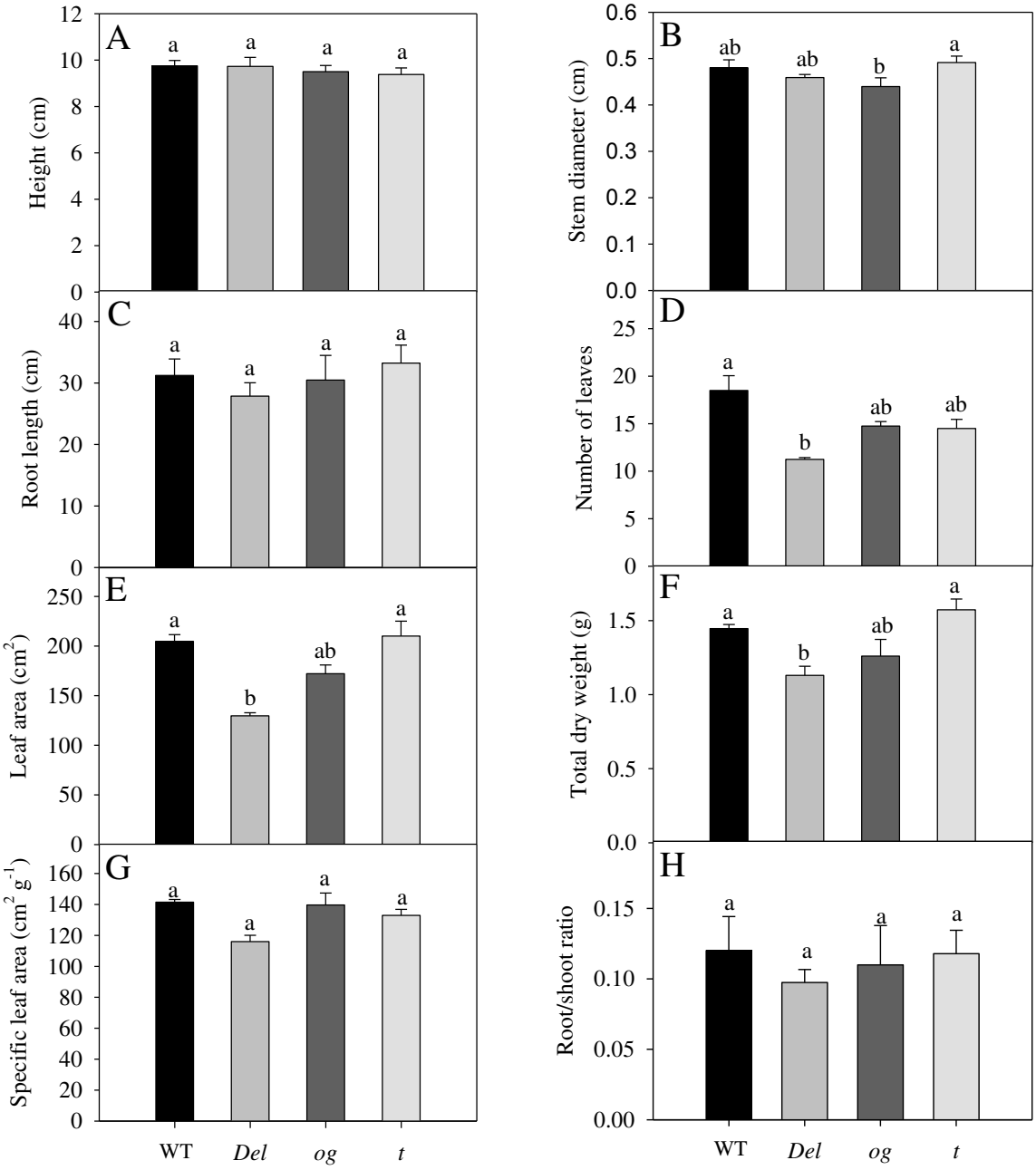

Figure 1 - Changes in growth plants in the Micro-Tom plants (WT) and *Del, g* and *t* mutants. Evaluations were carried out on six-week-old plants (44 DAP). (A) Height; (B) Stem diameter; (C) Root length; (D) Number of leaves; (E) Leaf area; (F) Total dry weight; (G) Specific leaf area; (H) Root/Shoot ratio. Means followed by the same letter do not differ according to Duncan's test ($P < 0.05$). Values are presented as relative means ± standard error ($n = 4$).

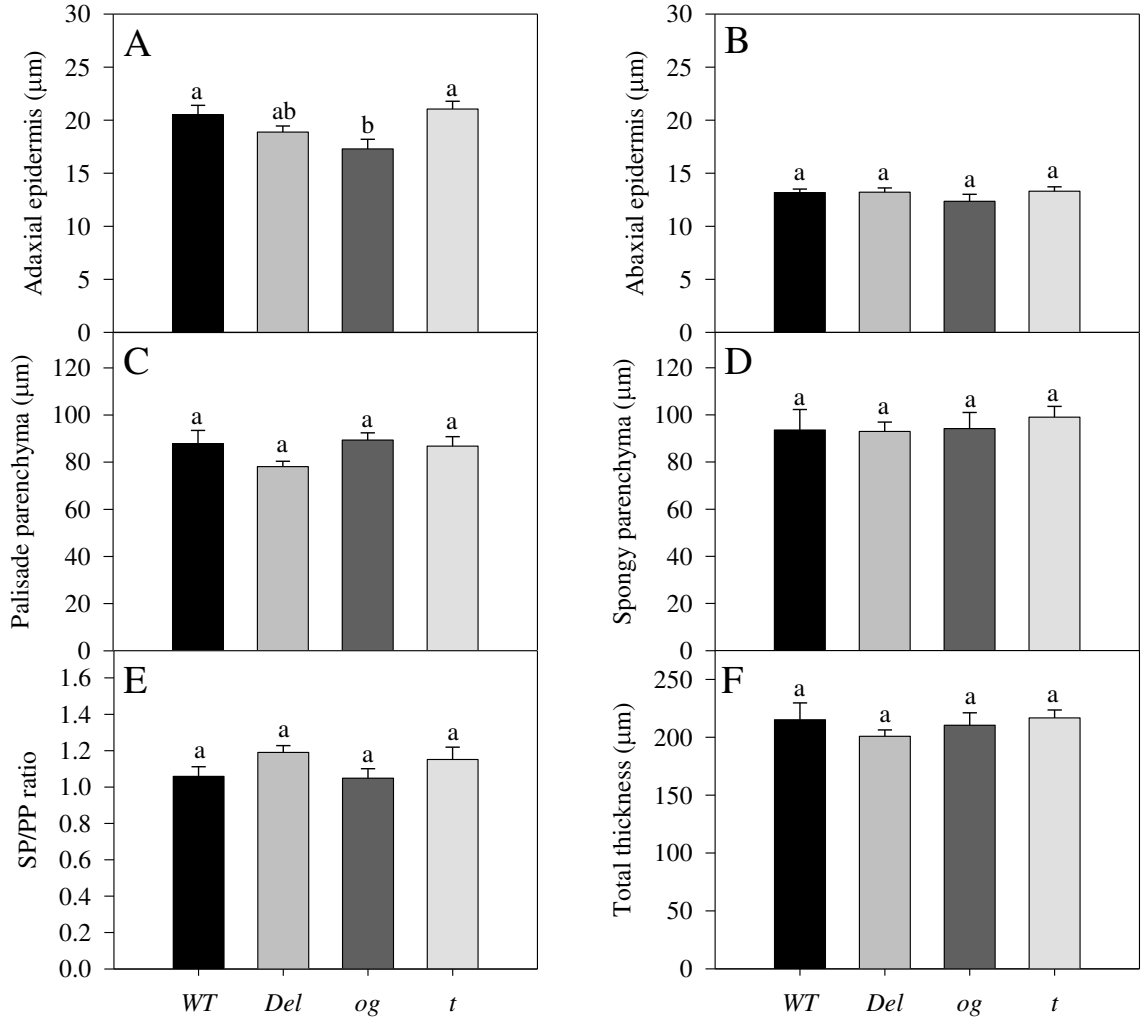

Figure 2 - Leaf limb measurements in the Micro-Tom plants (WT) and *Del, g* and *t* mutants. Evaluations were carried out on four-week-old plants (28 DAP). (A) Adaxial epidermis; (B) Abaxial epidermis; (C) Palisade parenchyma; (D) Spongy parenchyma; (E) SP/PP ratio; (F) Total thickness. Means followed by the same letter do not differ according to Duncan's test ($P < 0.05$). Values are presented as relative means ± standard error (n = 5).

Table 2 - Changes in gas exchange and fluorescence parameters in the Micro-Tom plants (WT) and *Del, g* and *t* mutants. Evaluations were carried out on four-week-old plants (28 DAP). *A*: Photosynthesis; *Rd*: Dark respiration; g_s: Stomatal conductance; C_i: Internal CO_2 concentration; *E*: transpiration; *Fv/Fm* ratio; *ETR*: electron transport rate; *ΦFSII*: effective quantum yield of Photosystem II. Means followed by the same letter on the horizontal did not differ (P <0.05) by the Duncan's test. Values are presented as means ± standard error (n = 5).

	WT	*Del*	*og*	*t*
A	16.46 ± 0.72 ab	14.71 ± 0.78 b	17.29 ± 1.06 a	15.67 ± 0.43 ab
R_d	2.69 ± 0.09 a	2.84 ± 0.12 a	2.53 ± 0.16 a	2.60 ± 0.13 a
g_s	0.17 ± 0.01 a	0.11 ± 0.01 b	0.17 ± 0.02 a	0.16 ± 0.01 a
C_i	225.98 ± 7.57 a	196.57 ± 6.22 b	207.94 ± 2.95 ab	211.90 ± 5.89 ab
E	3.42 ± 0.12 a	2.51 ± 0.24 a	3.39 ± 0.23 a	4.00 ± 0.19 a
Fv/Fm	0.82 ± 0.003 a	0.82 ± 0.007 a	0.81 ± 0.002 a	0.82 ± 0.003 a
ETR	238.77 ± 1.92 ab	235.41 ± 1.17 ab	230.48 ± 6.57 b	250.09 ± 1.72 a
ϕPSIIe	0.55 ± 0.004 b	0.54 ± 0.003 b	0.53 ± 0.015 b	0.58 ± 0.004 a
qP	0.83 ± 0.003 a	0.83 ± 0.005 a	0.81 ± 0.005 b	0.84 ± 0.003 a
qN	2.96 ± 0.06 ab	2.87 ± 0.02 b	2.76 ± 0.10 b	3.21 ± 0.05 a

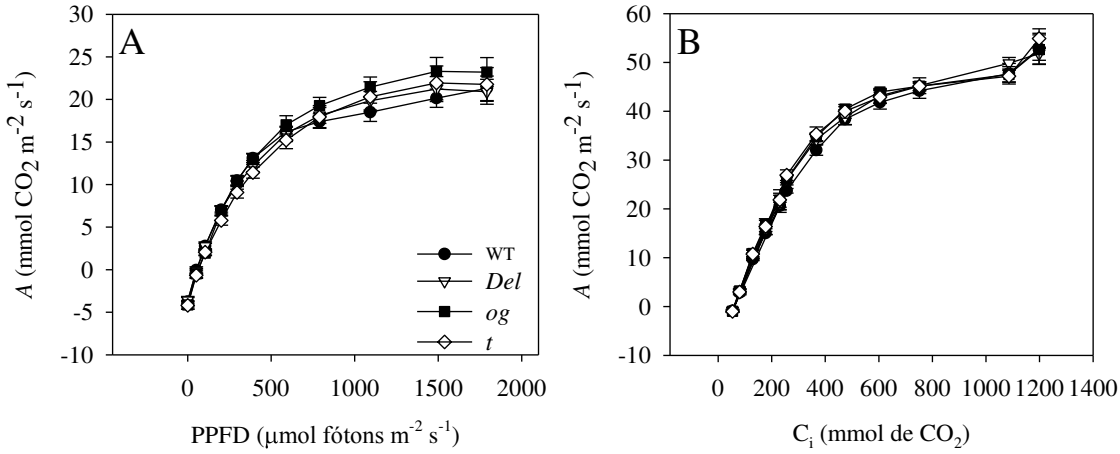

Figure 3 - Photosynthesis curves in response to variation in the photosynthetic photon flux density (PPFD) and substomatic CO_2 concentration (C_i) in the Micro-Tom plants (WT) and *Del, g* and *t* mutants. Evaluations were carried out on four-week-old plants (28 DAP). (A) *A*/PAR curves; (B) *A*/C_i curves. Values are presented as relative means ± standard error (n = 5).

Table 3 - Photosynthetic parameters derived from the light curves (*A*/PPFD) for Micro-Tom plants (WT) and *Del, g* and *t* mutants. A_{max}: net assimilation rate of carbon saturated by light, *LCP*: light compensation point; *LSP*: light saturation point and $1/\Phi$: efficiency of light use. Means followed by the same letter on the vertical do not differ (P <0.05) by the Duncan's test. Values represent means ± standard error (n = 5).

	A_{max} (μmol CO_2 m^{-2} s^{-1})	*LCP* (mmol m^{-2} s^{-1})	*LSP* (mmol m^{-2} s^{-1})	$1/\phi$ (μmol fótons mol^{-1} CO_2)
WT	27.47 ± 1.78 a	56.73 ± 9.22 a	832. 60 ± 57.18 a	14.20 ± 1.20 a
Del	28.07 ± 2.05 a	55.92 ± 5.53 a	881.39 ± 33.39 a	15.20 ± 0.93 a
og	31.19 ± 2.08 a	65.01 ± 6.78 a	910.73 ± 34.31 a	15.23 ± 0.29 a
t	30.07 ± 2.49 a	69.06 ± 7.11 a	947.83 ± 30.95 a	17.06 ± 0.60 a

Table 4 - Photosynthetic parameters derived from the *A/Ci* curve for Micro-Tom plants (WT) and *Del, g* and *t* mutants. V_{cmax}: maximum carboxylation rate, J_{max}: maximum carboxylation rate limited by electron transport, J_{max}/V_{cmax}: ratio between J_{max} and V_{cmax} and TPU: triose phosphate utilization. Means followed by the same letter on the vertical do not differ (P <0.05) by the Duncan's test. Values represent means ± standard error (n = 5).

	Vc_{max} (μmol m^{-2} s^{-1})	J_{max} (μmol m^{-2} s^{-1})	J_{max}/Vc_{max}	TPU (mmol m^{-2} s^{-1})
WT	89.76 ± 1.17 b	175.65 ± 1.90 a	1.96 ± 0.04 a	13.40 ± 0.23 a
Del	105.05 ± 4.16 a	176.61 ± 9.40 a	1.69 ± 0.09 b	13.18 ± 0.42 a
og	101.30 ± 2.68 a	170.57 ± 4.14 a	1.68 ± 0.03 b	12.75 ± 0.17 a
t	106.10 ± 3.84 a	161.61 ± 5.33 a	1.52 ± 0.03 b	12.20 ± 0.24 a

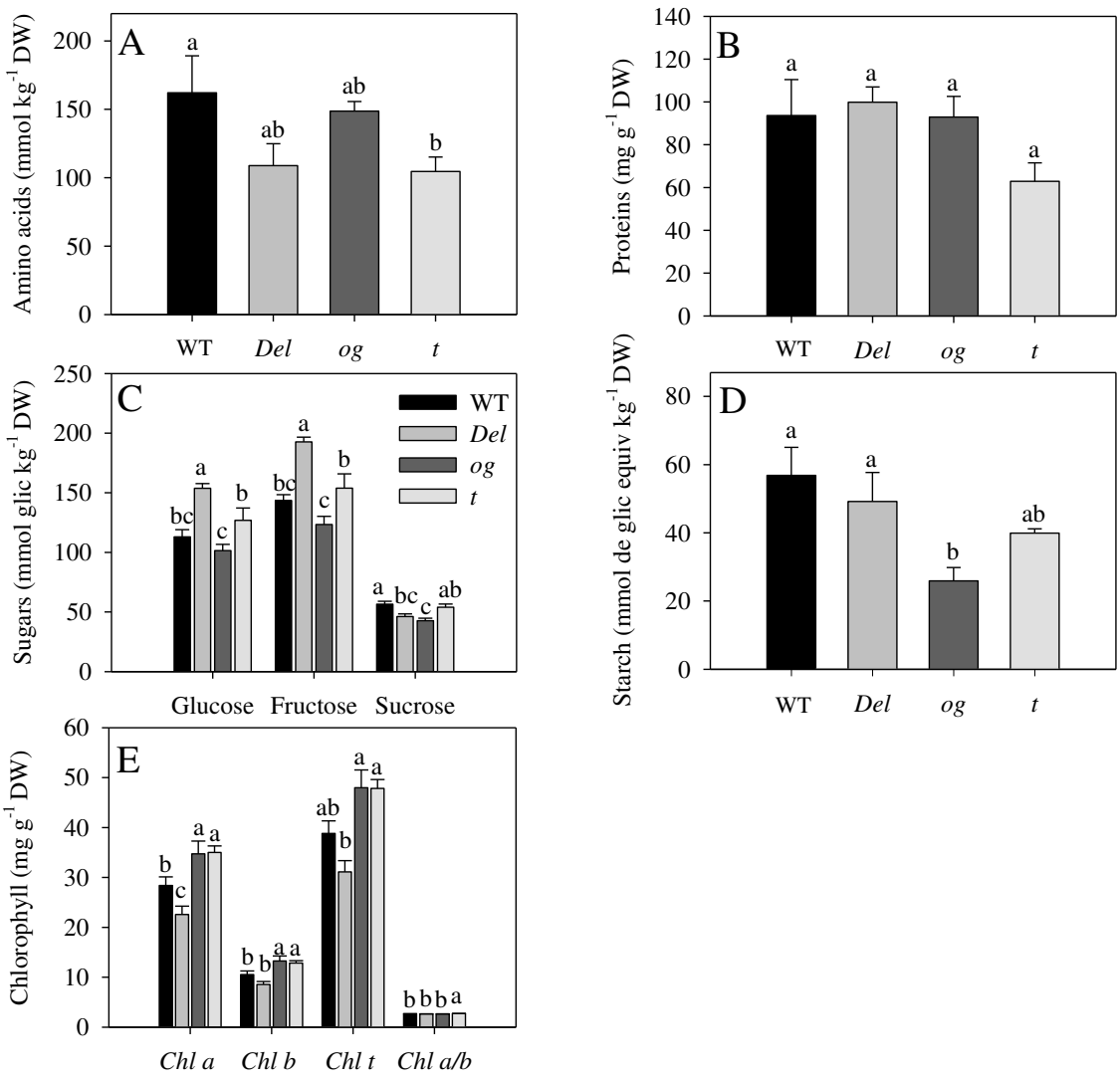

Figure 4 - Comparison of metabolite and pigment levels in the Micro-Tom plants (WT) and *Del, g* and *t* mutants. Evaluations were carried out on four-week-old plants (28 DAP). (A) Amino acids; (B) Proteins; (C) Starch; (D) Sugars; (E) Chlorophyll. Means followed by the same letter do not differ according to Duncan's test ($P < 0.05$). Values are presented as relative means ± standard error (n = 5).

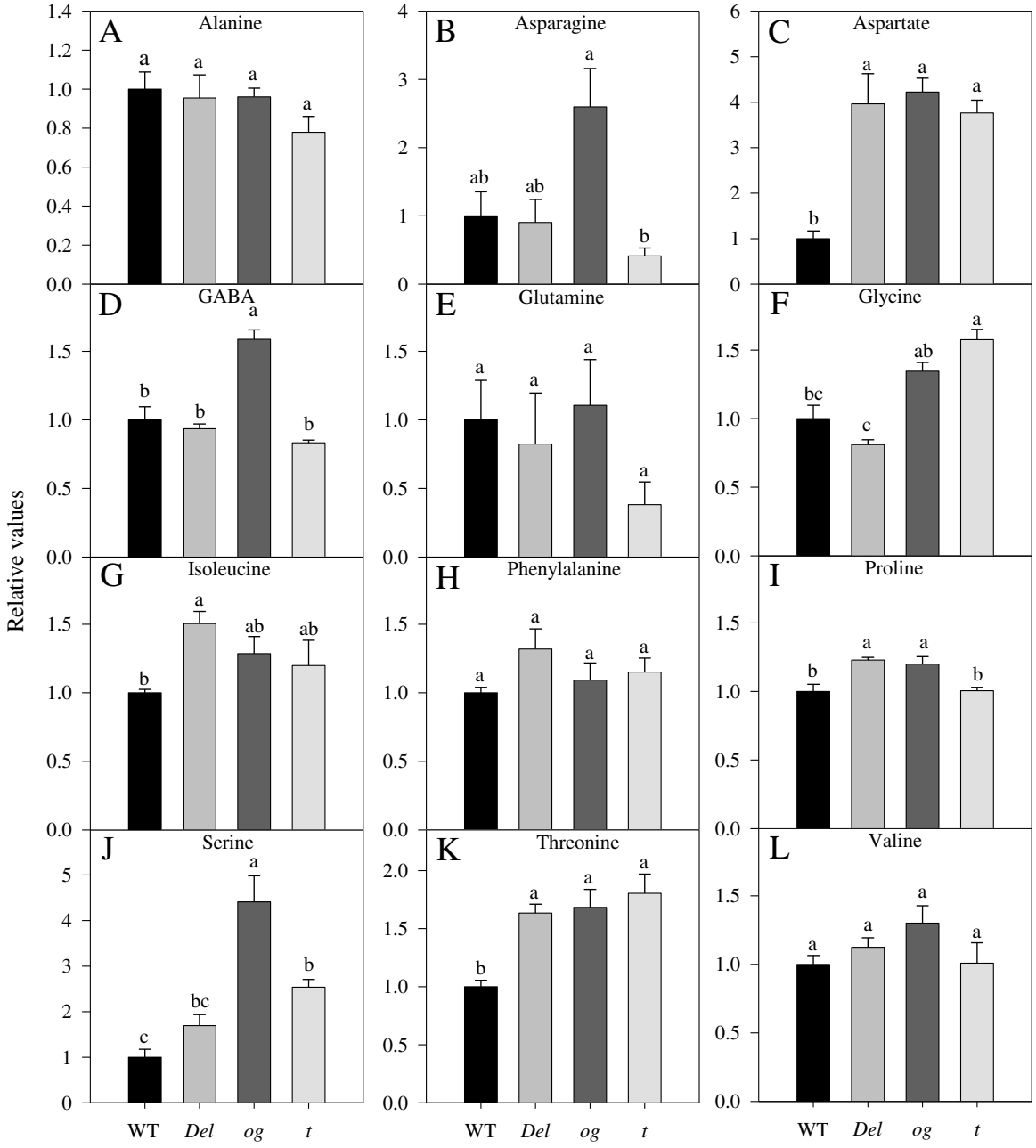

Figure 5 - Relative levels of amino acids in the Micro-Tom plants (WT) and *Del, g* and *t* mutants. Evaluations were carried out on four-week-old plants (28 DAP). (A) Alanine; (B) Asparagine; (C) Aspartate; (D) GABA; (E) Glutamine; (F) Glycine; (G) Isoleucine; (H) Phenylalanine; (I) Proline; (J) Serine; (K) Threonine; (L) Valine. Data were normalized to the mean Wild Type values. Means followed by the same letter do not differ according to Duncan's test ($P < 0.05$). Capital letters compare the same genotype in different treatments; lower case letters compare the different genotypes within each treatment. Values are presented as relative means ± standard error (n = 4).

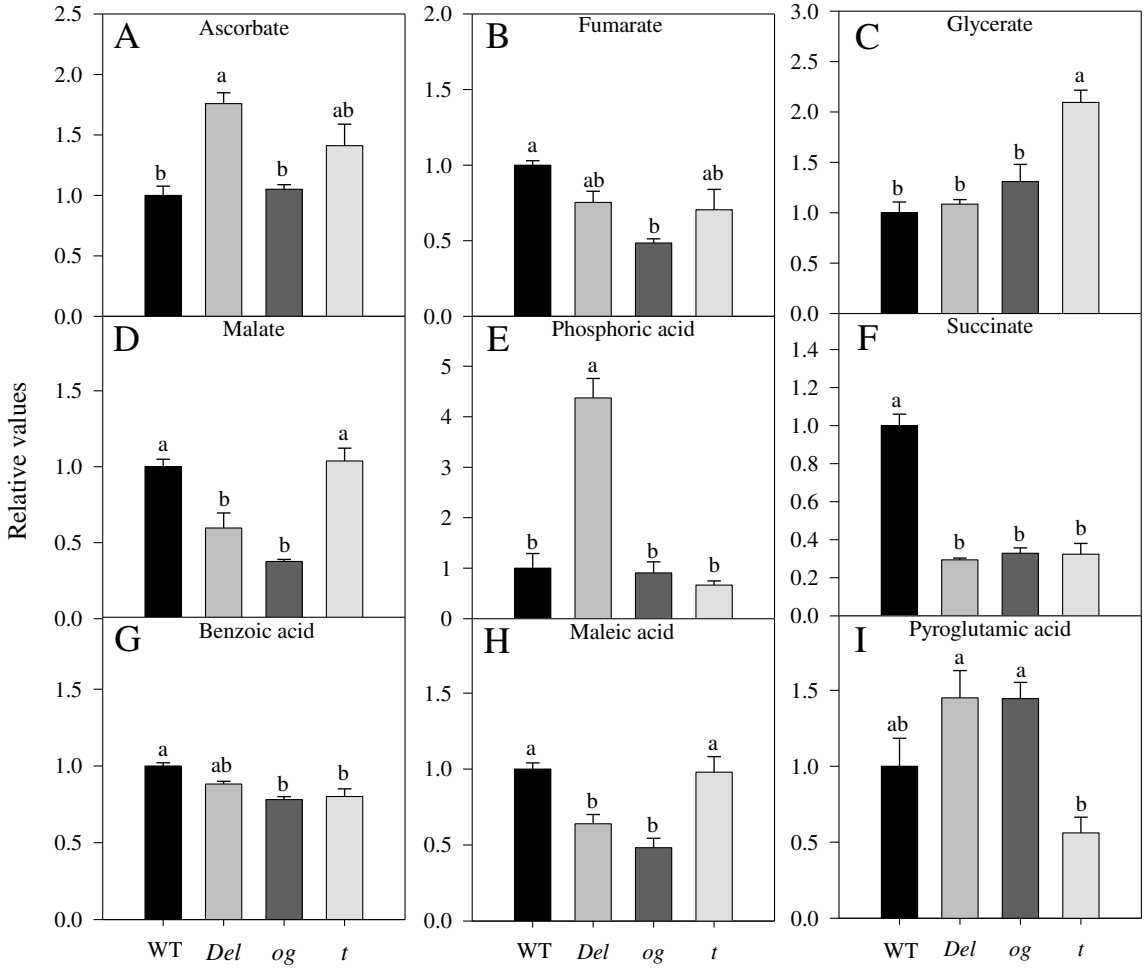

Figure 6 - Relative levels of organic acids in the Micro-Tom plants (WT) and *Del, g* and *t* mutants. Evaluations were carried out on four-week-old plants (28 DAP). (A) Ascorbate; (B) Fumarate; (C) Glycerate; (D) Malate; (E) Phosphoric acid; (F) Succinate; (G) Benzoic acid; (H) Maleic acid; (I) Pyroglutamic acid. Data were normalized to the mean Wild Type values. Means followed by the same letter do not differ according to Duncan's test ($P < 0.05$). Capital letters compare the same genotype in different treatments; lower case letters compare the different genotypes within each treatment. Values are presented as relative means ± standard error (n = 4).

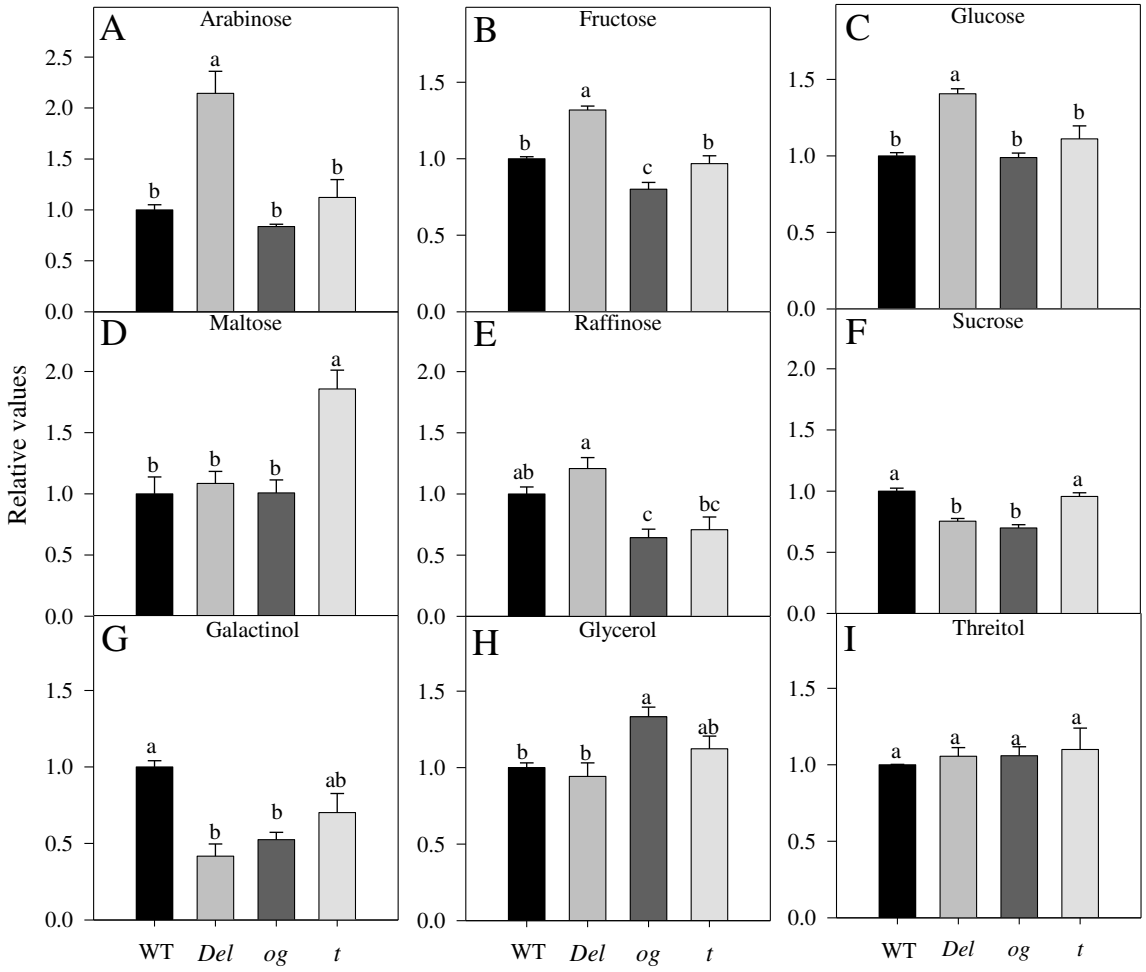

Figure 7 - Relative levels of sugars and polyols in the Micro-Tom plants (WT) and *Del, g* and *t* mutants. Evaluations were carried out on four-week-old plants (28 DAP). (A) Arabinose; (B) Fructose; (C) Glucose; (D) Maltose; (E) Rafinose; (F) Sucrose; (G) Galactinol; (H) Glycerol; (I) Threitol. Data were normalized to the mean Wild Type values. Means followed by the same letter do not differ from according to Duncan's test ($P < 0.05$). Capital letters compare the same genotype in different treatments; lower case letters compare the different genotypes within each treatment. Values are presented as relative means ± standard error (n = 4).

4.9 SUPPLEMENTARY DATA

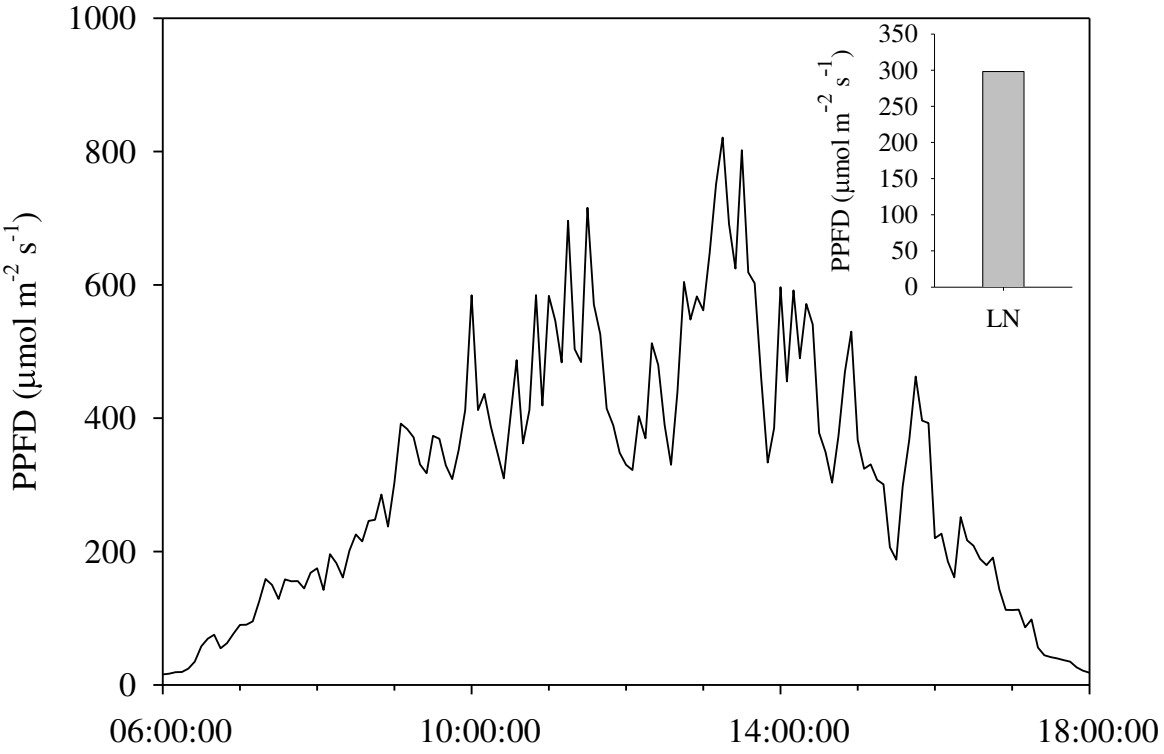

Supplementary Figure 1 - Time course of photosynthetic photon flux density (PPFD) throughout the day for WT plants and *Del, og* and *t* mutants. Plants were grown in greenhouse under natural light conditions (NL). Line represent the PPFD throughout the day and the inset bar represent the mean of PPFD measured from 6:00 to 18:00 hours in four days throughout the experiment.

Supplementary Table 1 - Sequence of primers used in qRT-PCR reactions.

Gene	Locus		Sequence
Actin	Solyc03g078400.2.1	FW	GGTCCCTCTATTGTCCACAG
		RV	TGCATCTCTGGTCCAGTAGGA
Lcy-e	Solyc12g008980.1.1	FW	TCCTACTGGTGCAACATTGATA
		RV	GAGAGACCGCGATTTCTGTT
Cyc-B	Solyc06g074240.1.1	FW	TGGCAATCTAGCAATAGAGAGC
		RV	GCTTGTTGACAGTATGTAGCTC
CrtISO	Solyc10g081650.1.1	FW	TGGTTGGTTAAGGACACTAGCA
		RV	CTCAATTGGAACCTCATTTTCCA

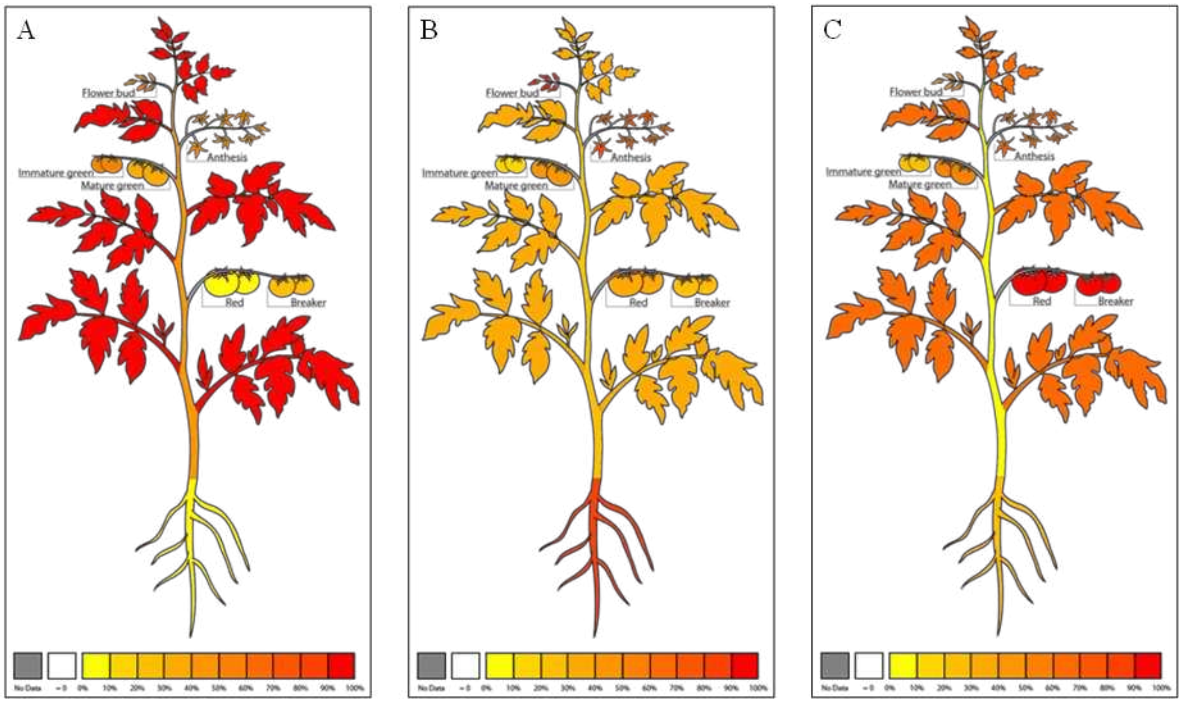

Supplementary Figure 2 - Expression levels of genes licopeno β-cyclase (*Cyc-B*) (A), licopeno ε-ciclase (*Lcy-e*) (B) and carotenoid cis-trans isomerase (*CrtISO*) (C) in different tissues of tomato (*Solanum lycopersicum* L). Font: TomExpress.

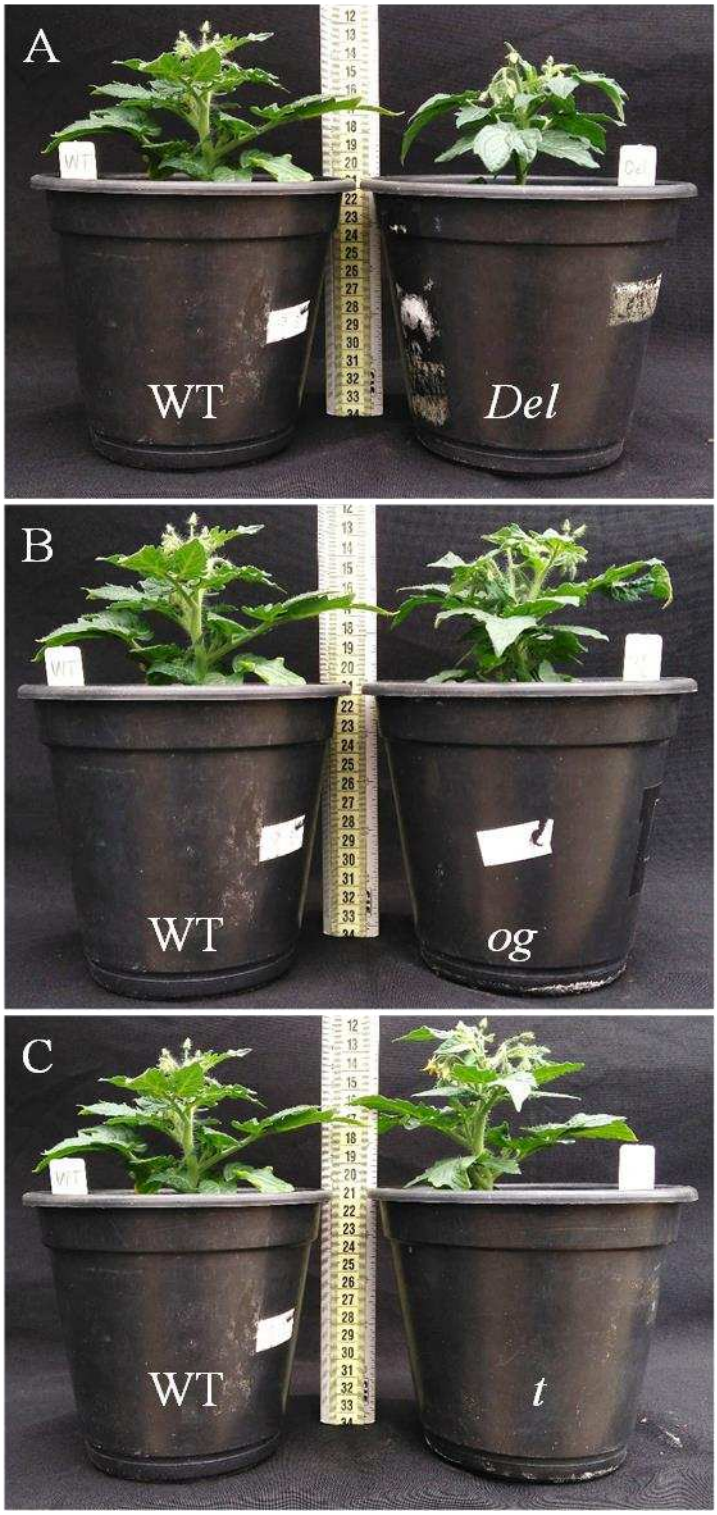

Supplementary Figure 3 – Representative photography of growth from plants WT, *Del* (A), *og* (B) and *t* (C), plants with five-weeks-old.

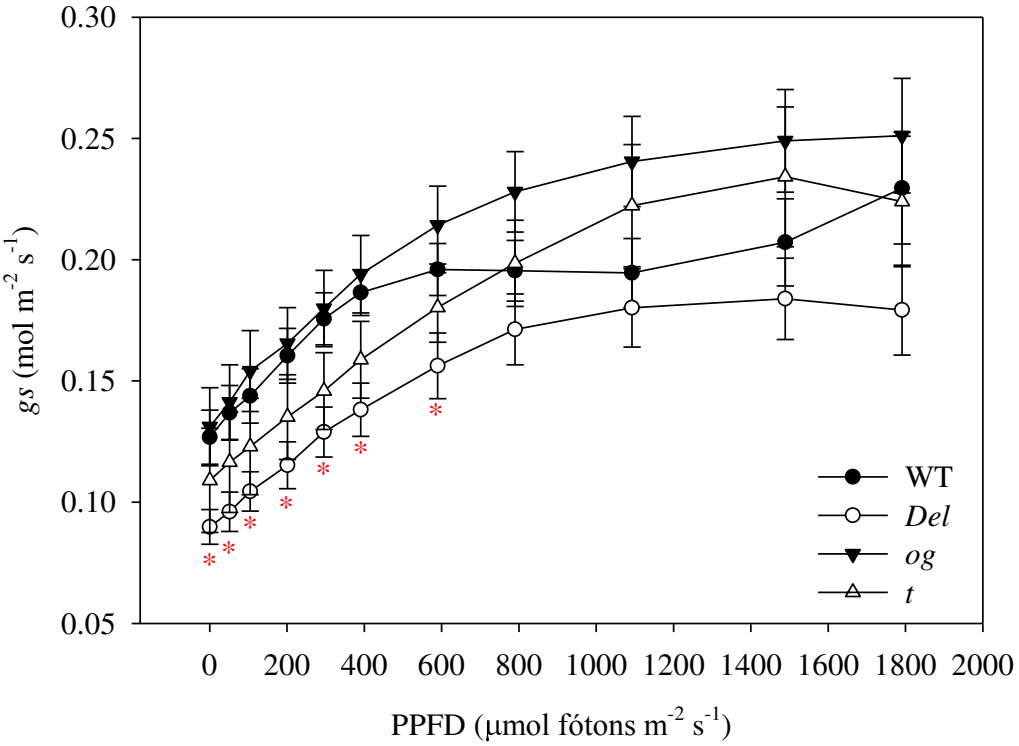

Supplementary Figure 4 - Stomatal conductance (*gs*) in response to changes in photosynthetic photon flux density (PPFD) of Micro-Tom plants (WT) and *Del*, *og* and *t*. Evaluations were carried out on four-week-old plants (28 DAP). Asterisks indicate at which point in the curve the mutants were significantly different to WT according to Student's t-test ($P < 0.05$); *Del* red asterisk, *og* green asterisk and *t* blue asterisk. Values are presented as means ± standard error (n = 6).

Supplementary Table 2 - Changes in stomatical indexes of Micro-Tom plants (WT) and *Del, og* and *t* mutants. Evaluations were carried out on eight-weeks-old plants (56 DAP). (SI) Stomatal idex; (SD) Stomatal density; (CD) Cells density. Means followed by the same letter on the vertical do not differ (P <0.05) by the Duncan's test. Values represent means ± standard error (n = 6).

ADAXIAL EPPIDERMIS			
	SI	SD (n° mm^{-2})	CD (n° mm^{-2})
WT	13.91 ± 1.05 a	98.73 ± 8.94 a	609.69 ± 20.28 b
Del	8.69 ± 1.50 b	65.82 ± 10.79 b	700.91 ± 37.76 a
og	11.22 ± 1.14 ab	73.60 ± 8.56 ab	581.39 ± 26.25 b
t	13.36 ± 1.51 a	88.73 ± 8.20 ab	588.39 ± 30.01 b
ABAXIAL EPPIDERMIS			
	SI	SD (n° mm^{-2})	CD (n° mm^{-2})
WT	21.16 ± 0.63 b	187.46 ± 11.30 b	696.02 ± 28.89 ab
Del	23.88 ± 0.91 a	238.60 ± 15.82 a	756.06 ± 17.77 a
og	22.49 ± 0.88 ab	203.41 ± 9.09 b	701.80 ± 25.39 ab
t	23.73 ± 0.63a	198.27 ± 5.55 b	641.23 ± 29.81 b

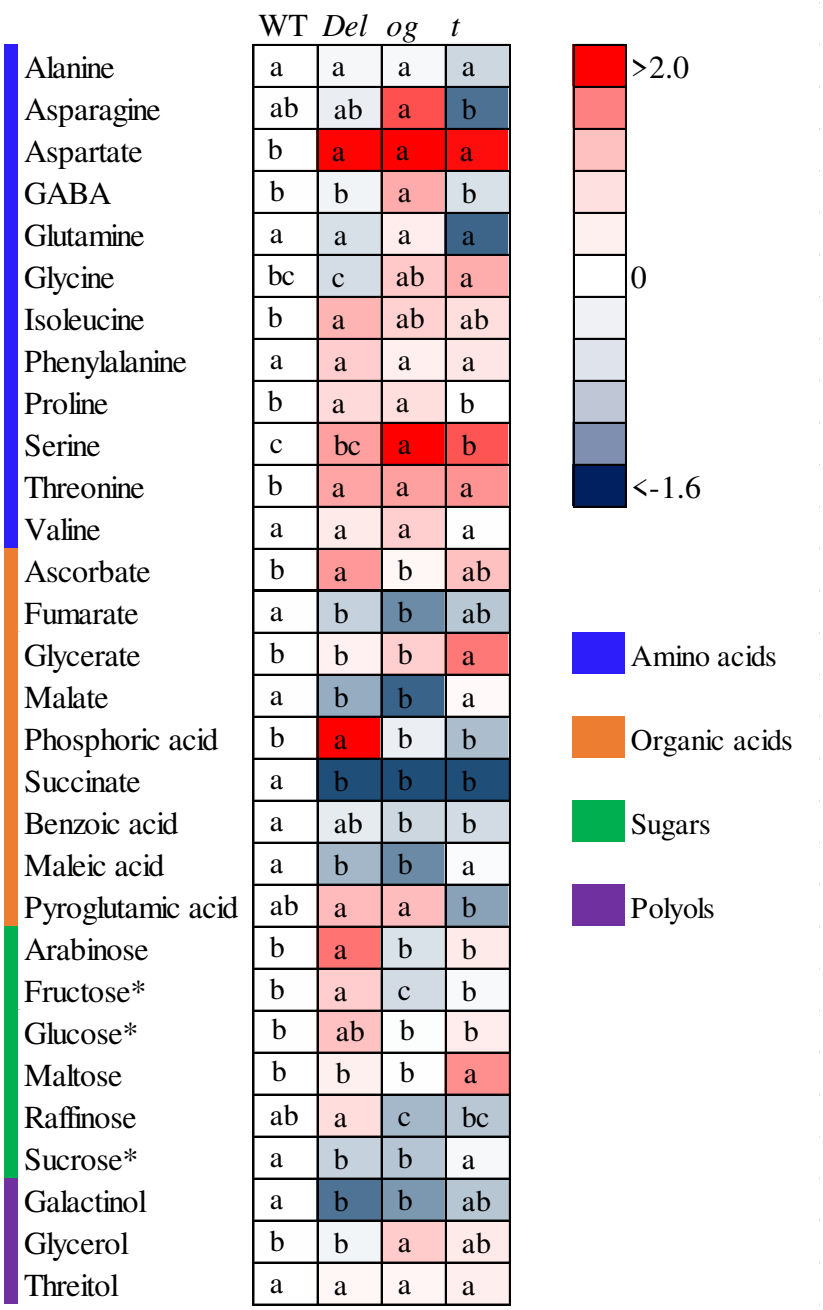

Supplementary Figure 5 - Heat map representing the variation on metabolite content in Micro-Tom plants (WT) and *Del, g* and *t* mutants. Evaluations were carried out on four-week-old plants (28 DAP). Different shades of blue and red express the extent of the change according to the color bar provide (control log2 ratio). Asterisk indicates that relative metabolite values were obtained by enzymatic method as described in the material and methods. Means followed by the same letter did on the horizontal not differ among genotypes ($P < 0.05$) according to Duncan's test. Values were plotted as log on base 2 of at least four independent plants.

Supplementary Table 3 - Mean values for metabolites of Micro-Tom plants (WT) and *Del, g* and *t* mutants. Evaluations were carried out on four-week-old plants (28 DAP). The data presented were obtained by gas chromatography coupled to mass spectrometry (GC-MS) and normalized by standard (Ribitol) and mass (g). Means followed by the same letter on the horizontal did not differ according to Duncan's test (P <0.05). Values are presented as means ± standard error (n = 4).

Compounds	WT	*Del*	*og*	*t*
Alanine	41.77 ± 3.68 a	39.88 ± 4.95 a	40.11 ± 1.87 a	32.53 ± 3.40 a
Asparagine	32.9 ± 11.57 ab	29.73 ± 11.06 ab	85.47 ± 18.47 a	13.59 ± 3.84 b
Aspartate	58.91 ± 9.93 b	233.55 ± 38.91 a	248.78 ± 17.87 a	221.69 ± 16.48 a
GABA	180.46 ± 17.16 b	168.82 ± 6.15 b	286.37 ± 12.55 a	150.2 ± 3,51 b
Glutamine	125.27 ± 36.07 a	103.24 ± 46.45 a	138.57 ± 41.73 a	47.83 ± 20.65 a
Glycine	91.48 ± 8.87 bc	74.14 ± 3.22 c	123.1 ± 5.81 ab	144.13 ± 6.87 a
Isoleucine	54.36 ± 1.32 b	81.8 ± 4.83 a	69.89 ± 6.75 ab	65.17 ± 10.02 ab
Phenylalanine	19.55 ± 0.78 a	25.79 ± 2.87 a	21.36 ± 2.44 a	22.5 ± 2.00 a
Proline	4958.29 ± 258.03 b	6095.29 ± 95.54 a	5948.05 ± 268.66 a	4983.6 ± 122.45 b
Serine	172.83 ± 30.19 c	292.69 ± 42.03 bc	762.23 ± 98.83 a	438.89 ± 29.39 b
Threonine	127.03 ± 7.05 b	207.6 ± 9.64 a	213.74 ± 19.70 a	229.15 ± 21.00 a
Valine	95.51 ± 6.13 a	107.44 ± 6.53 a	124.24 ± 12.09 a	96.33 ± 14.18 a
Ascorbate	7.06 ± 0.54 b	12.4 ±0.64 a	7.41 ± 0.26 b	9.95 ± 1.26 ab
Fumarate	6.03 ± 0.17 a	4.55 ± 0.44 ab	2.93 ± 0.17 b	4.25 ± 0.82 ab
Glycerate	59.45 ± 6.32 b	64.48 ± 2.69 b	77.8 ± 10.18 b	124.5 ± 7.18 a
Malate	772.84 ± 38.28 a	461.15 ± 76.19 b	291.15 ± 10.10 b	802.26 ± 65.01 a
Phosphoric acid	352.64 ± 101.91 b	1541.95 ± 136.39 a	319.89 ± 76.48 b	234.07 ± 29.21 b
Succinate	511.51 ± 31.04 a	150.63 ± 4.78 b	168.13 ± 14.42 b	165.69 ± 29.02 b
Benzoic acid	3.64 ± 0.08 a	3.21 ± 0.06 ab	2.84 ± 0.07 b	2.92 ± 0.18 b
Maleic acid	101.43 ± 4.08 a	64.9 ± 6.17 b	48.93 ± 6.27 b	99.34 ± 10.46 a
Pyroglutamic acid	472.09 ± 86.83 ab	684.49 ± 84.95 a	681.92 ± 50.69 a	264.76 ± 49.09 b
Arabinose	31.8 ± 1.61 b	68.19 ± 6.91 a	26.59 ± 0.73 b	35.68 ± 5.58 b
Fructose*	148.12 ± 1.99 b	195.29 ± 3.79 a	118.69 ± 6.43 c	143.42 ± 7.60 b
Glucose*	107.27 ± 2.29 b	150.79 ± 3.48 a	106.14 ± 3.14 b	119.21 ± 9.06 b
Maltose	14.49 ± 2.01 b	15.73 ± 1.42 b	14.59 ± 1.54 b	26.92 ± 2.22 a
Raffinose	9.94 ± 0.57 ab	12.01 ± 0.89 a	6.39 ± 0.69 c	7.04 ± 1.03 bc
Sucrose*	58.76 ± 1.42 a	44.3 ± 1.32 b	41.07 ± 1.57 b	56.25 ± 1.73 a
Galactinol	26.02 ± 1.06 a	10.85 ± 2.08 b	13.66 ± 1.23 b	18.25 ± 3.26 ab
Glycerol	25.05 ± 0.78 b	23.59 ± 2.21 b	33.37 ± 1.58 a	28.12 ± 2.08 ab
Threitol	2.91 ± 0.01 a	3.07 ± 0.17 a	3.08 ± 0.17 a	3.19 ± 0.40 a

Amino acids
Organic acids
Sugars
Polyols

5. CONCLUDING REMARKS

The work presented here is focused on the investigation of the role of pigments on the context of plant growth and leaf metabolism, which is largely dependent on photosynthesis. The main goals of this thesis were: (*i*) to revisit and highlight recent advances related to the improvement of photosynthesis; (*ii*) to investigate how and to which extent *high pigment* mutations (*hp1* and *hp2*) influence the metabolic machinery of tomato plants and how these plants adjust to different light conditions; and (*iii*) to increase our understanding of how mutations that alter carotenoid biosynthesis (*og*, *Del* and *t*) can affect the metabolic machinery of tomato plants. To this end, we used different but complementary approaches to evaluate growth and primary metabolism through morphological, physiological and biochemical analyzes. In each chapter we present and discuss the results obtained whereas within this section present coherently, although independently, an integrative discussion of the main findings found in each chapter. At the end, some perspectives to future research based on the results obtained from this work are further presented.

Rubisco is an extremely important enzyme for planet life since it participates in the carboxylation step of the photosynthesis. This fact aside, Rubisco is somewhat considered relatively inefficient due to its low catalytic velocity and also due to its ambiguous capacity to interact not only with CO_2 but also with O_2 starting the photorespiratory C_2 cycle at the expense of C fixed. Thus, Chapter I present a summary of the most recent studies that address photosynthetic improvements in land plants. It is important to mention, however, that lthough Rubisco is assumedly one of the main targets in the attempts to increase the photosynthetic process, we also highlight information on other important steps of the Calvin-Benson cycle. Thus, we summarize evidence showing that the activity of other enzymes can optimize the C flow within the Calvin-Benson cycle thereby eliminating bottlenecks throughout the cycle, or minimizing the effects of photorespiration (Kebeish et al., 2007; Maier et al., 2012; Nölke et al., 2014). Other significant and positive results have been found with the overexpression of native and foreign genes that clearly lead to increases in photosynthesis, although it not always culminated with increased biomass. On the other hand, improvements in light efficiency have been associated with positive results in biomass as deduced by the alterations

in the expression of genes of the major components of the xanthophyll cycle. This increased expression appears to help dissipation of the energy excess by relieving stress from the photosynthetic apparatus. Furthermore, changes in the amount of the main pigments of the antenna complex (chlorophylls and carotenoids) seems to additionally optimize light capture and, ultimately, changes in leaf optical characteristics, such as increased transmittance, can improve light utilization in overlapping canopy layers (Zhu et al., 2004; Melis, 2009; Blankenship et al., 2011; Kromdijk et al., 2016; Kirst et al., 2017). Advances in our current understanding of C_4 and CAM metabolism have been made and it clearly prompted significant research efforts aiming at including characteristics of these metabolism in C_3 plants to optimize photosynthesis. In addition, studies associated with carbon concentrating mechanisms (CCMs) have increased our knowledge on this exciting topic and further broadened the current attempts to include CCMs from other species into plants, aiming to increase the CO_2 concentration near the Rubisco catalytic sites and, thus improving Rubisco efficiency (Maier et al., 2012; Lin et al., 2014; Lundgren and Christin, 2017). In summary, we provided compelling evidence that while conventional breeding has been sufficient to increase agricultural productivity so far, new approaches must be explored to achieve higher yields in the near future. We further posit that among these approaches synthetic biology deserves special attention and presents itself as of tremendous value.

Natural mutations can also lead to increases in photosynthetic performance (Alves et al., 2016). Accordingly, *hp* mutants, which have more pigments (including photosynthetic pigments), are characterized by higher photosynthetic rate when compared to their WT counterpart (Levin et al., 2003; Lieberman et al., 2004). In Chapter II, we hypothesized that the high pigment levels observed in both *hp1* and *hp2* mutants may represent an additional energy expenditure for these plants and that major metabolic adjustments are required to maintain the successful performance of tomato plants under different growing light conditions. Therefore, these mutant plants were cultivated under low and normal light conditions, and our results demonstrated that *hp* mutations clearly affected all stages of tomato development. We additionally observed that shading reduces the differences between mutants and their respective WT. Growth was more affected during their vegetative phase, where mutants displayed lower height, but presented higher root length, number of leaves, leaf area, total dry weight and root/shoot ratio, and these differences were minimized under

shading conditions. During the reproductive phase, significant differences regarding plant growth were not observed; however, the final fruit production was negatively affected and the mutants also showed drastic reductions in the number of both flowers and fruits, mainly under the higher shade conditions. It is important to mention that these negative effected were observed in the mutants even though they showed higher *A*, lower stomatal limitation, greater V_{cmax} and anatomical changes that favor photosynthesis. It was also observed that overall metabolism was affected, as depicted by higher accumulation of amino acids in mutant plants, yet the content of sugars and organic acids was not altered in mutants despite the significant higher CO_2 assimilation. We additionally observed that *hp* mutant plants are generally more affected by shading than WT plants. It seems reasonable to assume that extensive physiological and metabolic reprogramming occurs to support enhanced biosynthesis of pigment and that due to the integrative nature of plant metabolic pathways, changes in the metabolism of pigment may have unavoidable consequences on other parts of metabolism, in general (Baghalian et al., 2014; Yuan et al., 2016; Sweetlove et al., 2017). We additionally postulate that overall changes promoted by the *hp* mutations are most likely involved more in protection against light-induced oxidative stress. In summary, complex metabolic adjustments appear to work in *hp* mutant plants not to improve photosynthetic performance *per se*, but rather to provide protection associated with energy dissipation and ROS scavenger at the leaf level.

Carotenoids play a significant role in plant life by actively participating in light capture in the photosystems and protecting the photosynthetic apparatus from excess energy, at same time it biochemically acts as dissipators of the singlet state of chlorophyll and avoiding ROS generation (Nisar et al., 2015). In Chapter III, we further explored the impacts of pigment-related mutations in the overall metabolism and physiology in tomato plants by investigating the effects of mutations on the carotenoid biosynthesis pathway (*og*, *Del* and *t*). To this end, we performed a detailed analyzes of the changes in photosynthetic traits, antioxidant capacity and the primary metabolism of these mutant plants. Taken together, our results shown that despite minor impacts on growth and gas exchange, the carbon flow is extensively affected, leading to significant adjustments in the overall metabolic machinery to support changes in carotenoid biosynthesis. It seems reasonable to anticipate that under

stress conditions, greater phenotypic changes would be observed due to the metabolic adjustments that are most likely required to support photosynthetic performance and growth.

Given the significance of photosynthesis and its improvement to assure food security, it is of utmost importance that more research efforts must be placed to achieve a more concrete and practical advance in terms of photosynthesis enhancements. Equally important, investments in long-term research projects are essential to achieve this goal. We are additionally aware that our knowledge on *hp1* and *hp2* mutations still remains limited, particularly given to their pleiotropic impacts in plant development. This fact aside, the positives impacts including higher amount of photosynthetic pigments, higher photosynthetic rate and higher concentration of health beneficial bioactive compounds [e.g., carotenoids (Lycopene), tocopherols and vitamin C (Levin et al., 2006)], might be incorporated into commercial crops, as observed for Wann (1997) and Ilahy et al. (2017). Mutations in the DDB1 protein seems to be a possible way to take full advantage of the *hp* mutation, as it culminates with highly similar benefits observed in the DET1 mutation, however, without major loss production. Moderate expression levels of the genes encoding these proteins could still be explored in order to minimize negative effects and take advantage of positive ones. Due to the growing demand for food that contains an adequate concentration of bioactive compounds, a real race has started aiming at the development of cultivars with this profile, either through conventional breeding or synthetic biology. Obviously, due to their proven effects, carotenoids have been the preferred targets in several independent studies (Jomova and Valko, 2013; Park et al., 2015; Martí et al., 2016). Nevertheless, the precise connection between energy metabolism and carotenoid-mediated growth control is just beginning to be understood, and as such, further studies are required. We posit that this information will be culminated with the production of carotenoid-enriched foods without compromising plant growth and development and ultimately accumulation of biomass. Although we did not observe large variations in plant growth with mutations in the carotenoid biosynthetic pathway, it seems that under non-stressful conditions the metabolism is extensively reprogrammed in an attempt to avoid more pronounced impacts. Thus, changes in carotenoid biosynthesis may not show the true impact under optimal growth conditions, and therefore future research under stressful conditions is likely required. It seems reasonable to assume that a better understanding of the relationship between photosynthesis, pigments and

metabolism can provide an useful tool not only for the development of food enriched with biotic compounds, but also for increasing photosynthetic efficiency and increasing food production.

6. REFERENCES

Alves FRR, de Melo HC, Crispim-Filho AJ, Costa AC, Nascimento KJT, Carvalho RF (2016) Physiological and biochemical responses of photomorphogenic tomato mutants (cv. Micro-Tom) under water withholding. Acta Physiologiae Plantarum. doi: 10.1007/s11738-016-2169-8

Baghalian K, Hajirezaei MR, Schreiber F (2014) Plant metabolic modeling: Achieving new insight into metabolism and metabolic engineering. Plant Cell **26**: 3847–3866

Blankenship RE, Tiede DM, Barber J, Brudvig GW, Fleming G, Ghirardi M, Gunner MR, Junge W, Kramer DM, Melis A, et al (2011) Comparing photosynthetic and photovoltaic efficiencies and recognizing the potential for improvement. Science **332**: 805–809

Ilahy R, Siddiqui MW, Piro G, Lenucci MS, Hdider C, Helyes L (2017) A focus on high-lycopene tomato cultivars: Horticultural performance and functional quality. Acta Horticulturae **1159**: 57–64

Ilan Levin A, Vos CHR de, Tadmor Y, Bovy A, Lieberman M, Oren-Shamir M, Segev O, Kolotilin I, Keller M, Ovadia R, et al (2006) High pigment tomato mutants—more than just lycopene (a review). Israel Journal of Plant Sciences **54**: 179–190

Jomova K, Valko M (2013) Health protective effects of carotenoids and their interactions with other biological antioxidants. European Journal of Medicinal Chemistry **70**: 102–110

Kebeish R, Niessen M, Thiruveedhi K, Bari R, Hirsch HJ, Rosenkranz R, Stäbler N, Schönfeld B, Kreuzaler F, Peterhänsel C (2007) Chloroplastic photorespiratory bypass increases photosynthesis and biomass production in *Arabidopsis thaliana*. Nature Biotechnology **25**: 593–599

Kirst H, Gabilly ST, Niyogi KK, Lemaux PG, Melis A (2017) Photosynthetic antenna engineering to improve crop yields. Planta **245**: 1009–1020

Kromdijk J, Głowacka K, Leonelli L, Gabilly ST, Iwai M, Niyogi KK, Long1 SP (2016) Improving photosynthesis and crop productivity by accelerating recovery from photoprotection. Plant Science **354**: 857–861

Levin I, Frankel P, Gilboa N, Tanny S, Lalazar A (2003) The tomato dark green mutation is a novel allele of the tomato homolog of the DEETIOLATED1 gene. Theoretical and Applied Genetics **106**: 454–460

Lieberman M, Segev O, Gilboa N, Lalazar A, Levin I (2004) The tomato homolog of the gene encoding UV-damaged DNA binding protein 1 (DDB1) underlined as the gene that causes the high pigment-1 mutant phenotype. Theoretical and Applied Genetics **108**: 1574–1581

Lin MT, Occhialini2 A, Andralojc PJ, Parry MAJ, Hanson MR (2014) A faster Rubisco with potential to increase photosynthesis in crops. Physiology & Behavior **513**: 547–550

Lundgren MR, Christin PA (2017) Despite phylogenetic effects, C_3 -C_4 lineages bridge the ecological gap to C_4 photosynthesis. Journal of Experimental Botany **68**: 241–254

Maier A, Fahnenstich H, von Caemmerer S, Engqvist MKM, Weber APM, Flügge UI, Maurino VG (2012) Transgenic introduction of a glycolate oxidative cycle into *A. thaliana* chloroplasts leads to growth improvement. Frontiers in Plant Science **3**: 1–12

Martí R, Roselló S, Cebolla-cornejo J (2016) Tomato as a source of carotenoids and polyphenols targeted to cancer prevention. Cancers **8**: 1–28

Melis A (2009) Solar energy conversion efficiencies in photosynthesis: Minimizing the chlorophyll antennae to maximize efficiency. Plant Science **177**: 272–280

Nisar N, Li L, Lu S, Khin NC, Pogson BJ (2015) Carotenoid metabolism in plants. Molecular Plant **8**: 68–82

Nölke G, Houdelet M, Kreuzaler F, Peterhänsel C, Schillberg S (2014) The expression of a recombinant glycolate dehydrogenase polyprotein in potato (*Solanum tuberosum*) plastids strongly enhances photosynthesis and tuber yield. Plant Biotechnology Journal **12**: 734–742

Park SC, Kim SH, Park S, Lee HU, Lee JS, Park WS, Ahn MJ, Kim YH, Jeong JC, Lee HS, et al (2015) Enhanced accumulation of carotenoids in sweetpotato plants overexpressing IbOr-Ins gene in purple-fleshed sweetpotato cultivar. Plant Physiology and Biochemistry **86**: 82–90

Sweetlove LJ, Nielsen J, Fernie AR (2017) Engineering central metabolism – a grand challenge for plant biologists. Plant Journal **90**: 749–763

Wann EV (1997) Tomato germplasm lines T4065, T4099, T5019, and T5020 with unique genotypes that enhance fruit quality. HortScience **32**: 747–748

Yuan H, Cheung CYM, Poolman MG, Hilbers PAJ, Van Riel NAW (2016) A genome-scale metabolic network reconstruction of tomato (*Solanum lycopersicum* L.) and its application to photorespiratory metabolism. Plant Journal **85**: 289–304

Zhu XG, Ort DR, Whitmarsh J, Long SP (2004) The slow reversibility of photosystem II thermal energy dissipation on transfer from high to low light may cause large losses in carbon gain by crop canopies: A theoretical analysis. Journal of Experimental Botany **55**: 1167–1175